Active Separation Control Using Vortex Generator Jets

Active Separation Control Using Vortex Generator Jets

Hiroaki Hasegawa

Doctoral Program in Engineering
University of Tsukuba
Tennoudai, Ibaraki 305-8573

March 1999

ACKNOWLEDGEMENTS

The author gratefully acknowledges Prof. Kazuo Matsuuchi, Institute of Engineering Mechanics at the University of Tsukuba, for the kind guidance, insightful criticism, and incessant support of the whole study. Emeritus Prof. Yoshimasa Yoshizawa, the University of Tsukuba, provided valuable scientific suggestions. In finishing this work, the following professors guided him, Prof. Goichi Matsui, Prof. Masahide Murakami, Prof. Tatsuo Kawai, and Assoc. Prof. Hidenobu Shoji, Institute of Engineering Mechanics at the University of Tsukuba. He would like to express his appreciation for help to assemble the experimental apparatus and the suggestions to perform the experiments effectively provided by Mr. Takashi Nakajima and Masayuki Kobe, research engineers at the University of Tsukuba.

Dr. Naminosuke Kubota, a scientific advisor at Mitsubishi Electric Corporation, spent his precious hours for this dissertation to review from cover to cover, to give helpful comments and to correct expressions in English.

He would like to thank Mr. Jun Yamakami and Mr. Junsuke Tanaka for their contributions to perform experimental works as Master degree's student of the University of Tsukuba.

He would like to thank all the above people and his co-workers at the Technical Research and Development Institute, Japan Defense Agency who gave him a chance to research at the University of Tsukuba.

Finally, he thanks his wife and daughter for their patience and support during some hectic years.

ABSTRACT

Jets issuing through small holes in a wall into a freestream have proven effective in the control of boundary layer separation. Longitudinal (streamwise) vortices are produced by the interaction between the jets and the freestream. This technique is known as the vortex generator jet method of separation or stall control because it controls separation in the same general way as the well-known method using solid vortex generators. The vortex generator jet method is an active control technique which provides a time-varying control action to optimize performance under a wide range of flow conditions. The vortex generator jets can adjust the strength of longitudinal vortices by varying the jet speed and the jet speed control may be readily accomplished by the use of valves in the air supply lines of the jets. Therefore, they can achieve the adaptive control by properly adjusting the jet speed corresponding to flow parameters such as the angle of attack of an airfoil, the diffuser's divergence angle, and the freestream velocity. For the vortex generator jet method, it is not necessary to know whether the boundary layer is laminar or turbulent in advance. Longitudinal vortices strongly disturb the flow and the disturbance thus induced is dominant in comparison with the turbulence of the boundary layer.

The mechanism for suppressing flow separation was studied experimentally by making a comparison between the effect of steady jets and that of pulsed jets on generating longitudinal vortices. The suppression of flow separation is accomplished by the secondary flow of longitudinal vortices which transports the high momentum fluid of the freestream to the lower wall. The beneficial effect of separation control is obtained only if the jets are pitched to the lower wall and skewed with respect to the freestream direction. The effect of the jet pitch angle on suppressing flow separation was studied in three cases with the jet pitch angle set at 30, 45, and 60 degrees. In the 60-deg case, the longitudinal vortices moved apart more rapidly from the lower wall than in the other cases and therefore the 60-deg case is inferior to the others in terms of the control of flow separation. Accordingly, it is desirable for a jet pitch angle to be selected less than 60 degrees.

The important advantages of vortex generator jets are that 1) they can be adapted for various flow changes and that 2) they can avoid parasitic drag with the

jet flow turned off for flow situations where separation control is not needed, e.g., steady cruise conditions. Therefore, the vortex generator jet method is useful for both design and off-design conditions. The active separation control feedback system developed in this study has been based on the examinations of the mechanism of the boundary layer control and the effect of the jet pitch angle on suppressing flow separation. This active separation control system can suppress the flow separation by controlling the jet speed alone. The system has been actually applied to the flow separation control of a two-dimensional diffuser. Consequently, the active separation control system developed in this study can adaptively suppress separation for all the flow fields examined in the present study.

TABLE OF CONTENTS

LIST OF TABLES

LIST OF FIGURES

1. INTRODUCTION

1.1 Background

Separation is mostly an undesirable phenomenon because it entails large energy losses. In order to reduce drag and pressure losses it would be necessary to inhibit flow separation by suppressing boundary layer development. For this reason methods have been devised for the artificial prevention of separation. Boundary layer control has been used widely in aerodynamic applications to inhibit flow separation. The simplest method, for example, from the physical point of view, is to adopt a streamline shaped body in order to reduce the velocity difference between the stream and the flow near the solid wall, though this method sometimes has design restrictions in engineering practice. Another effective method for the prevention of separation is boundary layer mixing. In this method, the fluid particles which have large energy of the freestream are supplied to decelerated fluid particles in the boundary layer by longitudinal vortices. The techniques using longitudinal vortices are classified as passive and active methods. The passive control technique with solid vortex generators (rectangular, ramp, delta-shaped winglets, etc.) has advantages such as simplicity, ruggedness, and low cost. It has practical applications in stall control on airfoils and in diffusers. For example, solid vortex generators placed on the airfoils are useful to improve flight performance during aircraft take-off and landing. Furthermore, the generators placed in diffusers make the diffuser length shorter than those of the usual type. However, solid vortex generators have fatal shortcomings. Their disadvantages are that 1) they do not have the ability to provide a time-varying control action and therefore they can not be adopted for highly maneuverable aircraft and 2) they add parasitic drag in flow situations where stall suppression is not needed (e.g., an airfoil operating near its design condition). It is desirable for the control devices to be operated only when flow separation occurs. However, solid vortex generators are always exposed in the flow and they have increased drag.

On the other hand, pitched and skewed jets issuing through small holes in a wall into a freestream have proven effective regarding the control of boundary layer separation. Longitudinal vortices are produced by the interaction between jets and a freestream. This technique is known as the vortex generator jet method. The vortex generator jet method as an active control technique provides a time-varying control action to optimize performance under a wide range of flow conditions. For vortex generator jets, the strength of the longitudinal vortices are controllable by varying the jet speed. Furthermore, for flow situations where stall control is not needed, parasitic drag can be avoided with the jet flow turned off. The vortex generator jet method may accomplish separation control only when it is necessary and therefore it is available for both design and off-design conditions. Stall control with airplane or fluid machinery is not needed in usual operations because they are designed to produce no separation. If the control device operates only when it is necessary and can adaptively suppress flow separation, the ideal flow corresponding to the flow under its design condition is always attained without any changes in design of airfoils or diffusers.

1.2 Literature Review

The vortex generator jet method was first examined by Wallis [1] in the 1950's. However, solid vortex generators which were suggested by Taylor [2] some years earlier than that, had been energetically investigated at that time in comparison with vortex generator jets. They have practical applications in the stall control of airfoils and diffusers. It is not going too far to say that the vortex generator jet method has been neglected. Therefore, aspects for study related to the vortex generator jet method still remain.

A large body of literature describing studies of solid vortex generators exists. The principle of controlling a boundary layer using solid vortex generators such as those shown in Fig. 1.1 was first suggested by H. Bruynes and H. D. Taylor of the United Aircraft Corporation in 1947. Bruynes (1951) obtained U.S. Patent 2,558,816 for his fluid mixing device. H. D. Taylor [2] reported on the manner in which these solid vortex generators might be used in diffusers. This began a period during which wind tunnel testing was performed to determine the effects of

solid vortex generators on suppressing boundary layer separation. Schubauer and Spangenberg [3] studied forced mixing in boundary layers. They investigated various types of solid vortex generators to determine which were more effective in suppressing boundary layer separation. Mehta [4] studied the effects of longitudinal vortices on the turbulent mixing layer. He reported that the mixing between the two streams was enhanced due to longitudinal vortices without significant decay in the vortex strength due to the mixing layer. He also studied the effects of vortices on separated subsonic [5] and supersonic boundary layers [6]. He concluded that the longitudinal vortex delayed separation on the downwash side and encouraged separation on the upwash side of a vortex for subsonic flow. For supersonic flow the longitudinal vortex reduced the entire region of separation, not just in the downwash region.

The processes of Reynolds stress modification and streamwise vorticity transport are important in understanding the development of the embedded vortices. The structure of turbulent boundary layers with embedded longitudinal vortices has been studied by Bradshaw and his co-workers at Imperial College [7]. Vortices were generated by placing half-delta-wing vortex generators in a wind tunnel settling chamber. These vortices pass through the contraction and into the test section with no significant wake remaining, and are embedded in the boundary layer. Their studies concentrated on the turbulent structure modification in the boundary layer due to interaction with the embedded longitudinal vortices. Mehta et. al. [8] reported the early results of these studies. A detailed data presentation and an analysis of the results were summarized in several parts. For a single longitudinal vortex embedded in a boundary layer, the results appeared in Shabaka, Mehta, and Bradshaw [9] or Mehta [10]. The vortex interaction with common flow between the vortices directed toward the wall was the most extensively studied, because it caused a strong distortion of the boundary layer. Results for the vortex pair with common flow-up were reported by Mehta and Bradshaw [11]. Pauley and Eaton [12] provided more detailed data for a variety of configurations with respect to rotational direction and strength of longitudinal vortices. They reported that higher skin friction was observed in the region with secondary flow toward the lower wall for the common-flow-down vortex pair and lower skin friction was observed in the region with the secondary flow away from the lower wall for the common-flow-up vortex pair. Shizawa and Eaton [13] indicated the suppression effect and the downstream development of longitudinal vortices.

Matsumoto [14] measured the mean flow and Reynolds stress in the vicinity of an embedded common-flow-up vortex pair. He noted distortion of the boundary layer velocity profiles, particularly a decrease in the shape factor due to the vortices. The streamwise vorticity was mostly concentrated in the vortex core region, and this was accounted for as being produced by the anisotropy of the normal Reynolds stresses term in the streamwise vorticity transport equation. He observed the mean and fluctuating velocities in a turbulent boundary layer with no pressure gradient, but with longitudinal vortices introduced artificially by a series of vane-type vortex generators.

On the other hand, the image of generating longitudinal vortices using vortex generator jets is shown in Fig. 1.2. Jets issue through small holes in a lower wall into a freestream. Longitudinal vortices are generated by the interaction between the jets and the freestream. The vortex generator jet method was first examined almost 40 years ago by Wallis [1] and Wallis and Stuart [15] in Australia. Wallis' work indicated that a single vortex, which is similar to one from a solid vortex generator, might be formed by a jet which was skewed with respect to the freestream direction and was pitched to the lower wall. The vortex generator jet method was examined primarily for the purpose of delaying shock-induced separation of turbulent boundary layers. For vortex generator jets, the beneficial effect of separation control is obtained only if the pitched and skewed jets are issued. A more recent study by Ball [16] on stall suppression for jet-engine-inlet diffusers employed vortex generator jets alone and together with solid vortex generators.

Johnston and Nishi [17] examined five configurations of jet directions. They provided engineering design data (e.g., minimum jet speeds and angles) for effective utilization and showed that jet arrays which give counter-rotating vortex pairs can cause significant spanwise variations. Compton and Johnston [18] investigated the strength and decay rate of a longitudinal vortex for seven cases of jet skew angle. They concluded that the maximum vorticity levels are strongly dependent on jet velocity and skew angle, and an optimal jet skew angle may be between 45 and 90 degrees to the downstream direction. Furthermore, they indicated that the property of longitudinal vortices produced by vortex generator jets is different from that by solid vortex generators. The suppression effect of flow separation using pulsed vortex generator jets in a stalled two-dimensional diffuser was demonstrated by McManus et al [19]. In order to realize pulsed flow,

they used a pulsed valve which was driven by a timing controller. A comparison between pulsed and steady flow jets was performed in order to confirm the relative efficiencies of the two techniques. It was indicated that the mass flow requirements for effective separation control using pulsed vortex generator jets were greatly reduced over those for steady jets.

Nishi et al. [20, 21] examined the applicability of vortex generator jets to suppressing separation in a conical diffuser which had a diffuser's divergence angle of 14 degrees. Selby et al. [22] performed a parametric study on controlling flow separation associated with low-speed turbulent flow over a two-dimensional rearward-facing ramp. In their study, they investigated the effects of several parameters such as the jet orifice diameter, jet orientation, jet speed, jet skew angle, and jet pitch angle on separation control. Furthermore, they made a comparison between slot blowing and vortex generator jets. A computational study was performed for the longitudinal vortices produced by a single jet and co-and contra-rotating jets in a turbulent cross flow by Zhang [23]. He selected control parameters such as jet angle, jet-to-cross flow velocity ratio, and jet spacing. The longitudinal vortices have the ability of convecting kinetic and thermal energy in the lateral plane. The ability could be utilized to enhance the film cooling efficiency of turbine blades (Honami et al. [24]) and heat transfer (Zhang and Collins [25]). Leylek and Zerkle [26] made a comparison of computational results with experiments on discrete jet film cooling and obtained reasonable agreement. Goldstein and Eckert [27] indicated that the effect of jet orifice geometry on the film cooling downstream of the secondary gas injection. Johnston and Khan [28] made a visual study using fluorescent dyes in a water flow channel in order to investigate the origin of the dominant vortex formed from a pitched and skewed jet.

As has been seen above, the effect of boundary layer control using vortex generator jets has begun to be understood in recent years. However, studies with respect to the vortex generator jet method have not been sufficiently carried out in comparison with those on solid vortex generators. In particular, the mechanism of the active boundary layer control by vortex generator jets and the generation mechanism of longitudinal vortices by the pulsed jets are not yet understood. Although the optimal jet skew angle which can strengthen the maximum vorticity level at a pitch angle of 45 degrees has already been reported, the effect of the jet pitch angle on separation control is unknown. The advantage of the vortex generator jet method is that it has the ability to adaptively control the various flow

conditions. However, applications of vortex generator jets to time-varying flow fields have not been reported.

1.3 Objectives of This Study

The purpose of present study was to investigate the effects of active separation control using vortex generator jets on suppressing flow separation. The more specific objectives of this study were the following:

1. To understand the mechanism of boundary layer control by using vortex generator jets [29, 30],

2. To determine the effects of the jet pitch angle on separation control [31, 32],

3. To understand the difference between the steady and pulsed jets in the downstream development of longitudinal vortices, and

4. To develop an active separation feedback system which can adapt time-varying flow fields and confirm the effectiveness of this system for changes in the flow fields of this experimental facility [33].

In this paper, the description is arranged in the following way: we begin in Chapter 1 by introducing the background and objectives of this study. In Chapter 2 we give an outline of the fundamental physical principles of the boundary layer and diffuser. The experimental apparatus are explained in Chapter 3 with a description of the velocity and pressure measurement instruments. In Chapter 4 we examine whether flow separation control is influenced by the boundary layer condition. In Chapter 5 the mechanism for suppressing flow separation using vortex generator jets is studied by making a comparison between the steady and pulsed jets in order to obtain data on the optimal conditions of longitudinal vortices for effective separation control. Furthermore, we make clear that the downstream development of longitudinal vortices for pulsed jets is different from that for steady jets. For these reasons we prepared Chapter 6. In Chapter 7 we describe the

effect of the jet pitch angle on separation control in order to obtain effective engineering design data. In Chapter 8 we take up the application of the active boundary layer control system which utilizes the data on the mechanism for the prevention of separation of the longitudinal vortices and the jet pitch angle. Finally, Chapter 9 contains a summary of the paper.

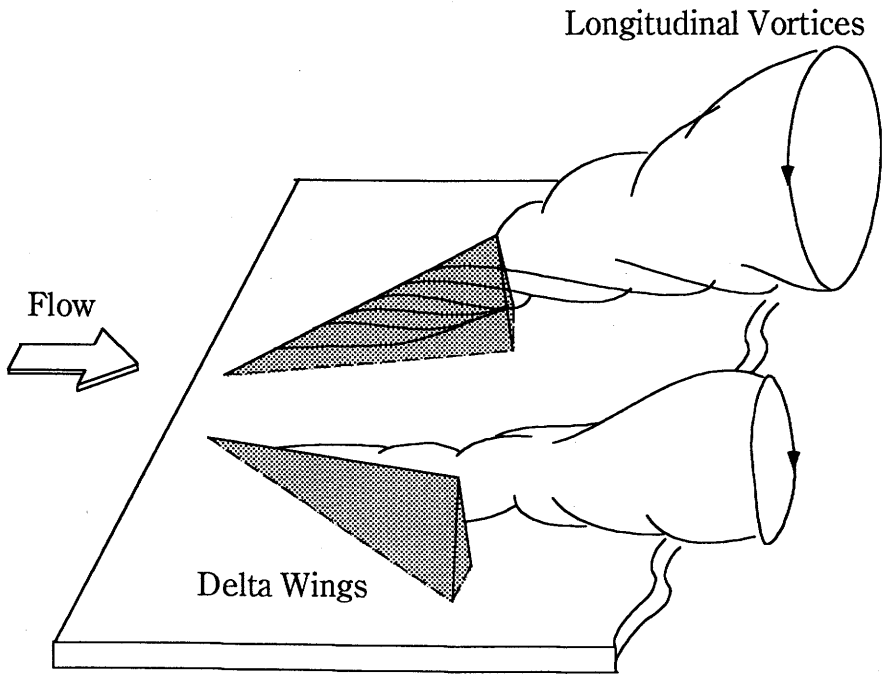

Figure 1.1 Longitudinal vortices generated by solid vortex generators.

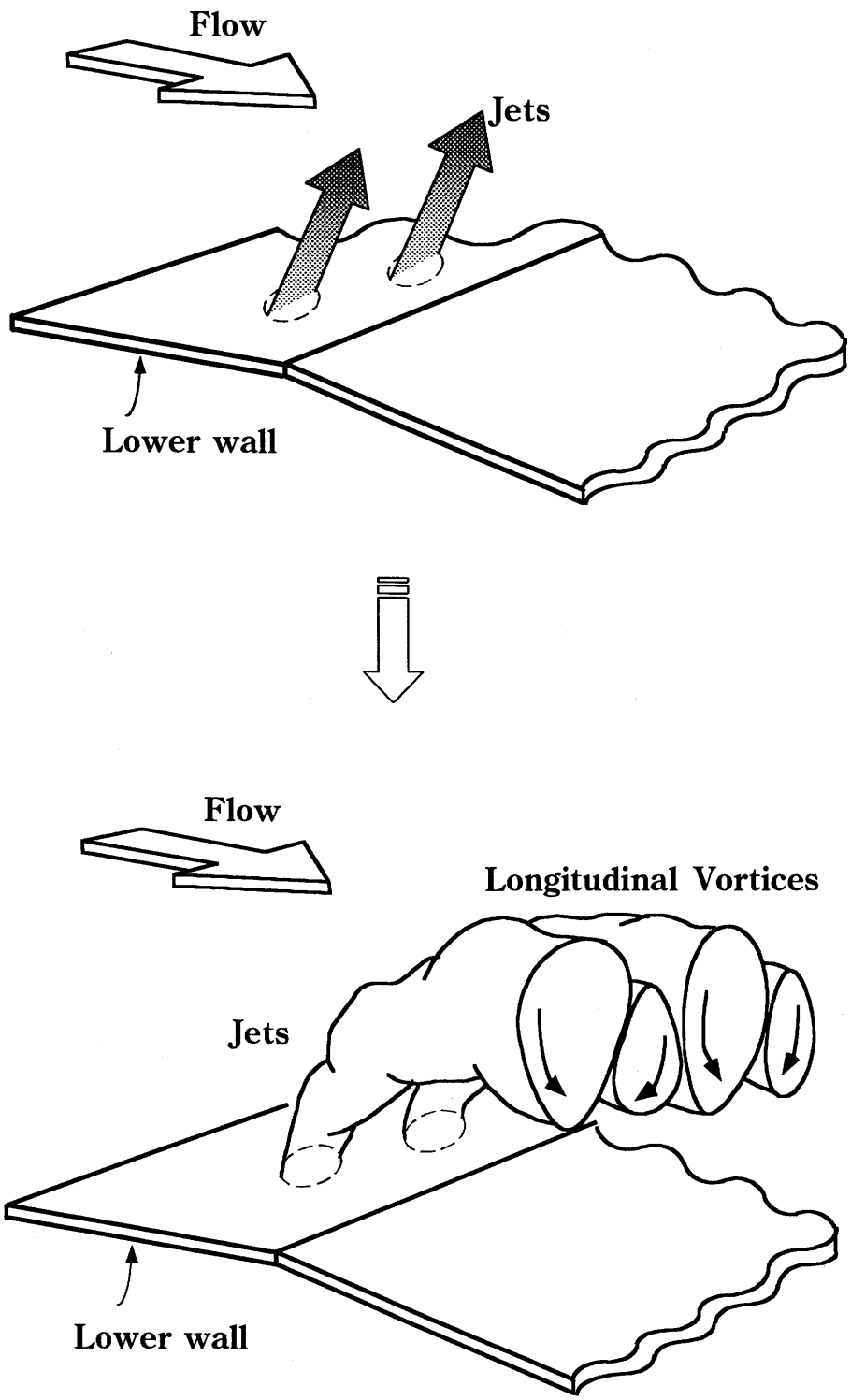

Figure 1.2 Longitudinal vortices due to jets issuing into freestream.

2. FUNDAMENTAL THEORY

2.1 Outline of Boundary Layer Theory [34-38]

2.1.1 The Boundary Layer Concept

The influence of viscosity at high Reynolds numbers is confined to a very thin layer near a solid wall. If the condition of no slip were not to be satisfied for the case of a real fluid, there would be no appreciable difference between the field of flow of the real fluid and that of a perfect fluid. However, the fact that the fluid adheres to the surface at the solid wall means that frictional forces retard the motion of the fluid in a thin layer near the wall. In the thin layer, the velocity of the fluid increases from zero on the solid wall (no slip) to its full value which corresponds to external frictionless flow (main stream). The thin layer which has a large velocity gradient exists near the solid wall. This thin layer is called the boundary layer.

The thickness of this boundary layer increases along a plate in a downstream direction. Figure 2.1 indicates diagrammatically the velocity distribution in a boundary layer on a flat plate. In front of the leading edge of the plate the velocity distribution is uniform. With increasing distance from the leading edge in the downstream direction, the thickness δ of the retarded layer increases continuously. Evidently, the thickness of the boundary layer increases with increasing viscosity.

When a region with an adverse pressure gradient exists along the wall, the retarded fluid particles near the wall cannot, in general, move far downstream against the increased pressure owing to their small kinetic energy. Thus the decelerated fluid particles in the boundary layer do not remain in the thin layer which adheres to the body. In some cases, if the boundary layer increases its thickness considerably in the downstream direction, the downstream movement of

the fluid near the wall which has small momentum is prevented and the flow in the boundary layer becomes reversed. This causes the decelerated fluid particles to be forced outwards, which means that the boundary layer is separated from the wall. This phenomenon is called boundary layer separation. Boundary layer separation is always associated with the formation of vortices and with large energy losses in the wake of the body. It occurs primarily near the sharp corner and blunt bodies, such as circular cylinders and spheres. Behind such a body there exists a region of strongly decelerated flow, in which the pressure distribution deviates considerably from that in a frictionless fluid. The large drag of such bodies can be explained by the existence of this large deviation in pressure distribution which is produced by a consequence of boundary layer separation.

Boundary layer separation is an undesirable phenomenon in engineering. For example, if flow separation occurs on airfoils, lift markedly decreases and a large drag of the body is produced. A deterioration in the performance of the diffuser and the impeller in the fluid machinery is produced by flow separation. Furthermore, the machinery is vibrated violently and broken by the surge from flow separation.

The Navier-Stokes equations are modified for the purpose of deriving the boundary-layer equation. In the case of steady flow two-dimensional incompressible boundary-layer equations are written as

$$\left.\begin{aligned} &\frac{\partial u}{\partial x}+\frac{\partial v}{\partial y}=0, \\ &u\frac{\partial u}{\partial x}+v\frac{\partial u}{\partial y}=-\frac{1}{\rho}\frac{dp}{dx}+\nu\frac{\partial^2 u}{\partial y^2}. \end{aligned}\right\} \tag{2.1}$$

The fact that separation in steady flow occurs only in decelerated flow ($dp/dx>0$) can be inferred from a consideration of the relation between the pressure gradient dp/dx and the velocity distribution $u(y)$ with the aid of the boundary-layer equation. From Eq. (2.1) with the boundary conditions $u=v=0$ we have at $y=0$

$$\mu\left(\frac{\partial^2 u}{\partial y^2}\right)_{y=0}=\frac{dp}{dx}. \tag{2.2}$$

In the immediate neighborhood of the wall the curvature of the velocity profile depends only on the pressure gradient, and the curvature of the velocity profile at the wall changes its sign with the pressure gradient. For flow with decreasing pressure (accelerated flow, $dp/dx<0$)) we have from Eq. (2.2) that $\partial^2 u/\partial y^2<0$

over the whole width of the boundary layer (see Fig. 2.2). For flow with increasing pressure (decelerated flow, $dp/dx>0$) we find $\partial^2 u/\partial y^2 > 0$ (see Fig. 2.3). However, in any case where $\partial^2 u/\partial y^2 < 0$ at a large distance from the wall, there must exist a point for which $\partial^2 u/\partial y^2 = 0$. This is a point of inflexion of the velocity profile in the boundary layer.

2.1.2 Boundary Layer Thickness

In general, the boundary layer thickness is defined as that distance from the wall where the velocity differs by one percent from the external velocity. However, it is impossible to determine a boundary layer thickness in an unambiguous way, because the influence of viscosity in the boundary layer decreases asymptotically outwards. Instead of the boundary layer thickness, another quantity, the displacement thickness δ_1 or the momentum thickness δ_2, is sometimes used in a physically meaningful measure for the boundary layer thickness. The displacement thickness indicates the distance by which the streamlines of the external potential flow are displaced as a consequence of the decrease in velocity in the boundary layer owing to the effect of friction near the wall. The decrease in volume flow due to the influence of friction is

$$\int_0^\infty (U_0 - u)dy \ ,$$

so that the displacement thickness δ_1 is given by

$$U_0\delta_1 = \int_0^\infty (U_0 - u)dy \ ,$$

or

$$\delta_1 = \int_0^\infty (1 - \frac{u}{U_0})dy. \tag{2.3}$$

The loss of momentum in the boundary layer due to the viscosity, as compared with potential flow, is given by

$$\int_0^\infty \rho u(U_0 - u)dy,$$

so that the momentum thickness δ_2 can be defined by

$$\rho U_0^2 \delta_2 = \rho \int_0^\infty u(U_0 - u)dy \ ,$$

or

$$\delta_2 = \int_0^\infty \frac{u}{U_0}(1 - \frac{u}{U_0})dy \ . \tag{2.4}$$

The displacement thickness and the momentum thickness have a relation to the conservation law of mass and momentum, respectively. The ratio H_{12} is called the shape factor and is defined by

$$H_{12} = \frac{\delta_1}{\delta_2} \ . \tag{2.5}$$

The shape factor indicates $H_{12} \fallingdotseq 2.6$ and $H_{12} \fallingdotseq 1.4$ for laminar flow and turbulent flow, respectively, in the boundary layer along a flat plate at zero incidence. As the value of H_{12} becomes smaller, the curvature of the velocity profile in the boundary layer indicates the type of flow with decreasing pressure (accelerated flow, see Fig. 2.2). As the value of H_{12} becomes larger, the curvature of the velocity profile in the boundary layer indicates the type of the flow with increasing pressure (decelerated flow, see Fig. 2.3).

2.2 Flow in Diffusers [35]

For the fluid transfer, pressure losses usually become smaller with decreasing velocity, because the pressure losses increase in proportion to the squared velocity. Therefore, it is important that the kinetic energy is converted to pressure by gradually decreasing the velocity. The flow path which can convert the kinetic energy to pressure energy is called a diffuser. Flow separation occurs easily for flows in the diffuser due to the adverse pressure gradient. Flow separation produces a decrease in the effective cross section of the flow path and therefore the pressure recovery in the diffuser markedly decreases.

Figure 2.4 indicates the characteristics of the flow in the diffuser with rectangular cross-sections. The area ratio AR (inlet to exit, $AR = W_e / W_i$) is defined as the ratio between the width of the inlet W_i and the width of the exit W_e of the diffuser. When the divergence angle of diffuser (2α) is small, flow along the surface is produced (see Fig. 2.4(a)). However, if the divergence angle becomes a

little wider, flow separation occurs locally because the flow in the boundary layer cannot overcome the pressure gradient (see Fig. 2.4(b)). As the divergence angle increases, the flow is perfectly separated from either wall and produces back-flow (see Fig. 2.4(c)). However, the flow adheres to the wall at the other side (see Fig. 2.4(c)). In this case, the flow is very unstable and therefore the losses then reach a maximum. If the divergence angle further increases, the flow is perfectly separated from the wall on both sides and changes into a jet flow (see Fig. 2.4(d)).

The pressure recovery coefficient C_p is defined as

$$C_p = \frac{p_e - p_i}{(1/2)\rho \overline{u}_i^2} \ . \tag{2.6}$$

Here p denotes the static pressure and $\overline{u}$ denotes the mean velocity over the cross section, whereas subscript i and e refer to conditions at the inlet and exit of the diffuser, respectively. The performance of the diffuser is evaluated by the diffuser effectiveness η. This is defined as

$$\eta = \frac{C_p}{C_{pth}} \ , \tag{2.7}$$

where

$$C_{pth} = 1 - \frac{1}{(AR)^2} \ ,$$

is the ideal pressure recovery coefficient. However, for the design of diffuser we, in general, prefer a shorter length diffuser to the maximum diffuser effectiveness. The pressure recovery in the diffuser becomes

$$\Delta p = p_e - p_i = \frac{1}{2}\rho(\alpha_i \overline{u}_i^2 - \alpha_e \overline{u}_e^2) - \widetilde{p}_l \ , \tag{2.8}$$

where

$$\alpha = \frac{1}{A}\int \left(\frac{u_L}{\overline{u}}\right)^3 dA \ .$$

In Eq. (2.8) α denotes the modified coefficient of kinetic energy due to the velocity fluctuation in the vertical plane, u_L denotes the local streamwise velocity, A denotes the sectional area of the diffuser, and $\widetilde{p}_l$ denotes the pressure losses (*cf.* Chapter 2 in Reference [35]). The value of $\widetilde{p}_l$ is usually large in the diffuser but the influence of the pressure losses can be neglected near the center axis of the diffuser. Therefore, if the streamwise velocity near the center axis is defined as u_c, the pressure recovery is given as

$$\Delta p \approx \frac{1}{2}\rho({u_{ci}}^2 - {u_{ce}}^2) \ . \tag{2.9}$$

If Eq. (2.9) is introduced into Eq. (2.6) and $\overline{u}$ is replaced by u_c, we obtain the local pressure recovery coefficient C_{p_L} written as

$$C_{p_L} = \frac{1}{2}\rho(u_{ci}^2 - u_{ce}^2)/\frac{1}{2}\rho u_{ci}^2 \ . \tag{2.10}$$

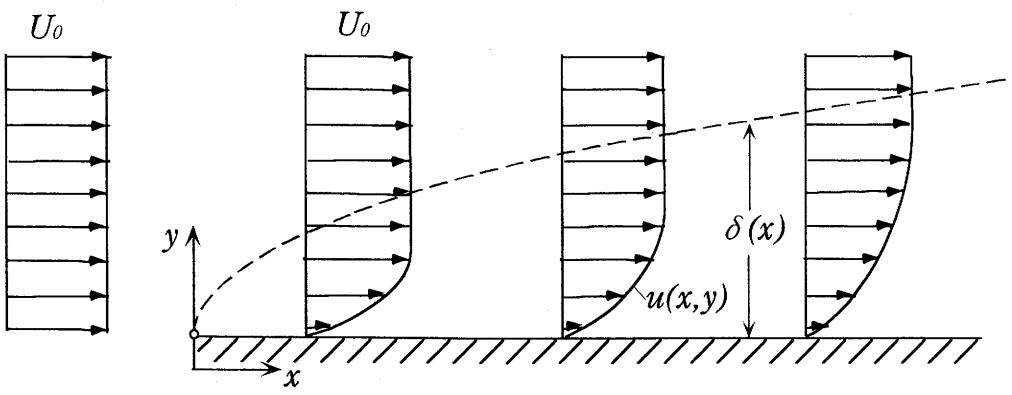

Figure 2.1 Image of boundary layer along a flat plate at zero incidence.

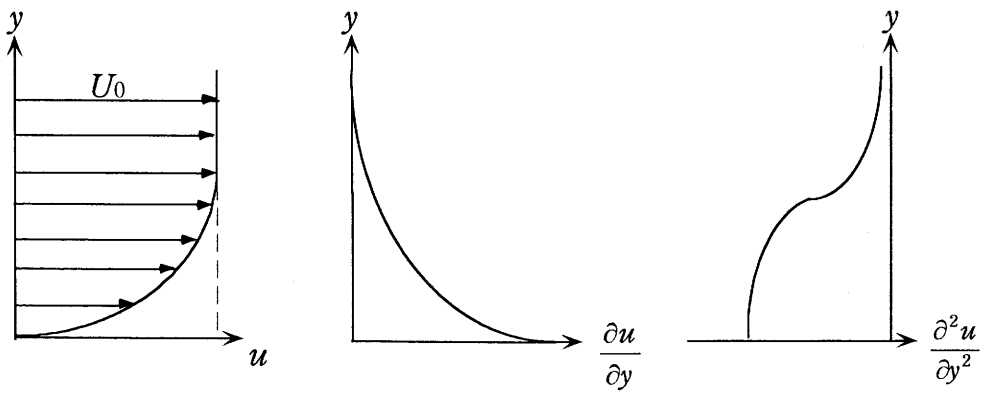

Figure 2.2 Velocity profile in a boundary layer with pressure decrease.

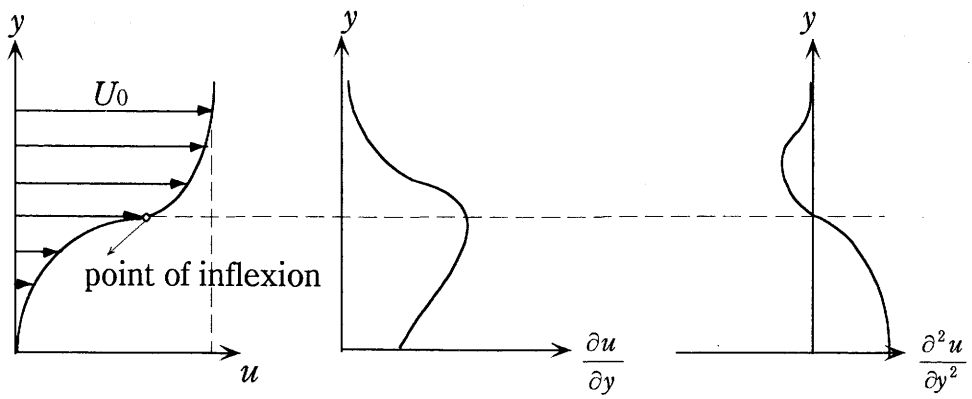

Figure 2.3 Velocity profile in a boundary layer with pressure increase.

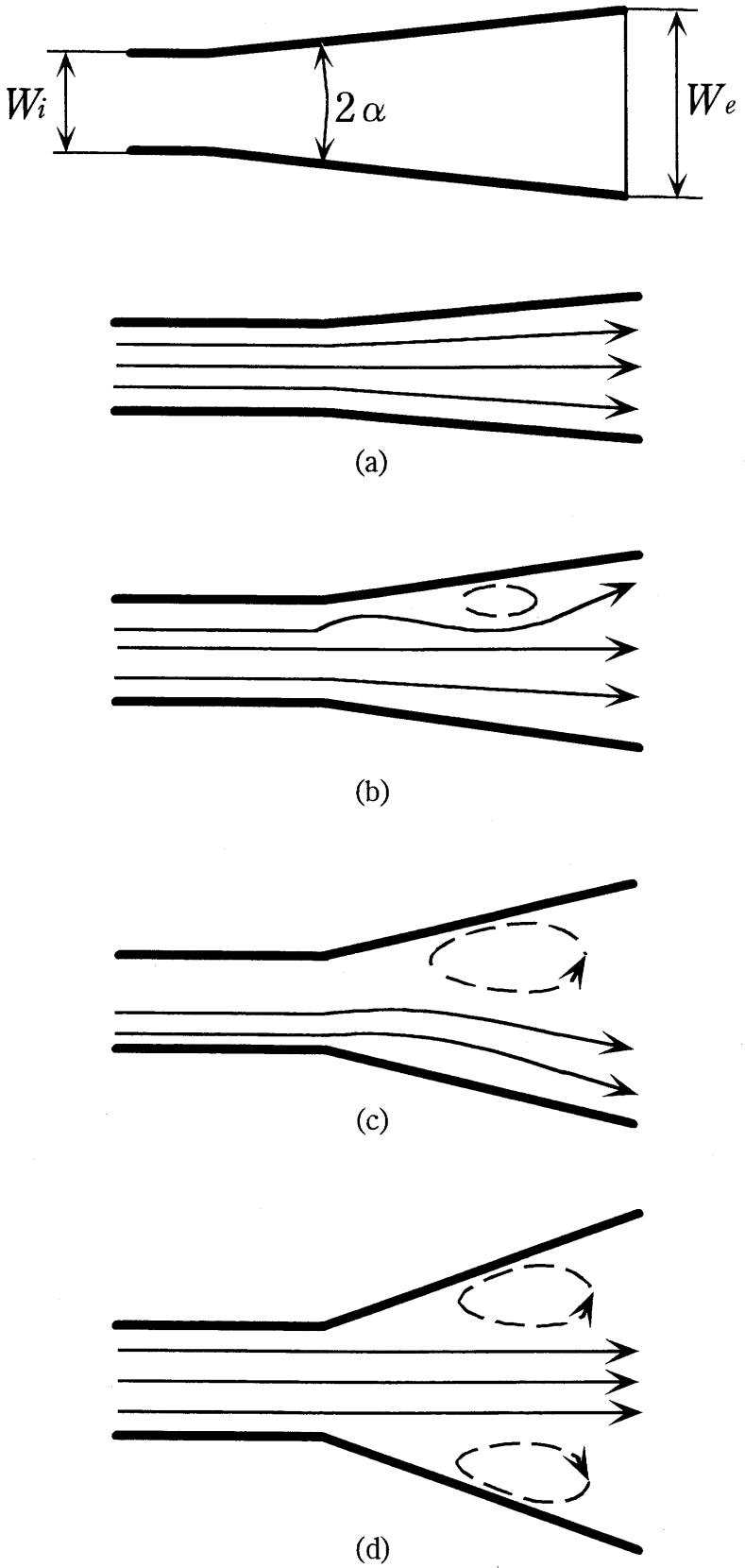

Figure 2.4 Flow in a diffuser with rectangular cross-section.

3. EXPERIMENTAL APPARATUS

3.1 Wind Tunnel

The experiments were conducted using a low speed wind tunnel. The schematic diagram and the whole view of the experimental facility are shown in Figs. 3.1 and 3.2, respectively. The wind tunnel consists of a driving section, rectification section, and test section. Low turbulence flow entering the test section was insured by conditioning the flow in the rectification section which was placed upstream of the test section. The wind tunnel was driven by an electric blower (model SFJ-304-IV-I). The flow leaving the blower entered a chamber with screens and a honeycomb. From the diffuser, the flow entered the honeycomb, passed through two fine-meshed screens, and entered the nozzle. The blower insured that the flow rate was steady and that the freestream velocity varied from 0 to 13 m/s with a freestream turbulence intensity of ± 1.5 percent. The test section inlet dimensions were 250×120 mm (W×H). The test section had the function of variable diffuser which could adjust the divergence angle α between 0 and 45 degrees. A detailed diagram of the test section is shown in Fig. 3.2. The jet flow was delivered through a needle valve and an electric valve (model 2AF5-10) after accumulating the air into a tank by using a compressor. A rotameter (model J-2693) was placed at the downstream of the metering valve. The magnitude of the jet flow rate was characterized by the jet-to-freestream velocity ratio VR $(=V_j/U_0)$. Figure 3.3 shows the configuration of jets and the coordinate system used to describe the flow field. The origins of coordinate X, Y, and Z were defined as the location of the jet orifice, the lower wall, and the left wall of the test section (viewed from upstream), respectively. Three jet orifices were placed at the upstream of the divergent lower wall and were configured on the right-hand side of the lower wall in the test section (viewed from upstream). The jets were skewed with respect to the freestream direction (0 degrees being downstream) and were pitched to the lower wall. The jet skew angle and the pitch angle were denoted as

θ and ϕ, respectively. In this study, the jet skew angle was set at 90 degrees (θ =90 degrees). The jet pitch angle and the jet orifice diameter could be changed by replacing the jet orifice unit shown in Fig. 3.4.

3.2 Laboratory Computer

Data acquisition and experiment control were accomplished using a SORD SRV4100-500 computer with an i486DX4 processor and had 20 MB of memory. The system included four interface boards connected to the ISA-Bus and VL-Bus which were used to sample the data and control the experimental instruments. The interface boards were a digital-to-analog converter (D/A), an analog-to-digital converter (A/D), and a stepping motor control unit. Both the A/D and D/A converters had 12-bit resolution. The A/D converter was utilized in the hot wire data and the differential pressure data acquisition. The D/A converter was utilized in the control of an electric valve.

3.3 Velocity Measurement Instruments

3.3.1 X-Array Hot Wire [39, 40]

The velocity field was measured using an X-array hot wire probe. A schematic of the X-array probe is shown in Fig. 3.5. This probe consists of two constant temperature anemometer sensors positioned nominally at 45 degrees to the streamwise direction and 90 degrees to each other. The probe was a Model 0252R-T5 with two tungsten wires 5μm in diameter and four support needles. The probe tip was rotated into the *U-V*, *U-W* planes in order to obtain three-dimensional velocity. Each of the two wires was connected to a Model 1010 Constant Temperature Anemometer bridge operating with an overheat ratio of 1.5.

A calibration technique used to find the calibration curves of output voltage versus velocity was performed by setting the probe into a freestream. The velocity

response was determined for nine velocities and a modified King's law was used to express the relationship between the fluid velocity and the output voltage of a hot wire anemometer. With an inclined hot wire the magnitude of the convection heat transfer from the wire is less than that with a hot wire set vertically in the flow, because the effective velocity component which has a relation to the convection heat transfer decreases. To understand how a heated sensor can be used to detect the angle between the hot wire sensor and the velocity vector, the velocity vector is separated into two components, a component normal to the wire and a component parallel to the wire. Although, both pass over the wire, the normal component is mainly responsible for sensor cooling. In other words, for a hot wire inclined at ($\pi/2+\theta$) degrees in the flow (see Fig. 3.6) the flow component along a hot wire can be assumed to be negligible and as a result the effective cooling velocity V_{eff} is written as

$$V_{eff} = v\cos\theta \ , \tag{3.1}$$

where v is the magnitude of the velocity vector and θ is defined as the angle between the velocity vector and the component normal to the wire. This relationship (3.1) is called the cosine law of a hot wire. The radiation heat transfer rate from the sensor to the surroundings is usually neglected, because the radiation heat loss is much lower than losses by convection to the fluid or conduction to the support needles for most applications. For a hot wire anemometer, King's law is usually written as

$$E^2 = a + bV_{eff}^n \ , \tag{3.2}$$

where E is the anemometer output voltage, V_{eff} is the effective cooling velocity, and a, b, and n are King's law constants determined through a least squares fit.

The mean velocity components, U and V, were measured by setting a hot wire in the U-V plane (see Fig. 3.7(a)). Measurements in the U-W plane were used to obtain the mean velocity components W after a hot wire probe was rotated at 90 degrees around the probe axis (see Fig. 3.7(b)). For the case shown in Fig. 3.7(a), from Eq. (3.1) and Fig. 3.7(c) the effective cooling velocity of each hot wire is written as

$$\left.\begin{aligned} V_{effa1}^2 &= (v\cos\theta_1)^2 = v_{a2}^2 + W^2, \\ V_{effa2}^2 &= (v\cos\theta_2)^2 = v_{a1}^2 + W^2, \end{aligned}\right\} \tag{3.3}$$

where V_{effa1} and V_{effa2} indicate the effective cooling velocity of the No.1 hot wire and the No.2 hot wire, respectively. Furthermore, v_{a1} and v_{a2} indicate the velocity component along the No.1 and No.2 hot wire of Fig. 3.7(a) or 3.7(c), respectively. The mean velocity components, U and V, become

$$\left.\begin{aligned} U &= (v_{a1} + v_{a2})\cos 45°, \\ V &= (v_{a1} - v_{a2})\cos 45°. \end{aligned}\right\} \tag{3.4}$$

Therefore, v_{a1} and v_{a2} are written as

$$\left.\begin{aligned} v_{a1} &= \frac{U-V}{\sqrt{2}}, \\ v_{a2} &= \frac{U+V}{\sqrt{2}}. \end{aligned}\right\} \tag{3.5}$$

Substituting Eq. (3.5) into Eq. (3.3) we obtain the relationship between the effective cooling velocity and the mean velocity components, U, V and W:

$$\left.\begin{aligned} V_{effa1}^2 &= \frac{(U+V)^2}{2} + W^2, \\ V_{effa2}^2 &= \frac{(U-V)^2}{2} + W^2. \end{aligned}\right\} \tag{3.6}$$

Thus

$$V_{effa1} = \sqrt{\frac{(U+V)^2}{2} + W^2} = \frac{U}{\sqrt{2}}\sqrt{\left(1+\frac{V}{U}\right)^2 + 2\left(\frac{W}{U}\right)^2}\ . \tag{3.7}$$

Hence, if the mean velocity components, V and W, are very small compared with the component U, we must have

$$\left(\frac{V}{U}\right)^2,\ \left(\frac{W}{U}\right)^2 \to 0\ . \tag{3.8}$$

Taking Eq. (3.8) into account, we can obtain in the following modified form:

$$V_{effa1} = \frac{U}{\sqrt{2}}\sqrt{1+2\frac{V}{U}} = \frac{U}{\sqrt{2}}\left(1+\frac{V}{U}\right) = \frac{U+V}{\sqrt{2}}\ , \tag{3.9}$$

and similarly we obtain

$$V_{effa2} = \frac{U-V}{\sqrt{2}}\ . \tag{3.10}$$

Finally, for the configuration of two hot wires in Fig. 3.7(a), the relationship between the mean velocity components and the effective cooling velocity is described as follows:

$$\left.\begin{aligned} U &= \frac{1}{\sqrt{2}}(V_{effa1} + V_{effa2}), \\ V &= \frac{1}{\sqrt{2}}(V_{effa1} - V_{effa2}). \end{aligned}\right\} \tag{3.11}$$

For the configuration of two hot wires in Fig. 3.7(b), Eq. (3.3) is modified in the following form:

$$\left.\begin{aligned} V_{effb1}^2 &= v_{b2}^2 + V^2, \\ V_{effb2}^2 &= v_{b1}^2 + V^2. \end{aligned}\right\} \tag{3.12}$$

Thus

$$\left.\begin{aligned} U &= \frac{1}{\sqrt{2}}(V_{effb1} + V_{effb2}), \\ W &= \frac{1}{\sqrt{2}}(V_{effb1} - V_{effb2}). \end{aligned}\right\} \tag{3.13}$$

3.3.2 Streamwise Vorticity

It is necessary to know an accurate vorticity field in order to understand the structure of the vortices and to compute their strength. In this study, secondary velocity measurements were carried out to determine the streamwise vorticity at each data point. The streamwise vorticity is given as

$$\omega_x = \left(\frac{\partial W}{\partial Y} - \frac{\partial V}{\partial Z}\right). \tag{3.14}$$

The two terms on the right-hand side in Eq. (3.14) are discretized in space using second-order central finite-difference approximation. W_{n+1} or W_{n-1} is written, by using the Taylor series around the point a_n (see Fig. 3.8), as

$$W_{n+1} = W(Y + \Delta Y) = W_n + \Delta Y W_n' + \frac{1}{2}(\Delta Y)^2 W_n'' + \cdots, \tag{3.15}$$

$$W_{n-1} = W(Y - \Delta Y) = W_n - \Delta Y W_n' + \frac{1}{2}(\Delta Y)^2 W_n'' - \cdots, \tag{3.16}$$

hence each term of Eq. (3.14) can be written as

$$\frac{\partial W}{\partial Y} = W_n' \approx \frac{W_{n+1} - W_{n-1}}{2\Delta Y}, \tag{3.17}$$

and

$$\frac{\partial V}{\partial Z} = V_n' \approx \frac{V_{n+1} - V_{n-1}}{2\Delta Z}\ , \tag{3.18}$$

where ΔY and ΔZ denote a uniform mesh spacing in the normal direction and the spanwise direction, respectively. One-side difference is used at the boundary in the computational domain and $W_{n\pm2}$ or $W_{n\pm1}$ is written, by using the Taylor series around the point a_n (see Fig. 3.9), as

$$W_{n\pm2} = W_n \pm 2\Delta Y W_n' + \frac{(\pm 2\Delta Y)^2}{2!} W_n'' + \frac{(\pm 2\Delta Y)^3}{3!} W_n''' + \cdots\ , \tag{3.19}$$

$$W_{n\pm1} = W_n \pm \Delta Y W_n' + \frac{(\pm \Delta Y)^2}{2!} W_n'' + \frac{(\pm \Delta Y)^3}{3!} W_n''' + \cdots\ , \tag{3.20}$$

hence each term of Eq. (3.14) at the boundary region can be written as

$$\frac{\partial W}{\partial Y} = W_n' \approx \frac{-3W_n + 4W_{n+1} - W_{n+2}}{2\Delta Y} \quad \text{(forward-difference)}, \tag{3.21}$$

$$\frac{\partial W}{\partial Y} = W_n' \approx \frac{+3W_n - 4W_{n-1} + W_{n-2}}{2\Delta Y} \quad \text{(backward-difference)}, \tag{3.22}$$

and

$$\frac{\partial V}{\partial Z} = V_n' \approx \frac{-3V_n + 4V_{n+1} - V_{n+2}}{2\Delta Z} \quad \text{(forward-difference)}, \tag{3.23}$$

$$\frac{\partial V}{\partial Z} = V_n' \approx \frac{+3V_n - 4V_{n-1} + V_{n-2}}{2\Delta Z} \quad \text{(backward-difference)}. \tag{3.24}$$

3.3.3 Single-Wire Probe

Figure 3.10 indicates a single-wire probe which is used in order to measure the streamwise mean velocity in the boundary layer. The single-wire probe was DANTEC Model 9055P0141, which had a single-wire sensor attached to the tips of two support needles, and was calibrated in the freestream near a Pitot tube which was used to measure the freestream velocity of the wind tunnel. The relationship between the output voltage of the single-wire probe and the fluid velocity was determined by using a linearizer Model 1013. The probe had a tip of a tungsten wire 5 μm in diameter. The single-wire was fixed vertically to the freestream.

3.3.4 Hot Wire Anemometer [39, 40]

The Wheatstone bridge is used in many electronic instruments to give an error signal proportional to the difference between a variable signal and a reference signal. Its use in hot wire anemometry is a typical application. The constant temperature anemometer uses a feedback amplifier to automatically maintain the sensor temperature constant. For constant temperature operation the adjustable resistor is set to a higher value than that for a balanced bridge based on the resistance of the unheated probe to prevent the oscillation of the circuit. The bridge voltage is increased to heat the sensor. This increases the sensor resistance and brings the bridge into balance. Any bridge imbalance caused by velocity variations is removed by readjusting the bridge voltage. The resulting bridge voltage is related to the fluid velocity through King's law.

3.3.5 Temperature Measurement Unit

Hot wire measurements required continuous temperature monitoring to make temperature corrections. The freestream temperature measurements for correcting temperature drift were made using a Model 1020 temperature measurement unit and probe. The probe sensor element is glass-plated platinum protected with a stainless steel pipe (see Fig. 3.11).

3.3.6 Three-Axis Automatic Probe Traversing Unit

Probe placement was achieved using a traversing mechanism that provided for automatic streamwise X, spanwise Z, and normal Y positioning and manual probe rotation about an axis parallel to the streamwise direction. Stepping motors (model KP6M2-005), stepping motor drivers (model SMD-301), and a stepping motor control unit (model SMC-3(PC)) were used to control the probe positioning. By using this method it was possible to control the probe placement at intervals of

0.1 mm in each direction.

3.4 Vortex Generator Jet Device

The vortex generator jet device is shown in Fig. 3.12. It consists of an electric motor (model M6100-201K) and a rotor disk. There is a hole 10 mm in diameter drilled into the rotor disk. The vortex generator can select steady flow or the pulsed flow jets. Pulsed flow was produced by passing or shutting off the secondary air from a compressor using the rotor which was driven by the electric motor. Steady jet flow was maintained if the rotor kept up the position passing the secondary air freely. In this study, the rotor allowed a pulse rate of up to 23 Hz. The revolutions per minute were measured with a revolution indicator (model 00204) which did not contact with the rotor.

3.5 Pressure Measurement Instruments

Static pressure measurements were made using a differential pressure transducer Model 3051CD which was very sensitive to pressure difference (0.01 mmAq). The pressure value was converted from the output voltage of the differential pressure transducer by a linear calibration fit. Static pressure measurements in the test section were carried out at wall mounted static pressure taps in the downstream (see Fig. 3.13).

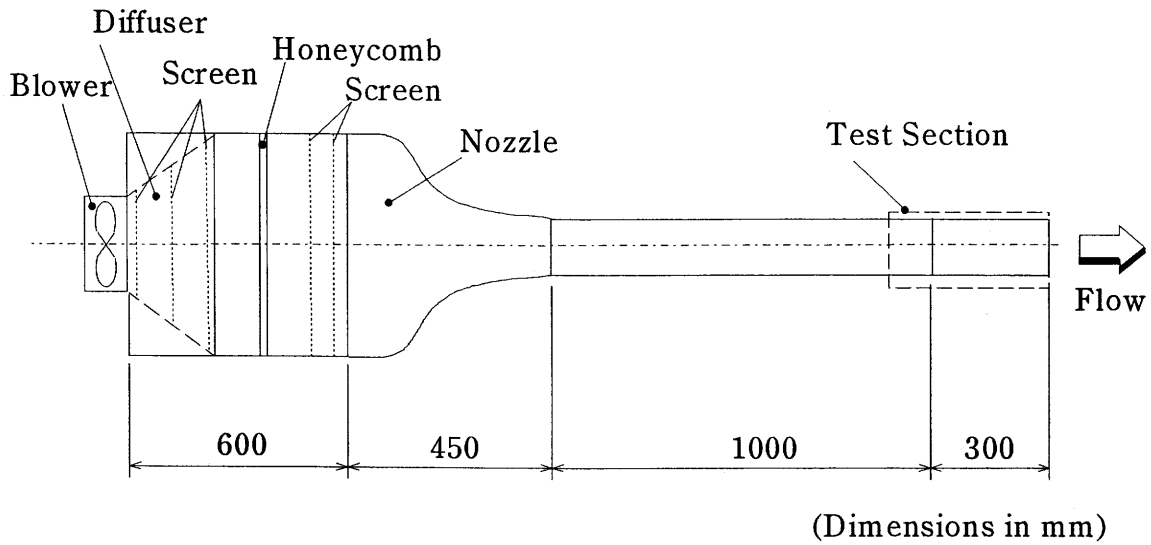

Figure 3.1 Schematic diagram of experimental facility.

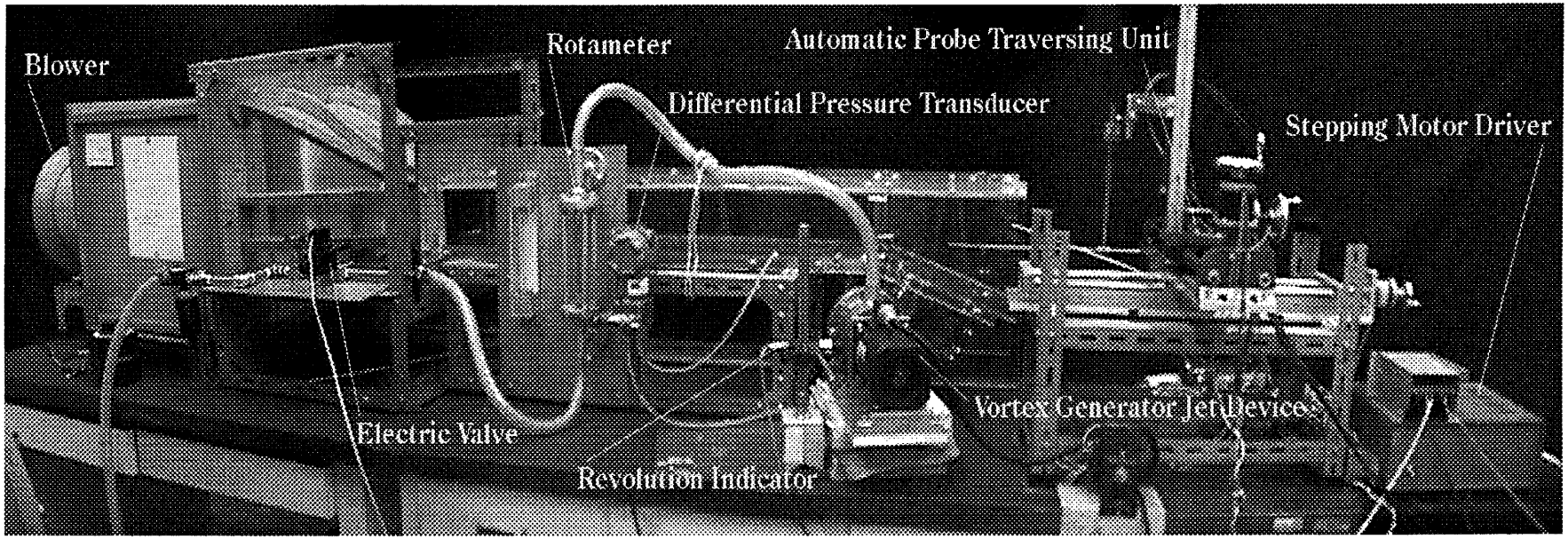

Figure 3.2 Whole view of experimental facility.

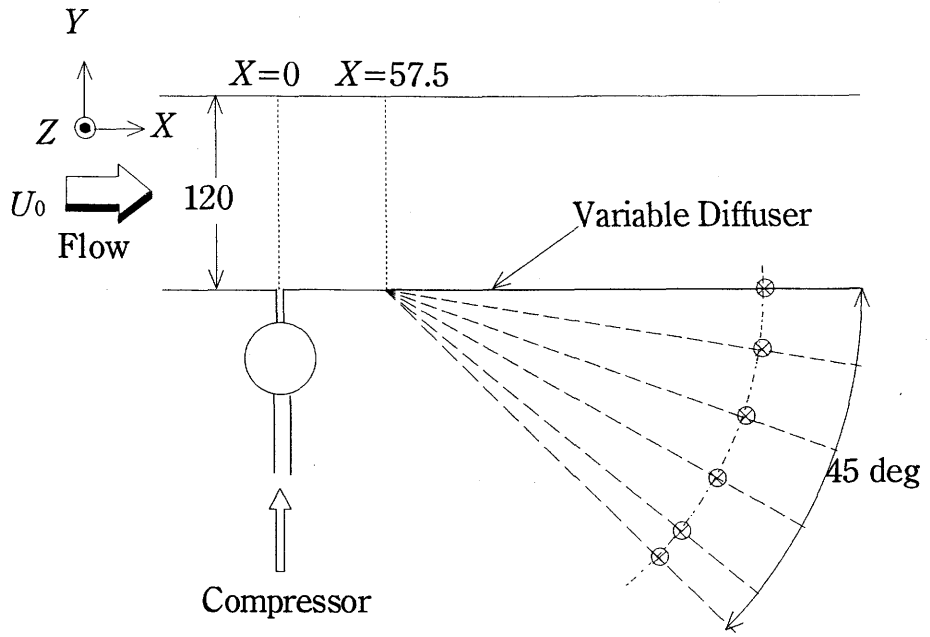

Figure 3.3 Test section geometry.

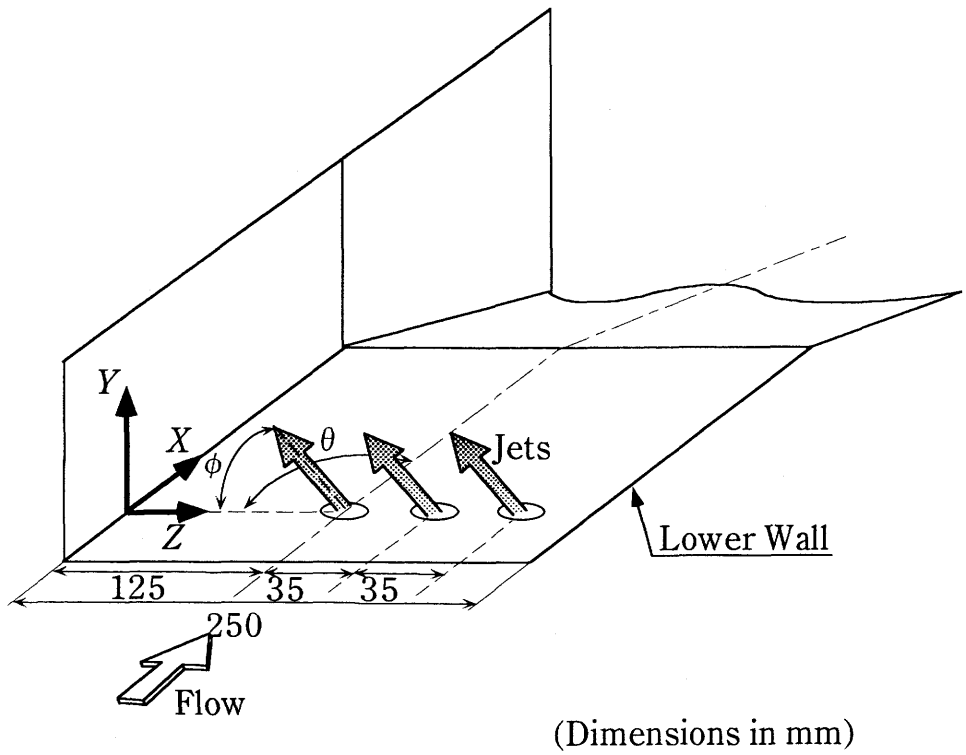

Figure 3.4 Jet configurations in test section.

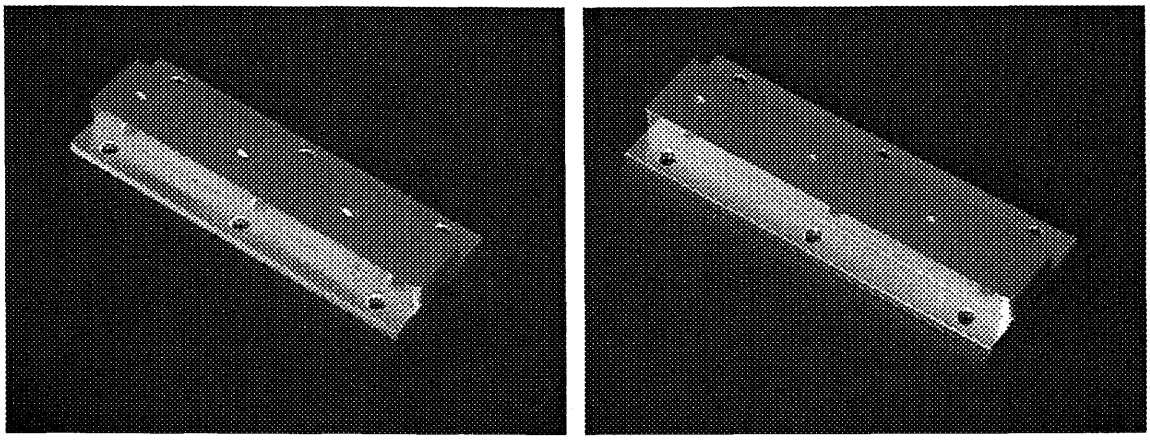

(a) D_j=2 mm, ϕ =30 deg

(b) D_j=2 mm, ϕ =45 deg

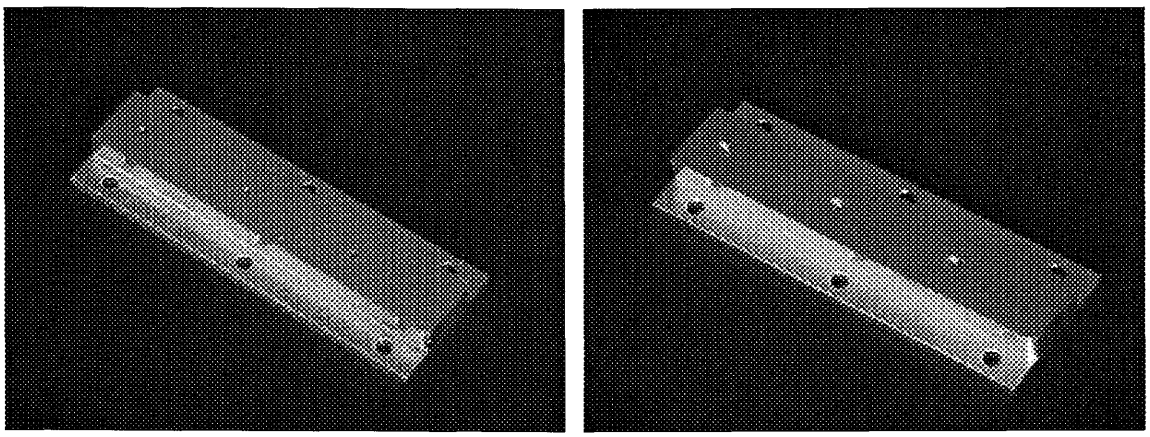

(c) D_j=2 mm, ϕ =60 deg

(d) D_j=3 mm, ϕ =45 deg

Figure 3.5 Jet orifice units.

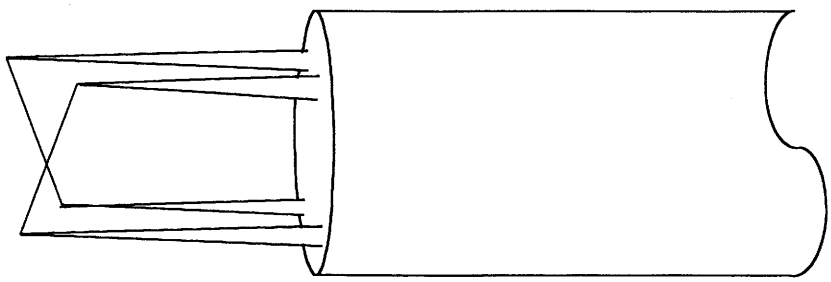

Figure 3.6 X-array hot wire probe.

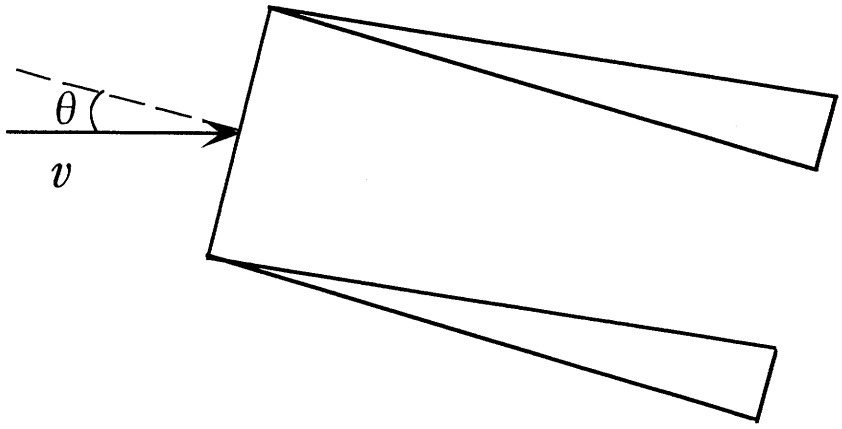

Figure 3.7 Inclined hot wire.

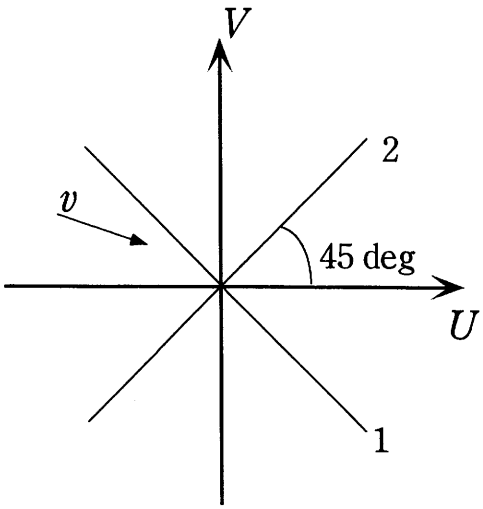

(a) *U-V* plane

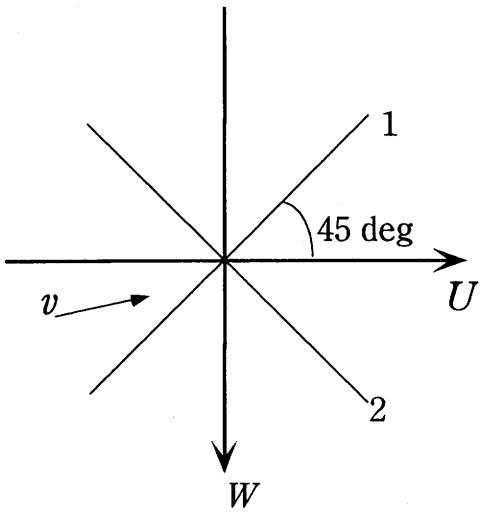

(b) *U-W* plane

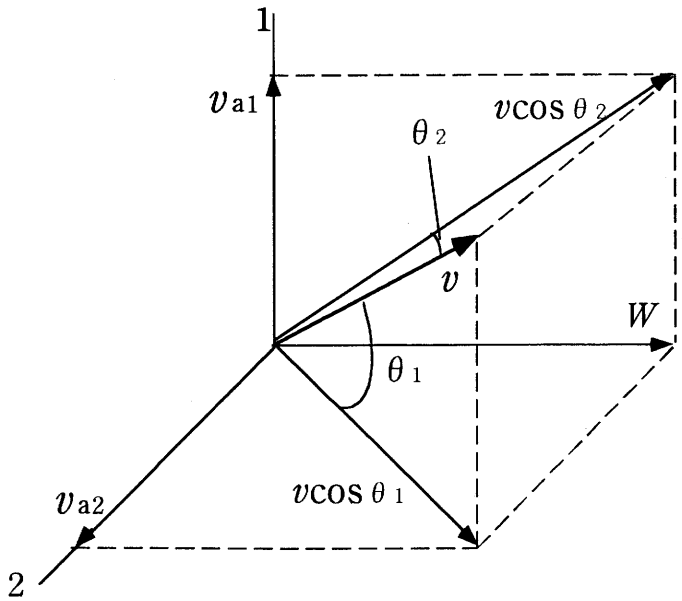

(c) No.1 or No.2 hot wire and velocity vector v

Figure 3.8 Hot wire configuration.

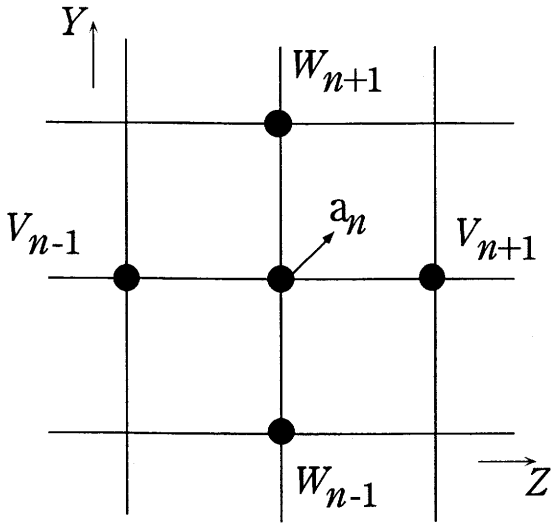

Figure 3.9 Inside of computational domain.

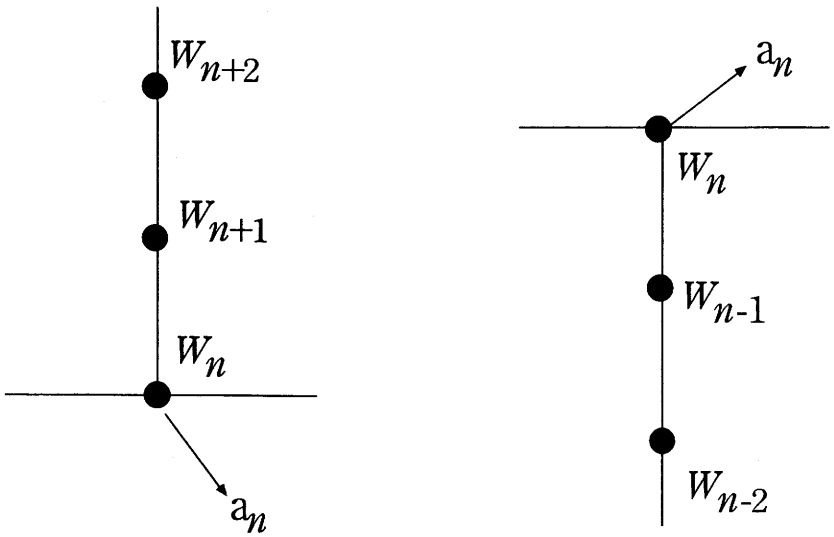

Figure 3.10 Boundary of computational domain.

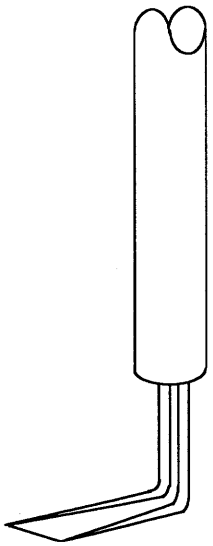

Figure 3.11 Single-wire probe.

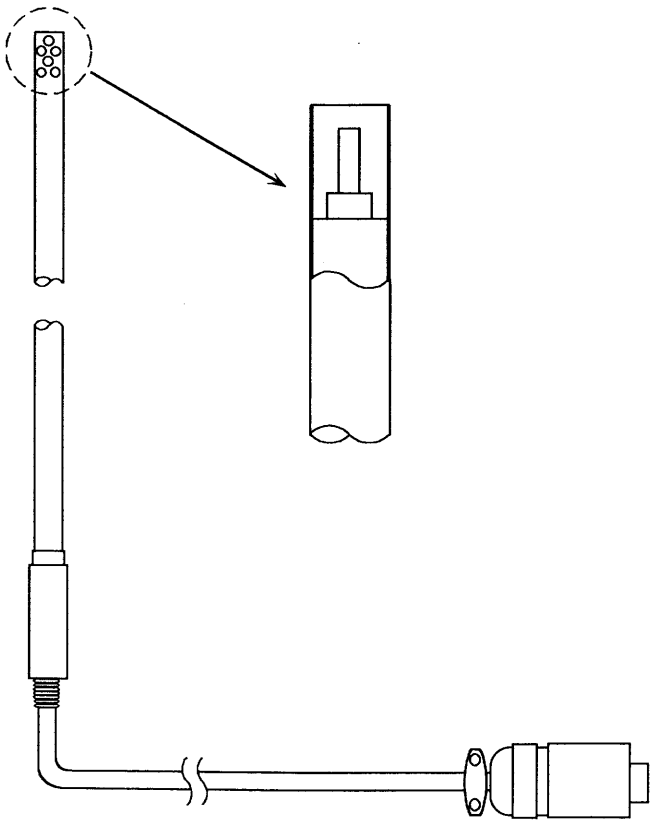

Figure 3.12 Temperature measurement probe.

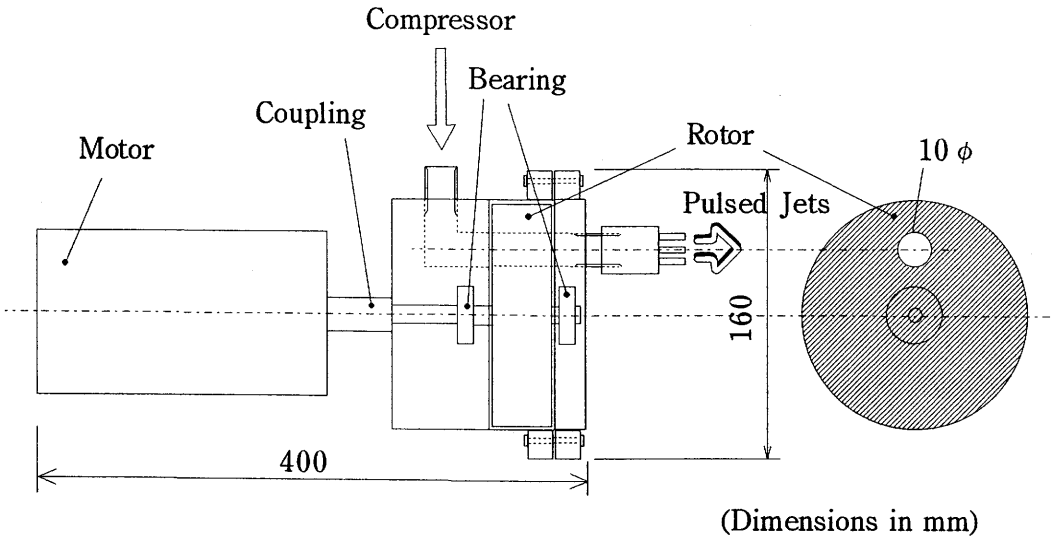

Figure 3.13 Vortex generator jet device.

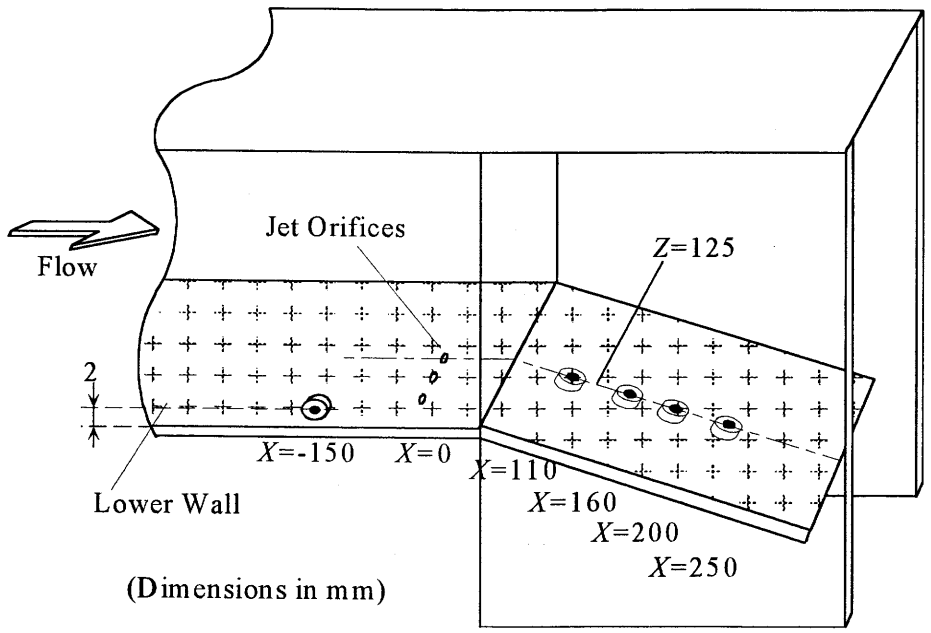

Figure 3.14 Location of static pressure holes in test section.

4. EFFECT OF BOUNDARY LAYER CONDITION ON SEPARATION CONTROL

In general, the boundary layer condition must be known before performing separation control. In this chapter, the effect of the boundary layer condition on separation control is investigated for the vortex generator jet method. It is clarified that it is not necessary to know in advance whether the boundary layer is laminar or turbulent.

4.1 Experimental Method

A detailed diagram of the test section is shown in Fig. 3.2. In this experiment, two freestream velocities U_0=6.5 and 11.1 m/s were chosen and the jet orifice was 2 mm in diameter. The jets were skewed at 90 degrees to the freestream direction and pitched at 45 degrees to the lower wall. A tripping wire which was 1.6 mm in diameter was set at X=-100 mm (X=0 indicates the location of issuing jets). The diameter of the tripping wire D_t which can cause a transition from laminar to turbulent flow was so determined as to satisfy $D_t \geqq 900\,\nu/U_0$ (*cf.* Chapter 5 in Reference [35]), where U_0 is the freestream velocity and ν is the kinematic viscosity. The velocity measurements in the boundary layer were carried out at 0.2 mm intervals in the normal direction from the position which was 0.3 mm from the lower wall of the test section (see Fig. 3.2). The boundary layer probe shown in Fig. 3.8 was used. The surface tuft method was adopted as a flow visualization technique. In this study, tufts were made of light and thin paper. In this experiment, the diffuser's divergence angle was set at 20 degrees (α =20 degrees).

4.2 Results and Discussion

4.2.1 Transition with a Tripping Wire

Figure 4.1 shows the streamwise velocity profiles with a tripping wire in comparison with those without a tripping wire for U_0=6.5 m/s. In Fig. 4.1, the velocity profiles without a tripping wire are comparable with the Blasius solution. The shape factor is calculated from Eqs. (2.3), (2.4), and (2.5). Equations (2.3) and (2.4) are integrated along the distance Y from the lower wall from Y=0 (lower wall) to $Y=\delta$. The upper limit of integration of Eqs. (2.3) and (2.4) could here be replaced by $Y=\delta$, which is defined as the distance of U/U_0=0.99. The velocity profile in the boundary layer is assumed to be the fourth (for the case without a tripping wire) or eighth (for the case with a tripping wire) power polynomial of the distance Y from the lower wall. For the cases of Figs. 4.1(a) and 4.1(b) the shape factor indicates H_{12}=2.27 and H_{12}=2.13, respectively. On the other hand, for the case with a tripping wire in Figs. 4.1(a) and 4.1(b) the shape factor indicates H_{12}=1.49 and H_{12}=1.77, respectively. Hence it is concluded that the boundary layer condition has been changed from laminar to turbulent flow by a tripping wire.

Figure 4.2 shows the flow visualization results in the divergent portion of the test section for an unforced (non-issuing jets) case. Figure 4.3 shows the flow visualization results when jets are issuing to suppress the flow separation. The air flows from left to right in these figures. From Fig. 4.2, it is seen that the separation point moves downstream by a tripping wire because the transition from laminar to turbulent boundary layer occurs. On the other hand, for the case of issuing jets it is clear that the control effect is not influenced by the boundary layer condition (see Fig. 4.3). This indicates that longitudinal vortices generated by the interaction between the jets and the freestream is dominant in comparison with the disturbance due to a tripping wire.

4.2.2 Transition without a Tripping Wire

Figure 4.4 shows the streamwise velocity profiles for the case without a tripping wire. This profile gives $H_{12}=1.89$. The boundary layer thickness δ for a flat plate at zero incidence is expressed as

$$\delta = 5.0\left(\frac{\nu x}{U_0}\right)^{1/2} = \frac{5x}{\sqrt{R_{ex}}}, \tag{4.1}$$

where

$$R_{ex} = \frac{U_0 x}{\nu},$$

and x is the length from the leading edge of the plate. According to Eq. (4.1), the boundary layer thickness on a flat plate increases in proportion to $\sqrt{x}$. The boundary layer on a plate is always laminar near the leading edge and becomes turbulent further downstream. The smallest Reynolds number with which transition occurs on a flat plate is the critical Reynolds number, as determined by

$$R_{ex,crit} = \left(\frac{U_0 x}{\nu}\right)_{crit} = 3.2\times10^5 . \tag{4.2}$$

In the case of a plate, the value $R_{ex,crit}=3.2\times10^5$ should be regarded as the lower limit to produce the transition from laminar to turbulent flow. For the case with a tripping wire (see Fig. 4.1(a)), letting the approximation curve fit the velocity profiles, we have $\delta=4.94$. The boundary layer thickness is defined as the location based on $U/U_0=0.99$. For the cases of $U_0=6.5$ and 11.1 m/s, it will be seen from Eqs. (4.1) and (4.2) that the Reynolds number is $R_{ex}=1.8\times10^5$ and $R_{ex}=6.9\times10^5$, respectively. This indicates that the boundary layer becomes turbulent for $U_0=11.1$ m/s in the case without a tripping wire. Figure 4.5 shows the flow visualization results for $U_0=11.1$ m/s. A difference between the two cases with and without a tripping wire does not appear.

4.3 Conclusions

Summarizing the above results on separation control using vortex generator

jets, the following conclusions were drawn:

1. In the present wind tunnel, transition from laminar to turbulent boundary layer takes place while increasing the freestream velocity.

2. A tripping wire changes the boundary layer condition from laminar to turbulent flow and the transition causes the separation point to move downstream.

3. In the vortex generator jet method, whether the boundary layer is laminar or turbulent has no influence on separation control.

4. For the vortex generator jet method, separation control can be achieved without surveying the boundary layer condition before control.

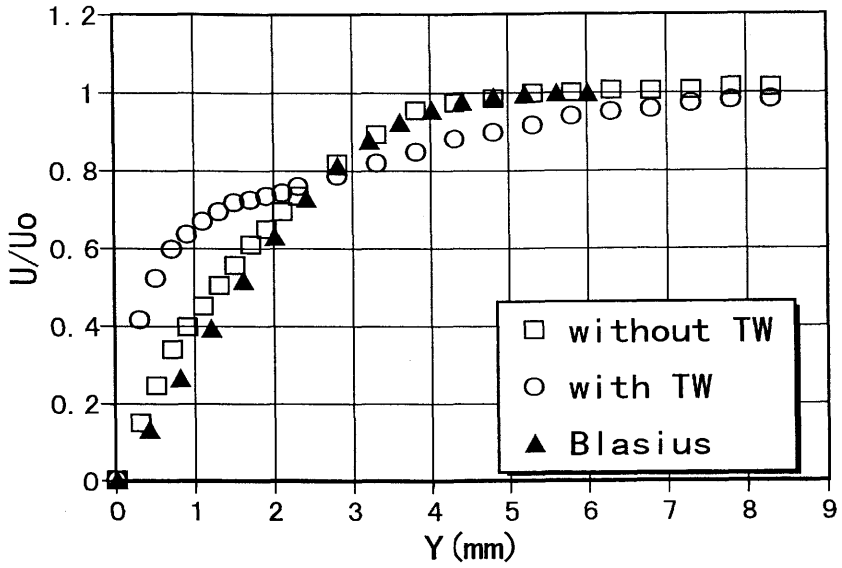

(a) X=0, Z=110 mm

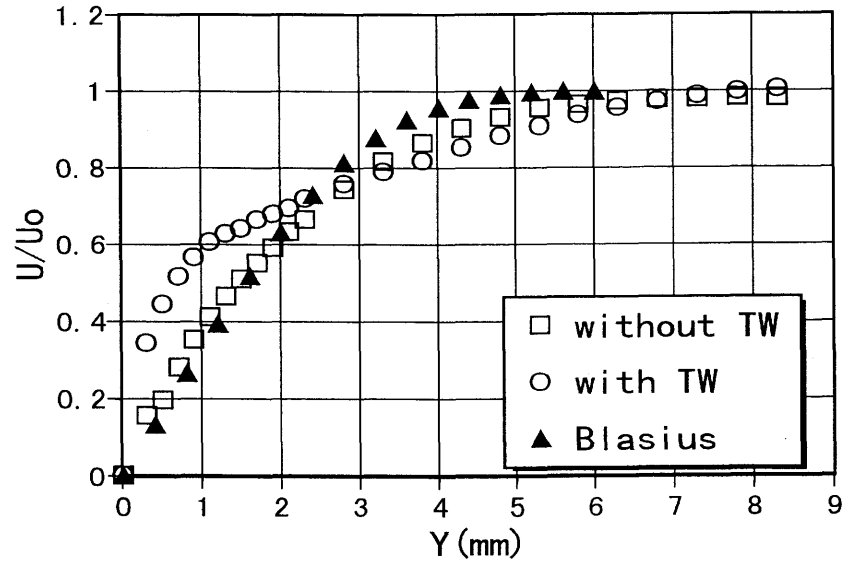

(b) X=0, Z=140 mm

Figure 4.1 Streamwise velocity profiles with and without tripping wire (TW) (U_0=6.5 m/s, unforced).

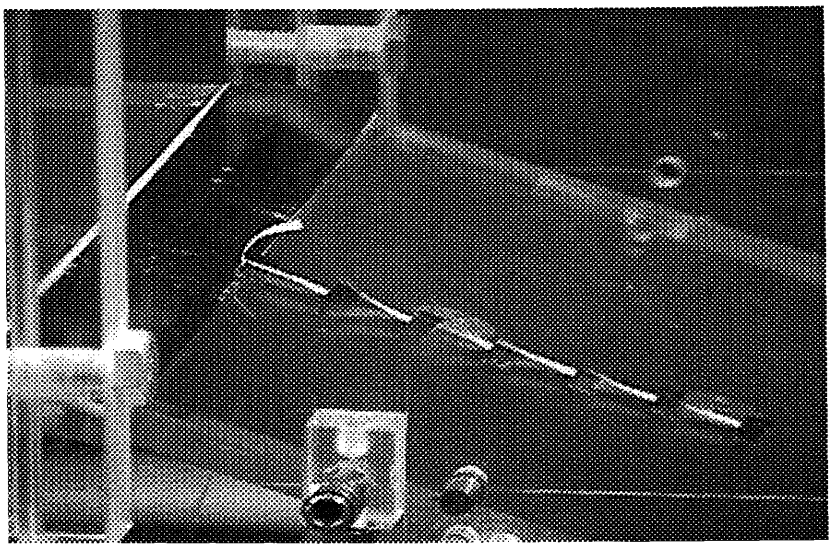

(a) Without tripping wire

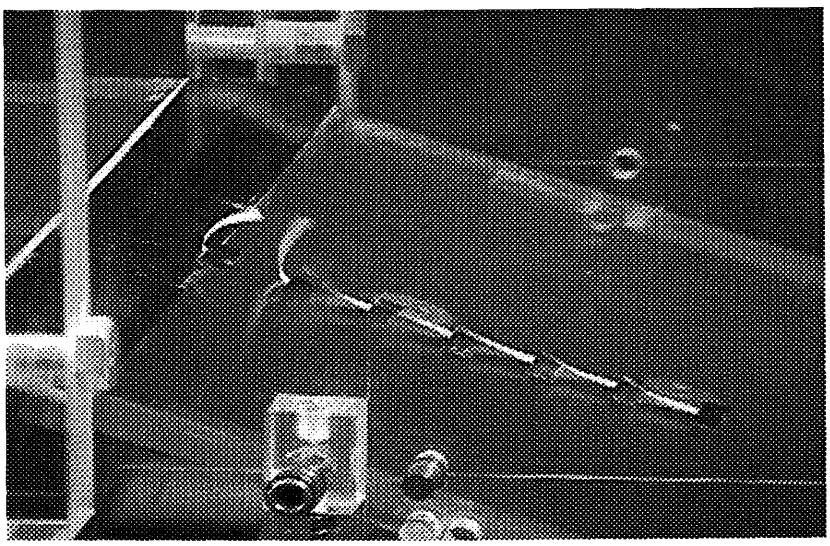

(b) With tripping wire

Figure 4.2 Surface flow in divergent portion of the test section (U_0=6.5 m/s, unforced).

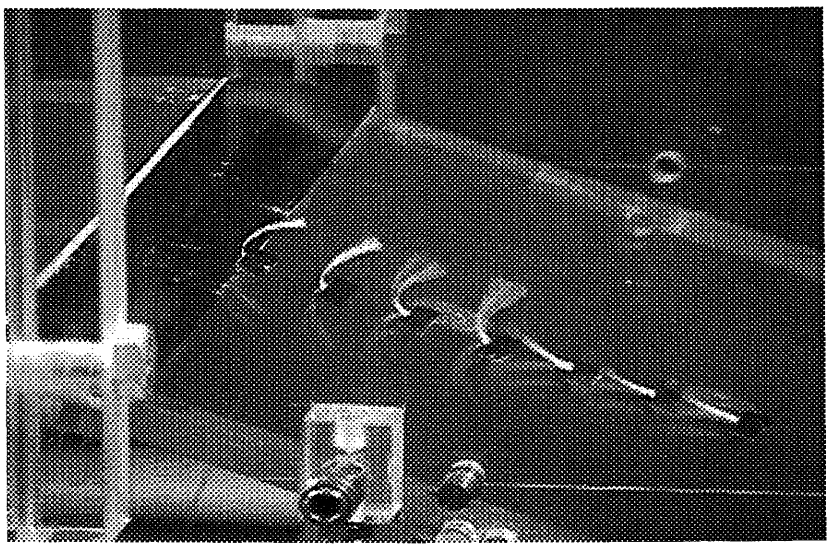

(a) Without tripping wire

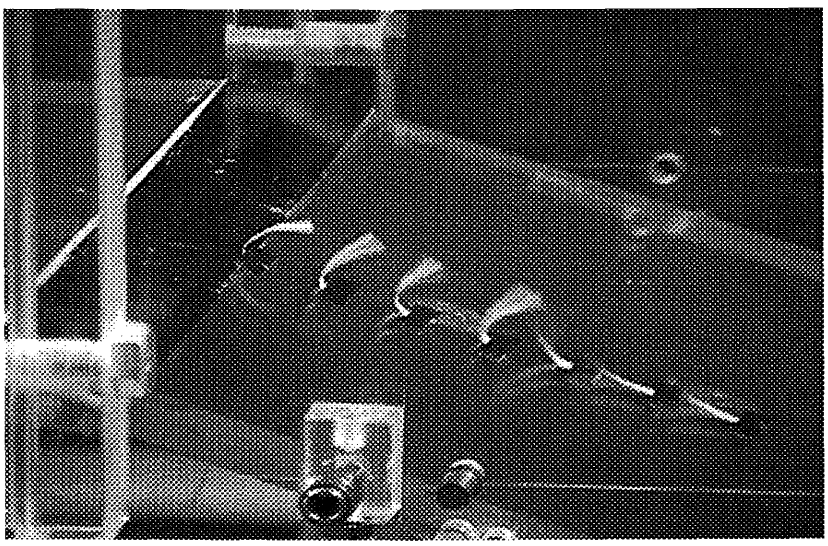

(b) With tripping wire

Figure 4.3 Surface flow in divergent portion of the test section (U_0=6.5 m/s, VR=6.5).

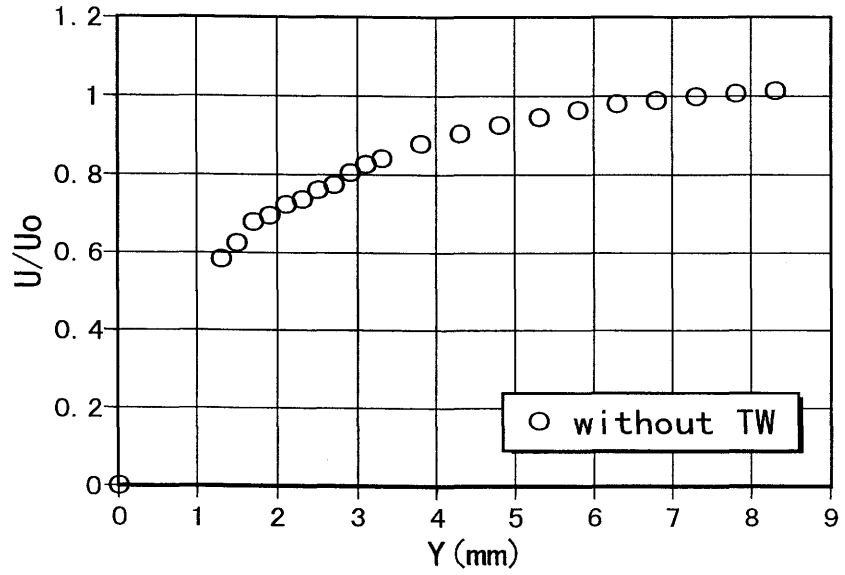

Figure 4.4 Streamwise velocity profile without tripping wire (TW) at $X=0$, $Z=140$ mm ($U_0=11.1$ m/s, unforced).

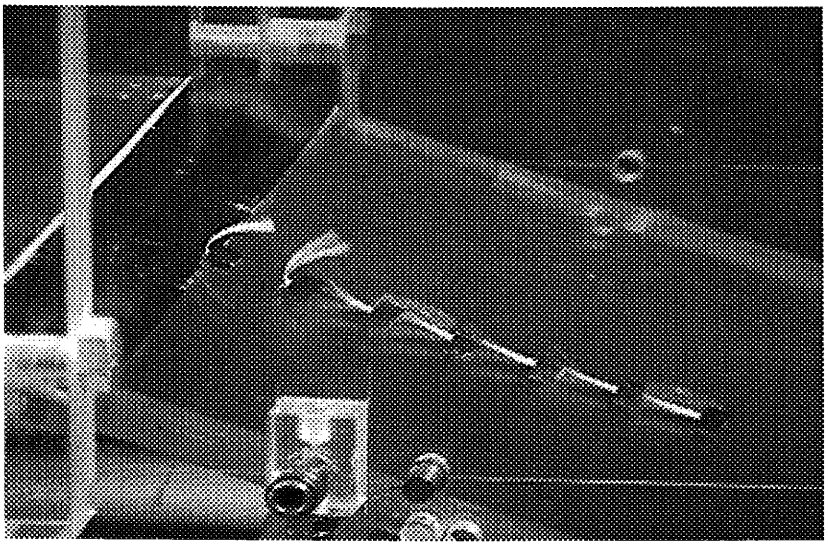

(a) Without tripping wire

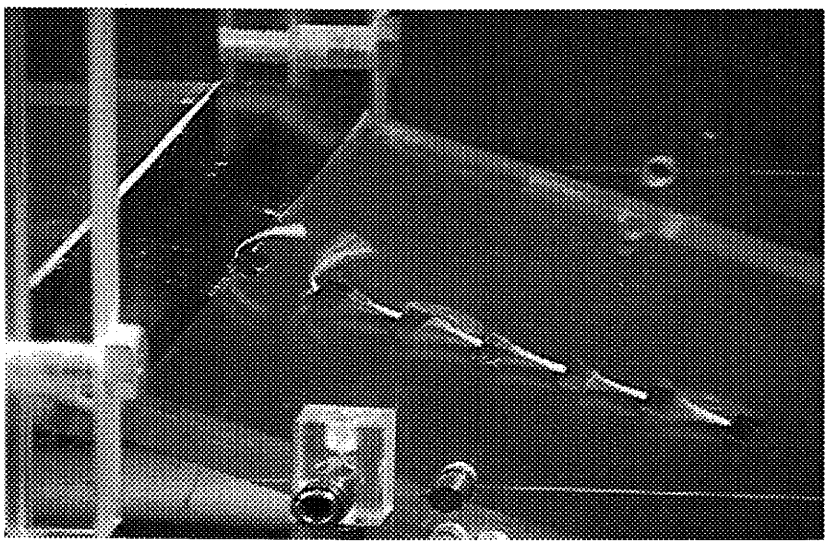

(b) With tripping wire

Figure 4.5 Surface flow in divergent portion of the test section (U_0=11.1 m/s, unforced).

5. MECHANISM OF ACTIVE BOUNDARY LAYER CONTROL

It is important to understand the mechanism of active separation control in the actual use of vortex generator jets. In this chapter, in order to investigate the mechanism for suppressing flow separation, experiments are described which make a comparison between the two roles of steady and pulsed jets in generating longitudinal vortices. Mean velocity profiles, the downstream development of longitudinal vortices, secondary flow vectors, and contours of streamwise vorticity will be presented for the purpose of understanding the mechanism for preventing flow separation.

5.1 Experimental Method

A schematic diagram of the wind tunnel used is shown in Fig. 3.1. In this experiment, two freestream velocities U_0=6.5 and 11.1 m/s were chosen. The test section was configured with a lower wall which had a divergence angle of 20 or 30 degrees. A detailed diagram of the test section is shown in Fig. 3.2. The magnitude of the jet flow rate was characterized by the jet-to-freestream velocity ratio *VR*. The vortex generator jet device is shown in Fig. 3.12. The pulse rate was allowed up to 23 Hz. The configuration of jets and the coordinate system used to describe the flowfield are shown in Fig. 3.3. Three jets 2 mm in diameter were placed at the upstream of the divergent lower wall and their orifices were configured on the right-hand side of the lower wall in the test section (viewed from upstream). The jets in this study were skewed at 90 degrees to the freestream direction and pitched at 45 degrees to the lower wall.

Velocity profiles in the test section were obtained using an X-array hot wire probe. The hot wire probe was supported by a three-axis computer-controlled

traverse unit. Streamwise velocity profiles were measured at $Z=110$ mm to avoid the effect of jet orifices. The downstream locations were chosen at $X=40$, 70, 110 mm. The velocity measurements in a Y-Z plane were carried out at equal spaces of 5 mm, in the X and Y directions.

5.2 Results and Discussion

5.2.1 Waveform of Pulsed Jets

Figure 5.1 shows the waveform of the pulsed jets in this study. The pulsed jet generator has a tendency to broaden the peak region of the waveform for both cases of increasing the jet flow rate (or equally increasing jet speed) and the lowering of a frequency. The feature of the frequency-lowering case results from the increased passage time of the secondary air due to decreased rotor speed.

5.2.2 Flow Visualization Results

The surface tuft method was used as a diagnostic technique to observe the effect of vortex generator jets on separated flow. Tufts were put on the lower wall of the test section at $Z=125$ and 140 mm. Figure 5.2 shows the surface flow in the divergent portion of the test section and the air flows from left to right. Figures 5.2(a), 5.2(b), and 5.2(c) indicate an unforced (non-issuing jets) case, the pulsed jet case, and the steady jet case, respectively. It is seen that steady or pulsed vortex generator jets can delay flow separation in comparison with the unforced case.

5.2.3 Streamwise Velocity Measurements

Figures 5.3 and 5.4 show the streamwise velocity profiles in the test section. The data are presented for a lower wall divergence of 20 degrees. The profiles for the unforced case in these figures indicate a boundary layer separation in the divergent portion of the test section. For U_0=6.5 and 11.1 m/s, pulsed jets lead to a greater velocity increase in the near-wall region at the measurement stations of the divergent portion in comparison with the unforced case. Figure 5.3 shows that the effective near-wall velocity increase is achieved by increasing the jet flow rate. This result coincides with the conclusion for steady jets by Compton and Johnston [18] which states that a strong vortex could be produced by increasing the jet flow rate in the same freestream speed.

On the other hand, the velocity profiles for the case of U_0=11.1 m/s are similar for the two different *VR* of the pulsed jet case (see Fig. 5.4). In this study, we define positive vortices in a *Y-Z* plane for clockwise rotating ones when we view from upstream. Figure 5.5 shows a comparison between the downstream decays of the maximum positive vorticity and the minimum negative vorticity of longitudinal vortices. The positive vorticity produced by the interaction between the jets and the freestream becomes strong with increasing freestream velocity at a fixed *VR*. In other words, the case of U_0=11.1 m/s generates longitudinal vortices that are strong enough to achieve the near-wall velocity increase.

Two cases of jet pulse frequency, f_p=10 and 20 Hz, were investigated. The shapes of peaks in the original waveform of pulsed jets broaden with respect to the time axis and also the jet flow rate per pulse is increased by lowering the pulse frequency. In contrast, increasing the pulse frequency leads to an increase in the number of peaks in the original waveform in a time interval. However, the profiles for f_p=20 Hz (see Fig. 5.6) show that the near-wall velocity is increased in comparison with those for f_p=10 Hz. In the present experiment, it is thus concluded that increasing the pulse frequency is more effective in the control of flow separation in comparison with broadening the shapes of peaks by lowering the pulse frequency.

The velocity profile for steady jets (see Fig. 5.4(a)) shows a velocity defect near the outer edge of the boundary layer of the unforced case, while the pulsed jets have the ability to thin the boundary layer thickness. Figure 5.7 shows

streamwise flow vectors at $X=40$, 70, 110 mm. For the case of pulsed jets, downward flow vectors exist in the measurement region. On the other hand, for the case of steady jets, upward flow vectors exist near the outer edge of the boundary layer. In the steady jet case, there is a velocity defect because downward flow does not exist near the outer edge of the boundary layer in contrast with the pulsed jet case (see Fig. 5.7).

The correlation of U and V with respect to the period of pulsed jets and the velocity measurements for the case of pulsed jets are shown in Fig. 5.8. For $f_p=20$ Hz and the sampling time of 30 ms of streamwise velocity, issuing jets coincides with the sampling at every interval of 150 ms. A streamwise velocity decrease is observed at that time. In other words, if the velocity is measured at the instant that the jets are blown, a streamwise velocity decrease is observed. It is hence supposed that steady jets have a tendency to increase the velocity in Y direction near the outer edge of the boundary layer and also to decrease the streamwise velocity there.

For the vortex generator jet method, an increase in the jet flow rate causes a near-wall velocity increase and makes effective the control of the separated flow for the same freestream speed. The increase in the jet flow rate corresponds to the broadening of the shape of the peaks of the pulsed jets. In order to avoid a velocity defect near the outer edge of the boundary layer, the pulsed jet method therefore is important.

5.2.4 Velocity Measurements in a Y–Z Plane

Figures 5.9 and 5.10 show the downstream development of longitudinal vortices for the case of pulsed jets. Secondary flow vectors at $X=70$, 110 mm are shown in Fig. 5.11. Figures 5.9 and 5.10 indicate that the longitudinal vortices persist near the lower wall in the downstream direction. No strong vortices exist apart from the lower wall. From Fig. 5.11 it is seen that the secondary flow toward the lower wall is induced by the effect of the longitudinal vortices in the near-wall region. The secondary flow of longitudinal vortices may transport the high momentum fluid of the freestream to the lower wall. The suppression of flow separation in a separated flowfield is accomplished by transporting the high

momentum fluid of the freestream to the lower wall.

Figure 5.12 shows the downstream development of longitudinal vortices for the case of steady jets. A comparison between Fig. 5.9 or 5.10 and Fig. 5.11 makes clear that the downstream development of longitudinal vortices for the case of pulsed jets is quite different from that for the case of steady jets. Pulsed jets keep the vortices near the lower wall. Because pulsed jets enhance the mixing process between the jets and the freestream further than steady jets, the upward movement of longitudinal vortices is suppressed.

From Fig. 5.12 counter-rotating vortices (with a negative sign) on the upwash side of the longitudinal vortices at $X=10$ mm are seen to be produced. It is supposed that the counter-rotating vortices are induced by the longitudinal vortices moving away from the lower wall. Vortex pairs are then formed. Three pairs of positive and negative vortices align on the right-hand side of Fig. 5.12 corresponding to the three jets. The formation of vortex pairs is due to the steady jets which make ineffective the mixing process between the jets and the freestream. The suppression of mixing brings about the upward movement of vortices. The pairs of vortices continue to be lifted away from the lower wall in the downstream direction due to the velocity induced by each vortex pair itself. The vortices, except for the edge vortices on both sides of this array, become weaker and disappear in the downstream direction. The secondary flow vectors at $X=70$, 110 mm are shown in Fig. 5.13. An upward secondary flow is produced near $Z=110$ mm. It is plausible that the upwash is induced by a vortex pair formed as a result of the production of a counter-rotating vortex of nearly equal strength (see Fig. 5.12).

For the case of steady jets, the minimum negative vorticity has a strength nearly equal to the maximum positive vorticity. On the other hand, for the case of pulsed jets, the maximum strength of positive vorticity increases with increasing freestream velocity, while that of negative vorticity is almost unchanged for various freestream velocities (see also Fig. 5.5). The suppression effect against the upward flow is achieved by keeping the longitudinal vortices near the lower wall. These vortices can effectively transport the high momentum fluid of the freestream to the lower wall.

Figure 5.14 shows the contours of the streamwise velocity. For the case of steady jets, the contours exhibit strong distortion near the outer edge of the boundary layer near $Z=110$ mm and therefore the boundary layer thickness

increases. This is due to the upwash induced by a pair of vortices of nearly equal strength at the spanwise location (see Fig. 5.13). Even if the suppression effect against separation is achieved, with the steady jet case the upwash makes ineffective the secondary flow toward the lower wall in a narrow spanwise region. Moreover, the velocity defect near the outer edge of the boundary layer is brought about by the upwash and thereby the boundary layer thickness varies largely in the spanwise direction. This characteristic is also confirmed in Fig. 5.3 where the mean velocity for the steady jet case is much lower than that for the unforced case. It should be noted that the streamwise velocity measurements are carried out just at $Z=110$ mm where the upwash occurs (see Fig. 5.14(b)).

5.2.5 Application for Divergence Angle of 30 Degrees

Figure 5.15 shows the streamwise velocity profiles at $X=110$ mm in the case of a divergence angle of 30 degrees for the pulsed jet case. The profiles indicate that the near-wall velocity hardly increases. Figure 5.16 shows the downstream development of the longitudinal vortices produced by the interaction between the pulsed jets and the freestream. The longitudinal vortices begin to lift away from the lower wall at $X=70$ mm and exist far from the lower wall at $X=110$ mm. A counter-rotating vortex of nearly equal strength exists below the longitudinal vortex because it moves away from the lower wall. Accordingly, the secondary flow toward the lower wall cannot be produced, as seen in Fig. 5.17. Figure 5.18 indicates the flow situation at $X=110$ mm for $U_0=11.1$ m/s. It is seen that the behavior of longitudinal vortices for $U_0=11.1$ m/s is similar to that for $U_0=6.5$ m/s. The high momentum fluid of the freestream is not carried effectively toward the lower wall and as a result the near-wall velocity in the divergent portion of the test section does not increase.

5.3 Conclusions

From the present experimental study on the mechanism of active boundary

layer control using longitudinal vortices, the following conclusions were drawn:

1. The suppression of flow separation is achieved by the secondary flow of longitudinal vortices, produced by the interaction between the jets and the freestream, which transports the high momentum fluid of the freestream toward the lower wall.

2. If a counter-rotating vortex is induced by the vortex which moves away from the lower wall, a pair of vortices is formed. An upwash is induced by the pair of vortices and as a result the boundary layer thickness is strongly distorted. The thickness becomes inhomogeneous in the spanwise direction because the streamwise velocity decreases in the upwash region.

3. The increase in near-wall velocity in the divergent portion of the test section is achieved by adjusting the strength of longitudinal vortices which depends on the jet flow rate. Pulsed jets enhance the mixing process between the jets and the freestream further compared with steady jets. This keeps longitudinal vortices close to the lower wall and never produces any upwash.

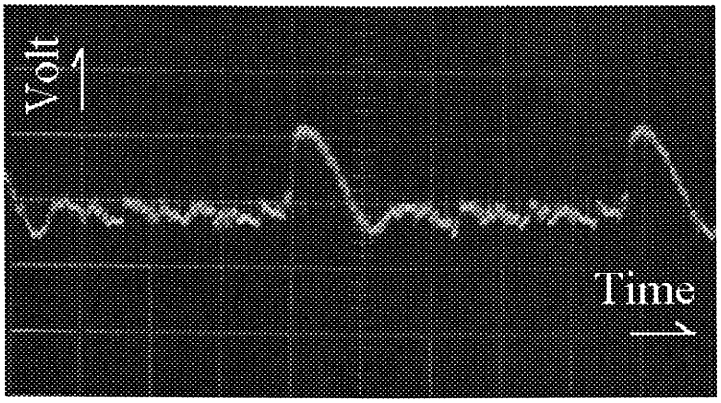

(a) f_p=20 Hz, Q_j=20 *l*/min (Time interval=10 ms)

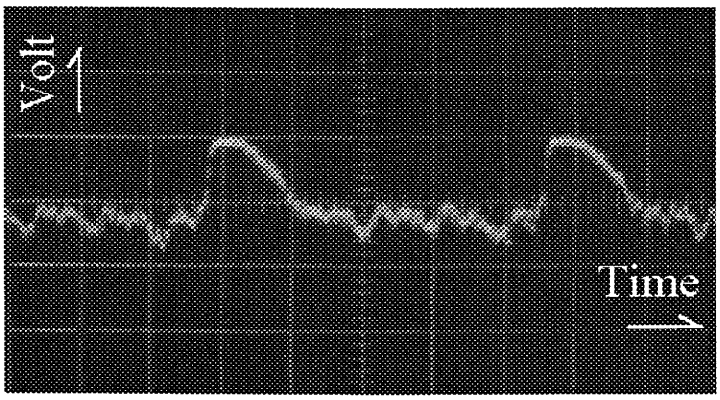

(b) f_p=20 Hz, Q_j=60 *l*/min (Time interval=10 ms)

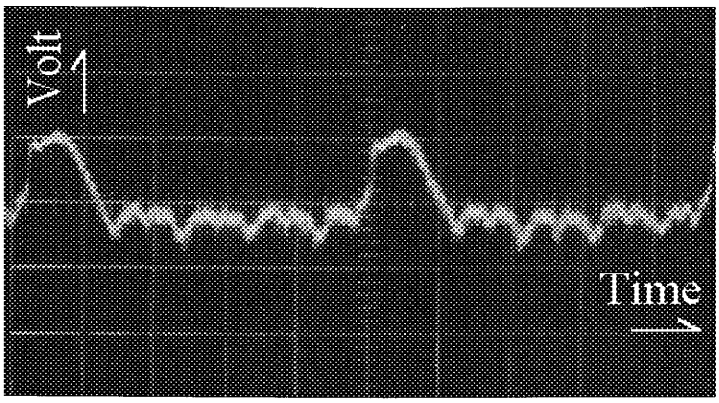

(c) f_p=10 Hz, Q_j=60 *l*/min (Time interval=20 ms)

Figure 5.1 Original waveform of pulsed jets.

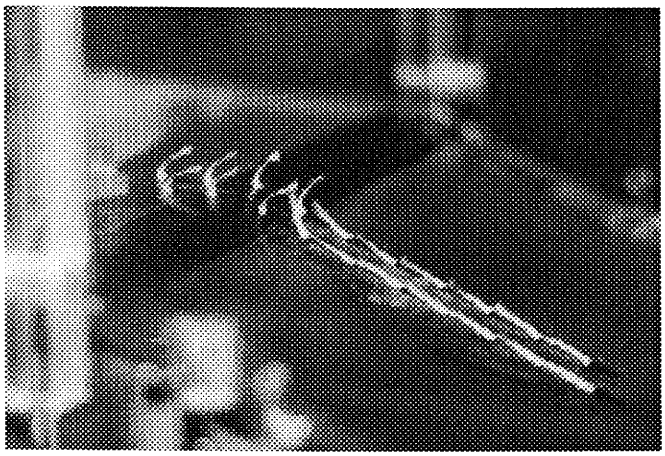

(a) Unforced

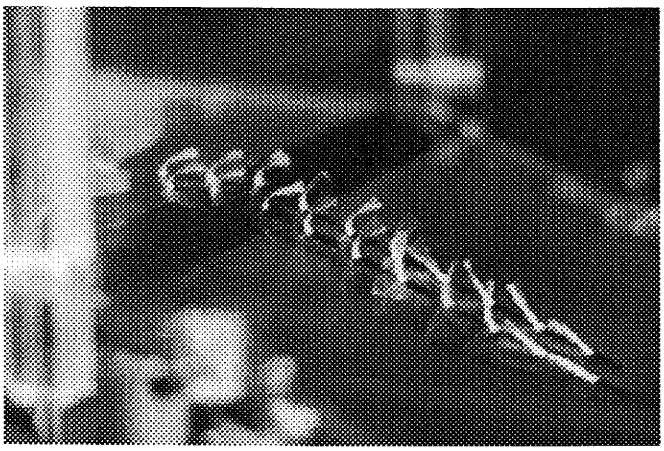

(b) $VR=9.5, f_p=20$ Hz

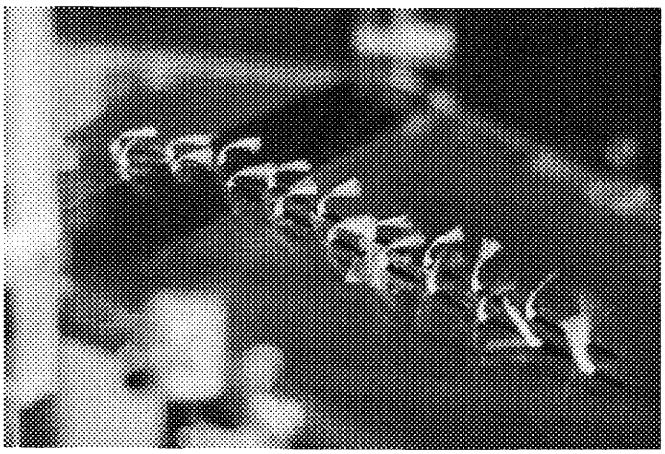

(c) $VR=13$

Figure 5.2 Surface flow in divergent portion of the test section ($U_0=6.5$ m/s).

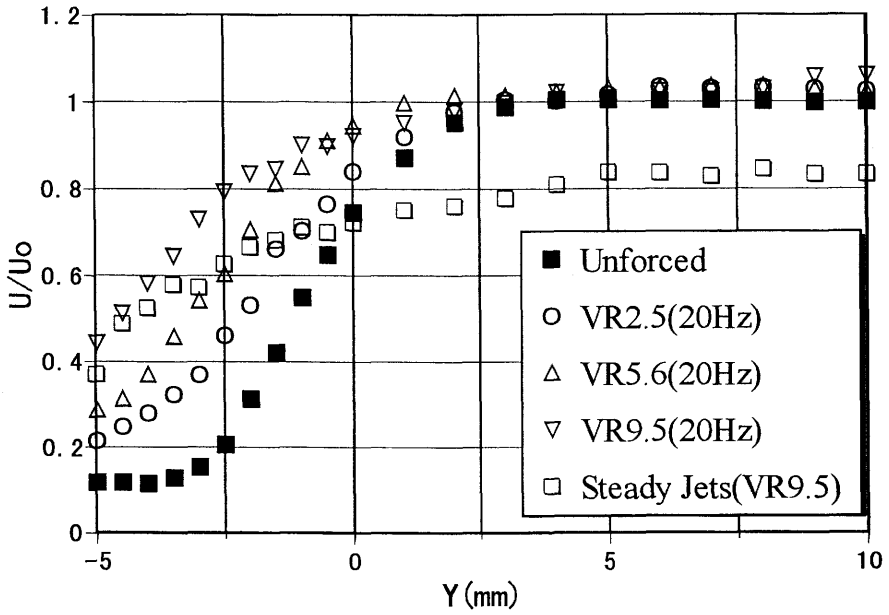

(a) X=70 mm

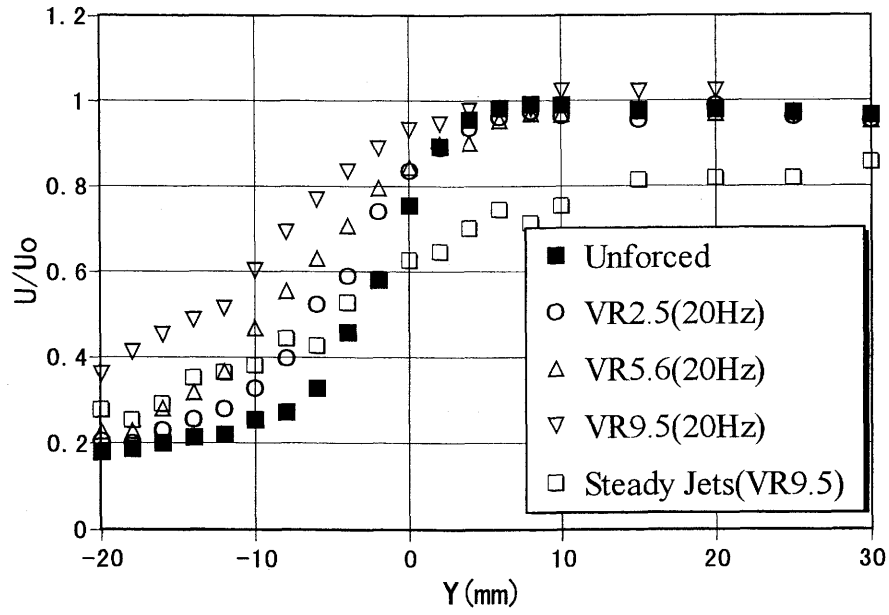

(b) X=110 mm

Figure 5.3 Streamwise velocity profiles (U_0=6.5 m/s, α =20 deg).

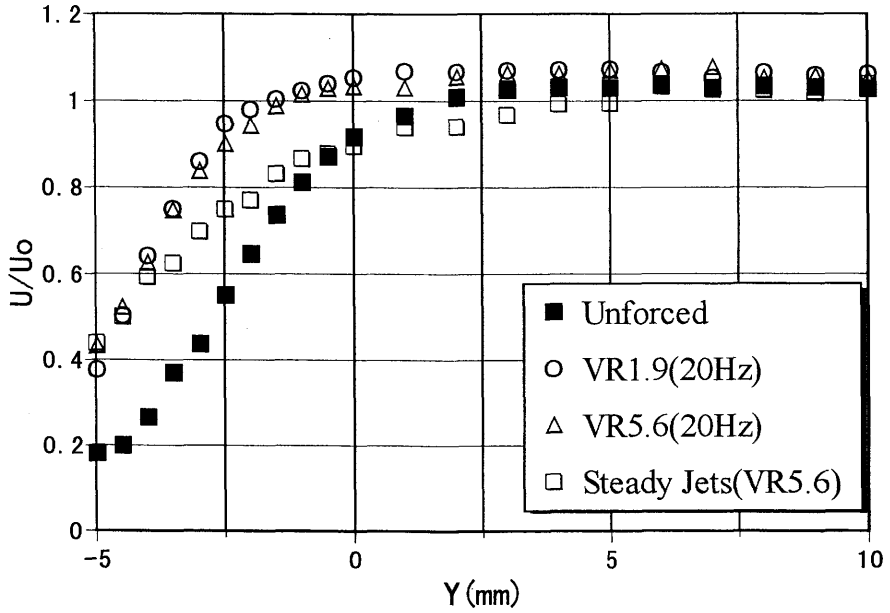

(a) X=70 mm

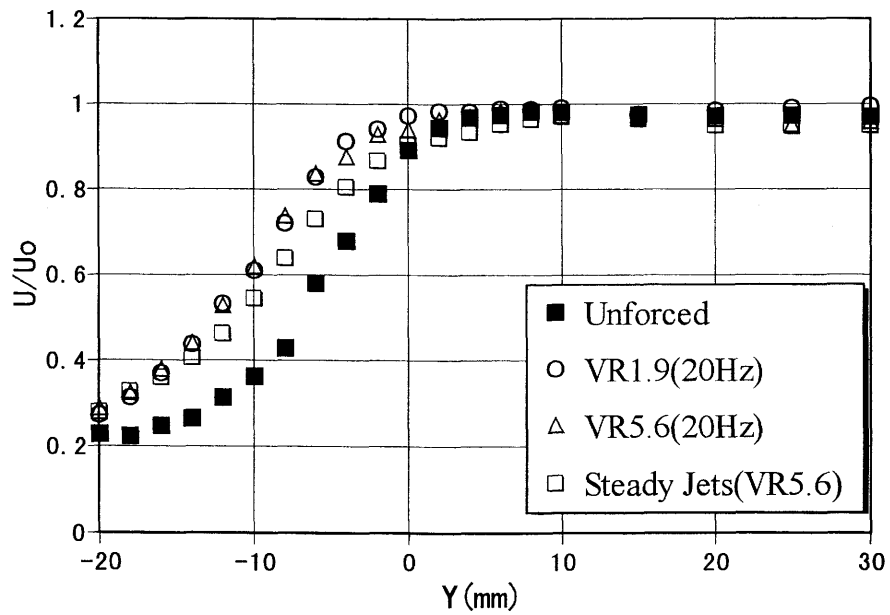

(b) X=110 mm

Figure 5.4 Streamwise velocity profiles (U_0=11.1 m/s, α=20 deg).

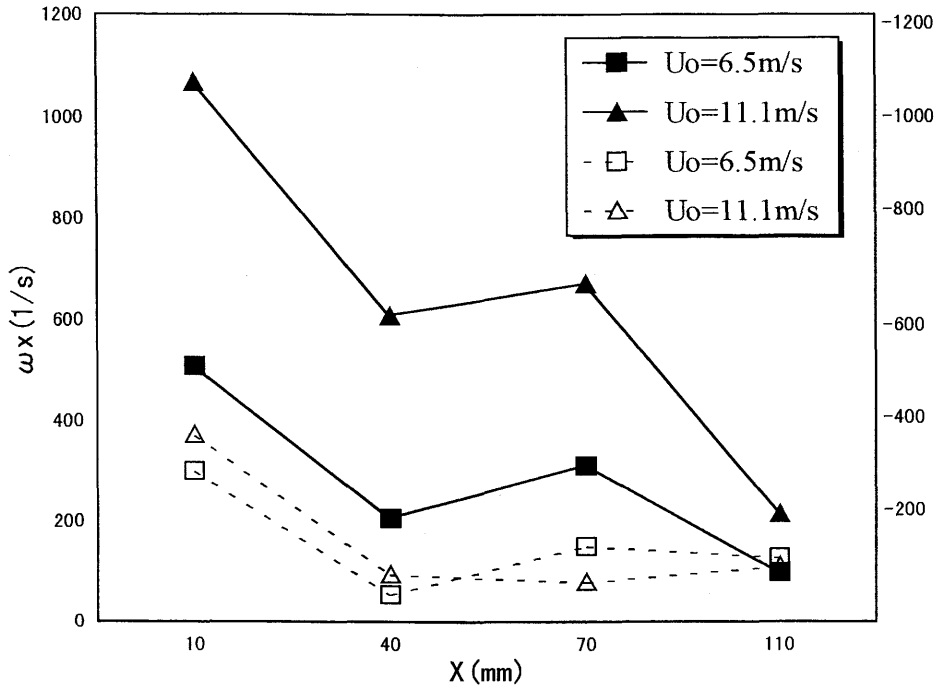

Figure 5.5 Comparison between the downstream decays of the maximum positive vorticity and the minimum negative vorticity. Open symbols denote negative vorticity (VR=5.6, f_p=20 Hz, α =20 deg).

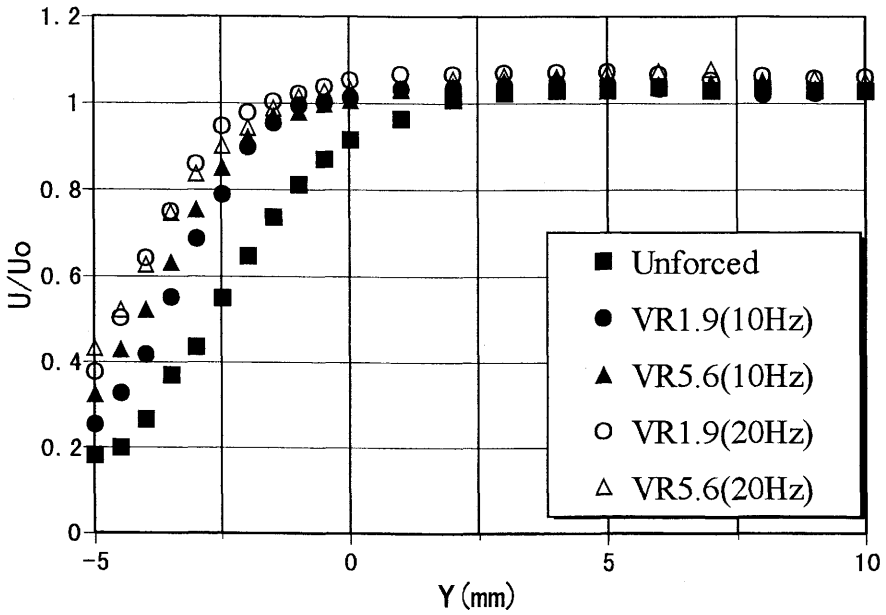

(a) X=70 mm

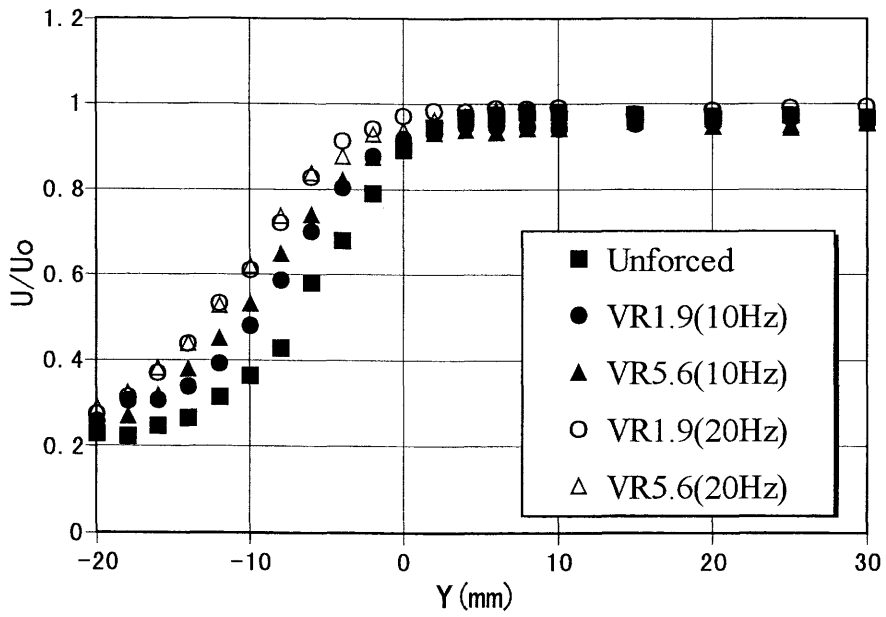

(b) X=110 mm

Figure 5.6 Streamwise velocity profiles for two cases of pulse frequency (U_0=11.1 m/s, α=20 deg).

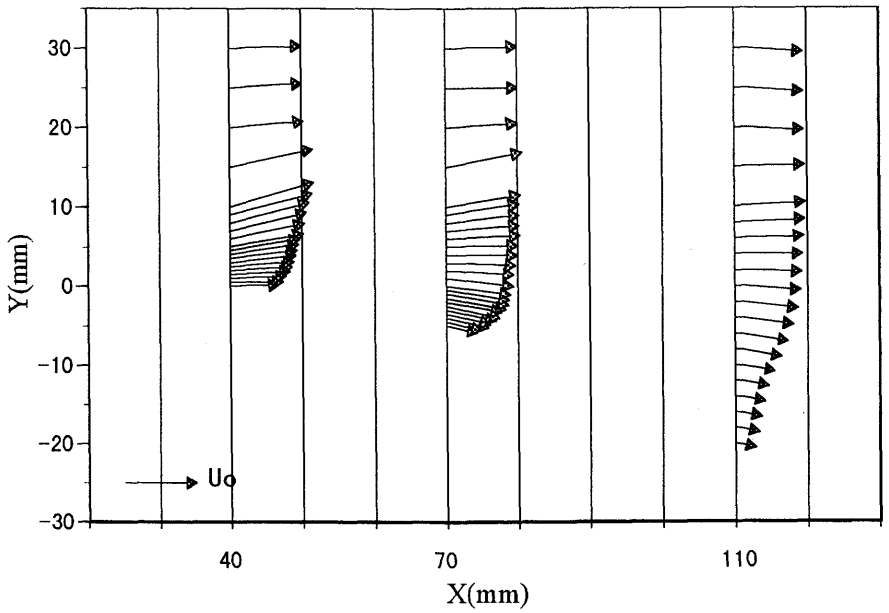

(a) Steady jets (VR=5.6)

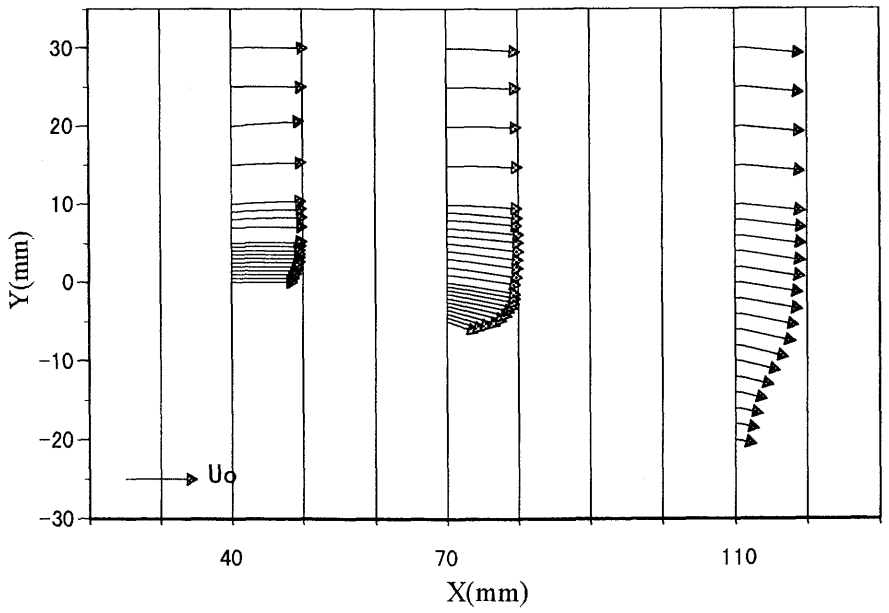

(b) Pulsed jets (VR=5.6, f_p=20 Hz)

Figure 5.7 Streamwise flow vectors (U_0=11.1 m/s, α=20 deg).

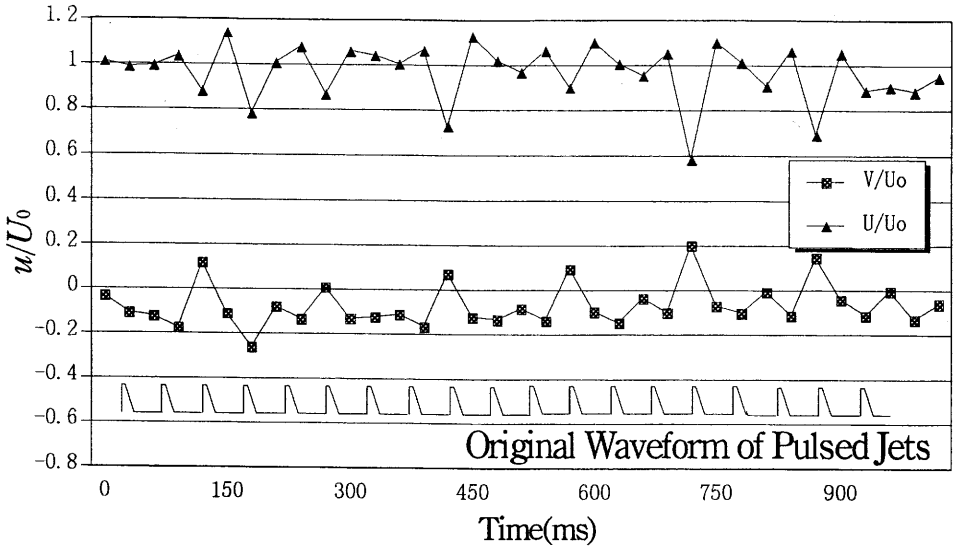

(a) U_0=6.5 m/s, VR=5.6, f_p=20 Hz

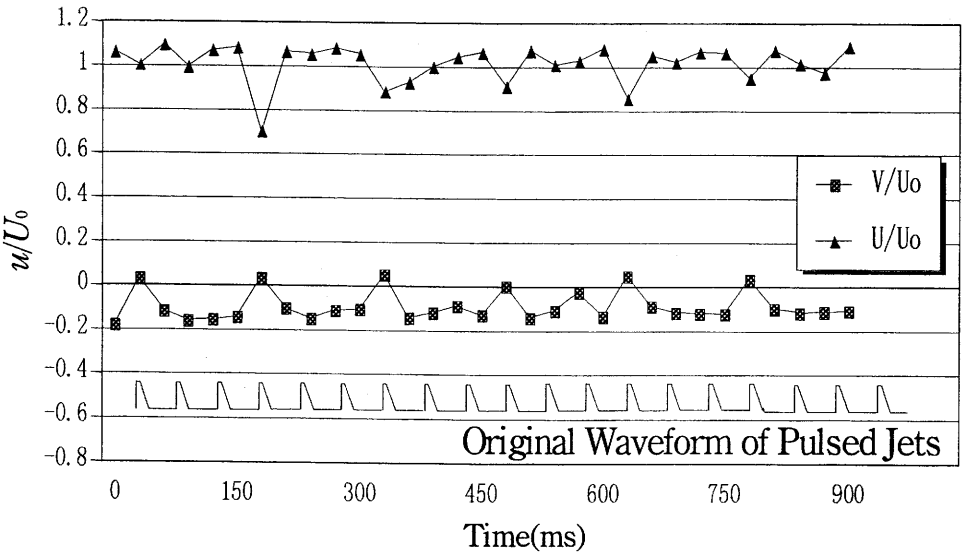

(b) U_0=11.1 m/s, VR=1.9, f_p=20 Hz

Figure 5.8 Sampling interval of streamwise velocity, compared to original waveform of pulsed jets at X=70 mm, Y=6 mm (α =20 deg).

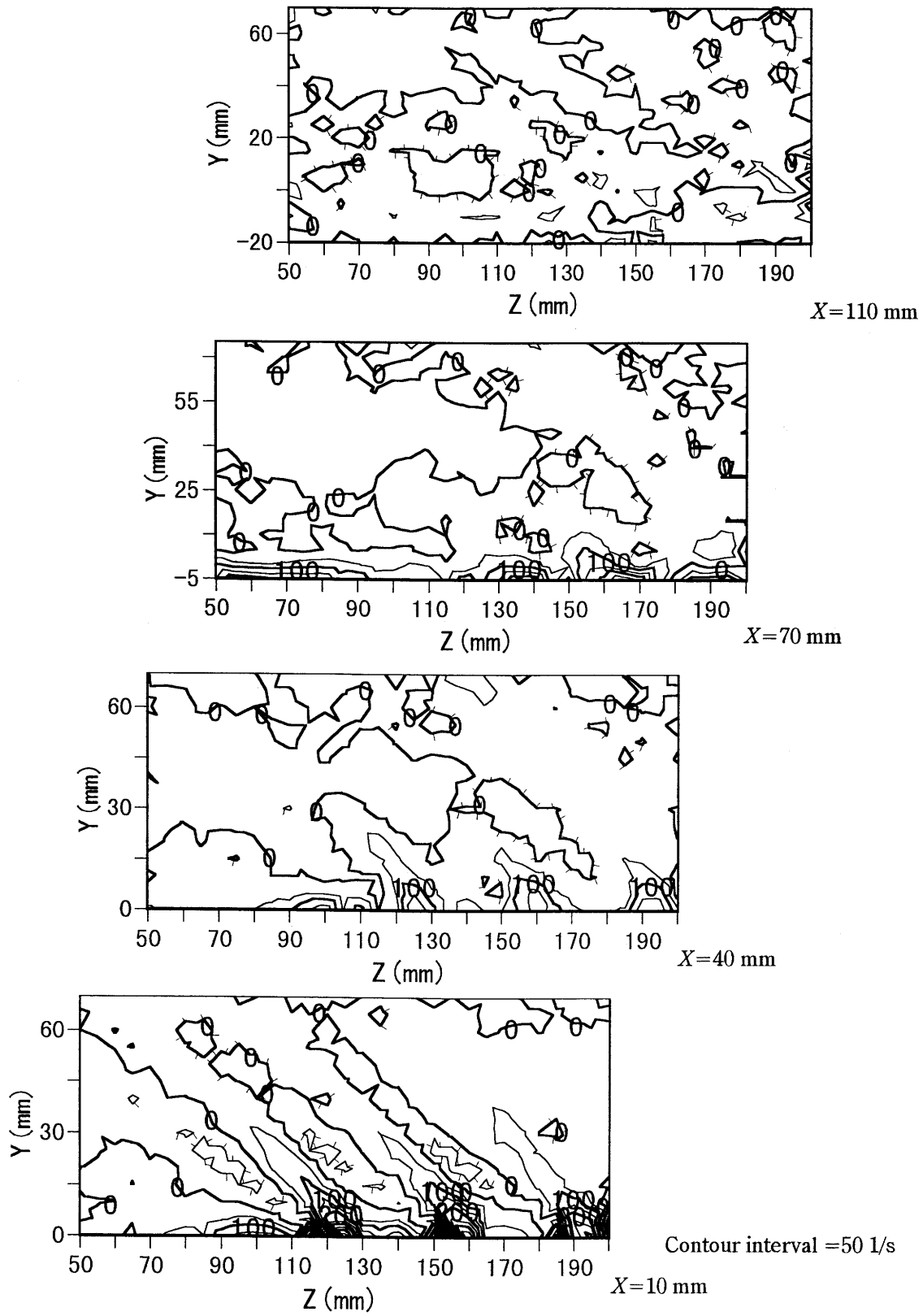

Figure 5.9 Contours of streamwise vorticity. Decorated lines denote negative vorticity (U_0=6.5 m/s, VR=5.6, f_p=20 Hz, α=20 deg).

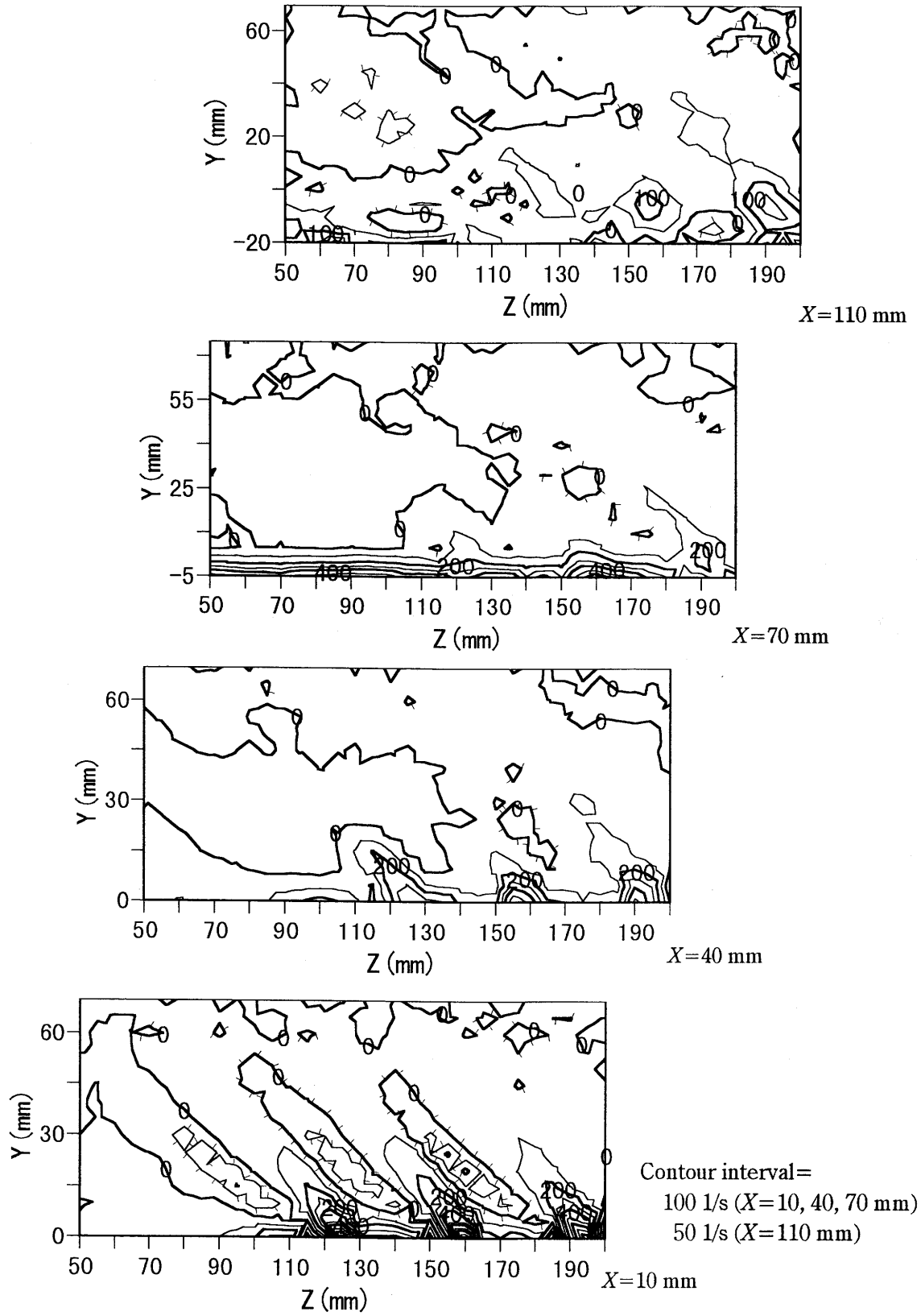

Figure 5.10 Contours of streamwise vorticity. Decorated lines denote negative vorticity (U_0=11.1 m/s, VR=5.6, f_p=20 Hz, α=20 deg).

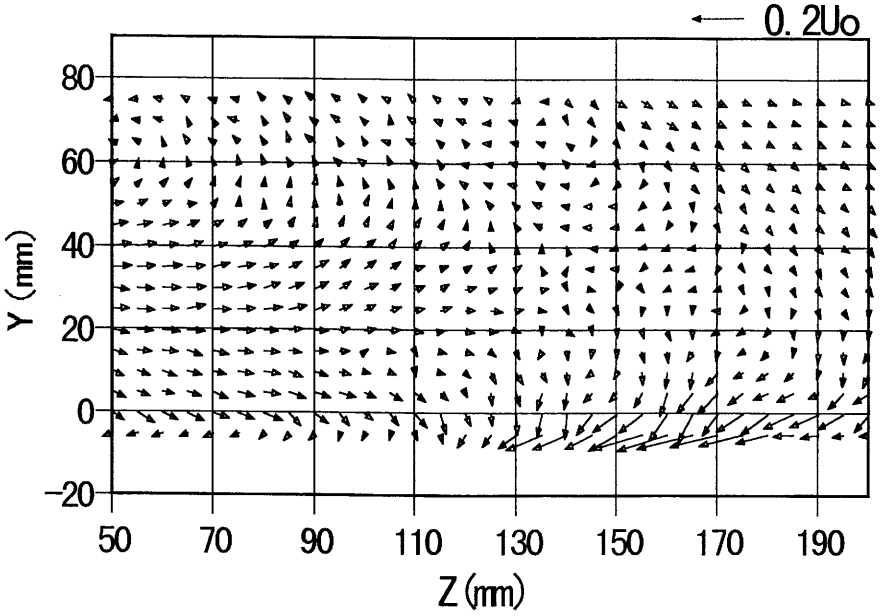

(a) X=70 mm

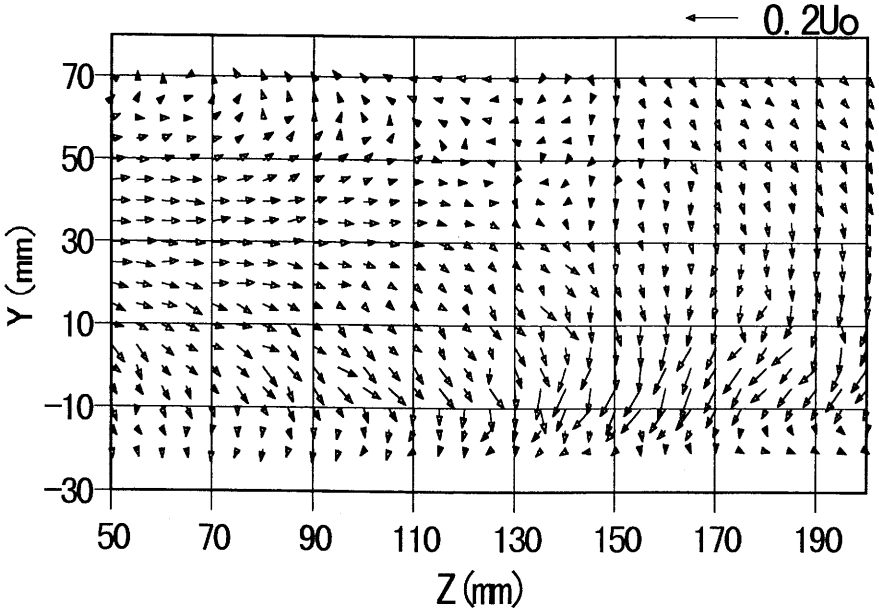

(b) X=110 mm

Figure 5.11 Secondary flow vectors (U_0=6.5 m/s, VR=5.6, f_p=20 Hz, α =20 deg).

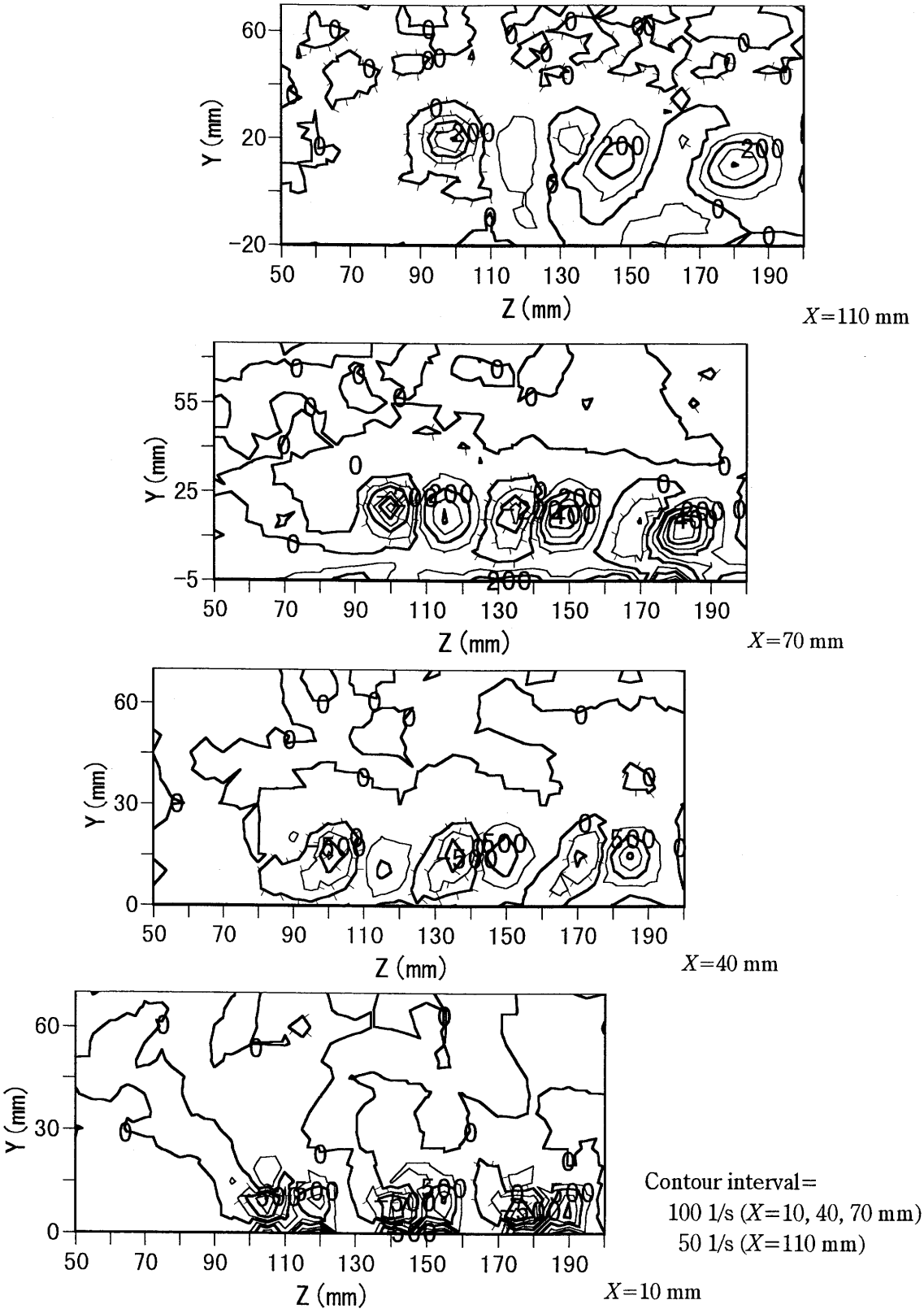

Figure 5.12 Contours of streamwise vorticity. Decorated lines denote negative vorticity (U_0=6.5 m/s, VR=9.5, α =20 deg).

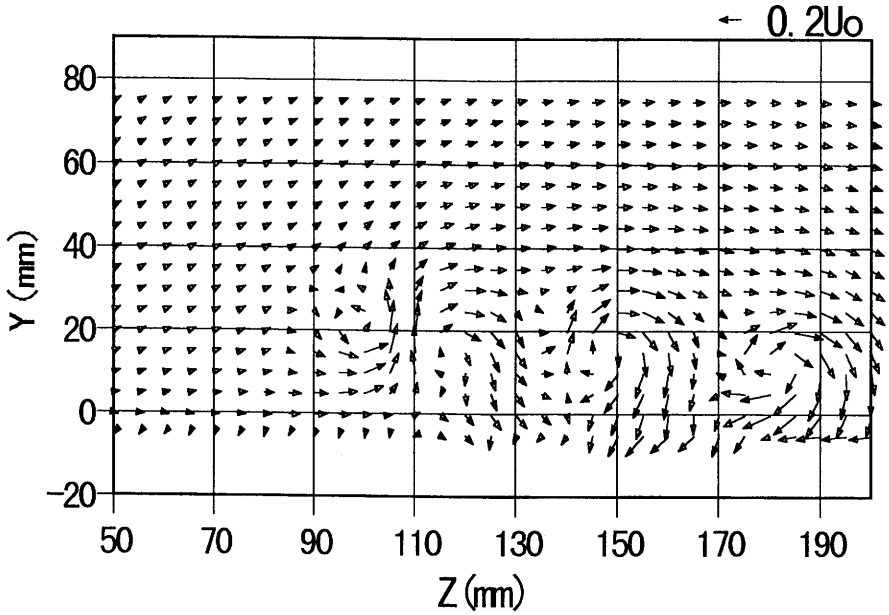

(a) X=70 mm

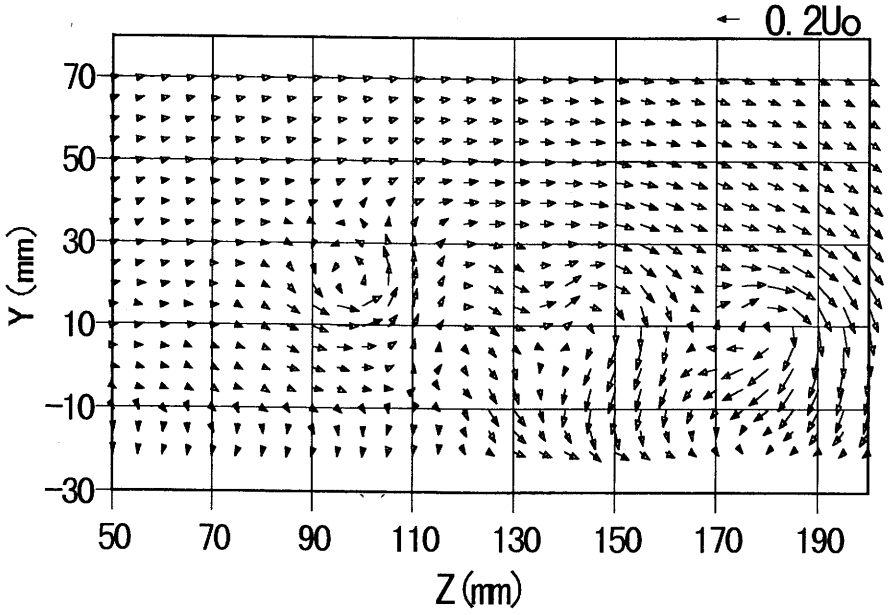

(b) X=110 mm

Figure 5.13 Secondary flow vectors (U_0=6.5, VR=9.5, α =20 deg).

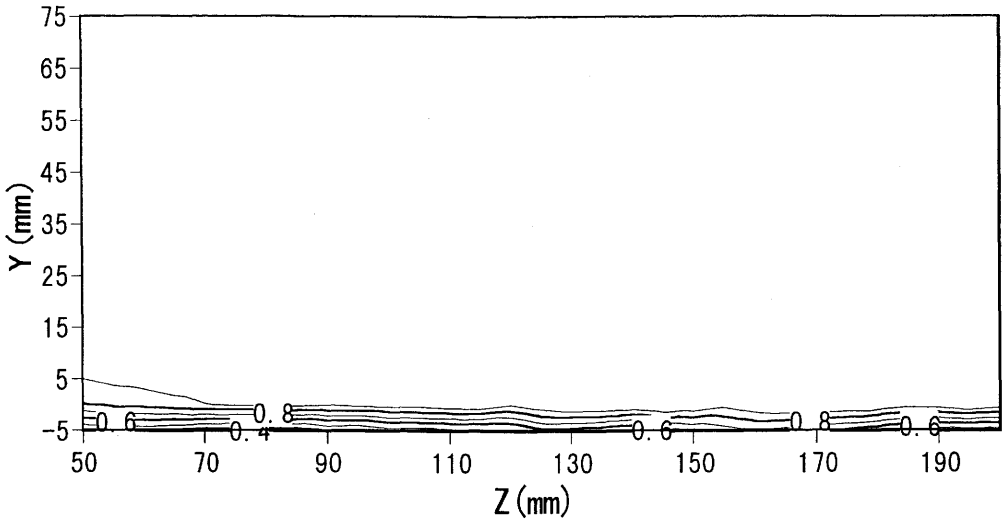

(a) Pulsed jets (VR=5.6, f_p=20 Hz)

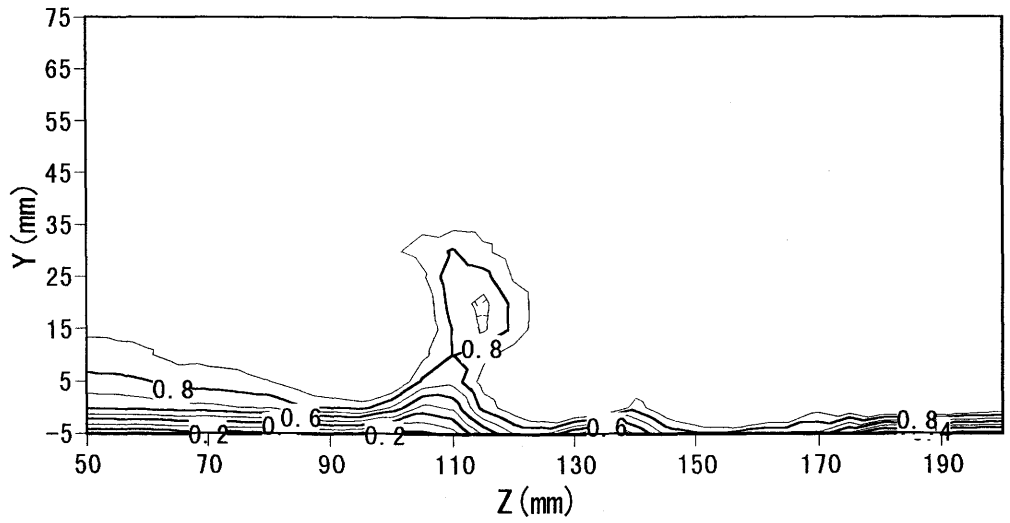

(b) Steady jets (VR=9.5)

Figure 5.14 U/U_0 contours at X=70 mm (U_0=6.5 m/s, α=20 deg). Contour interval=0.1.

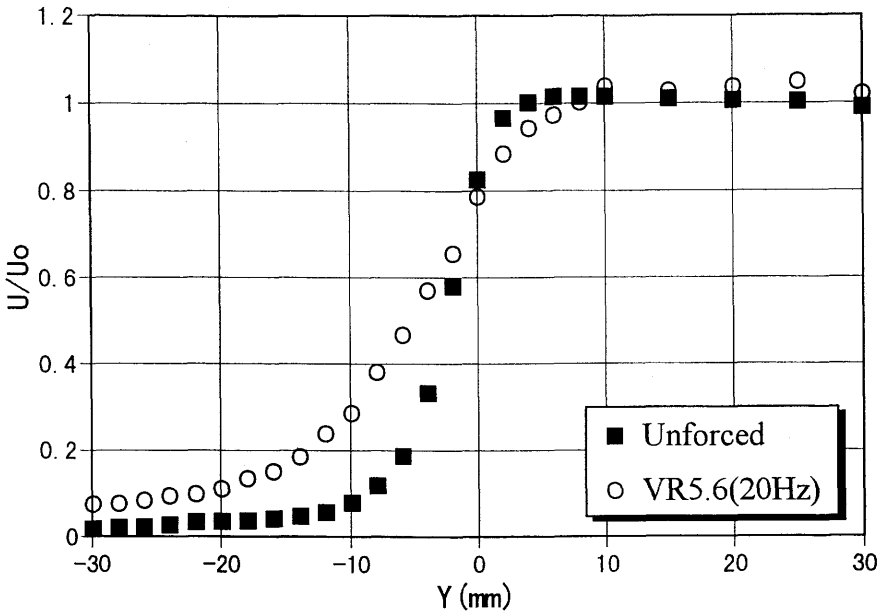

(a) U_0=6.5 m/s

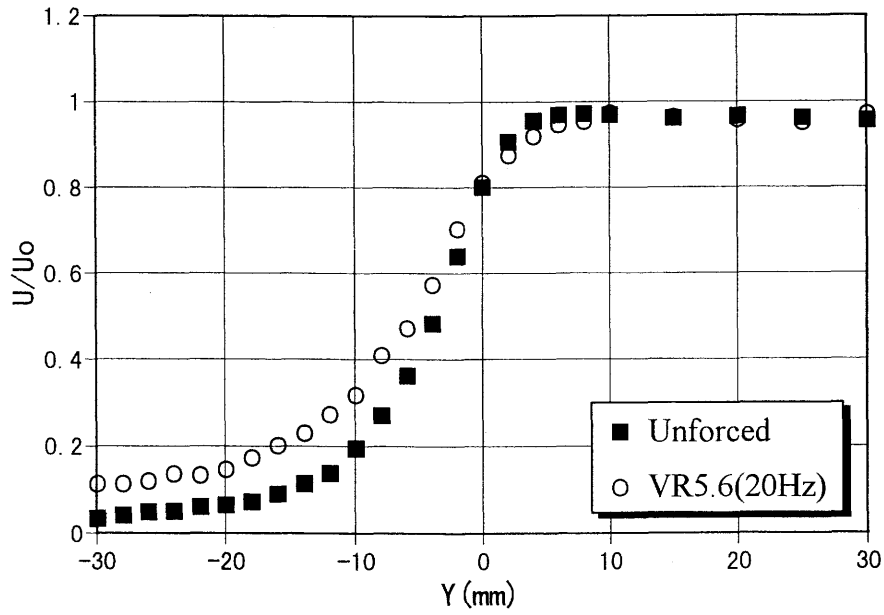

(b) U_0=11.1 m/s

Figure 5.15 Streamwise velocity profiles at X=110 mm (α =30 deg).

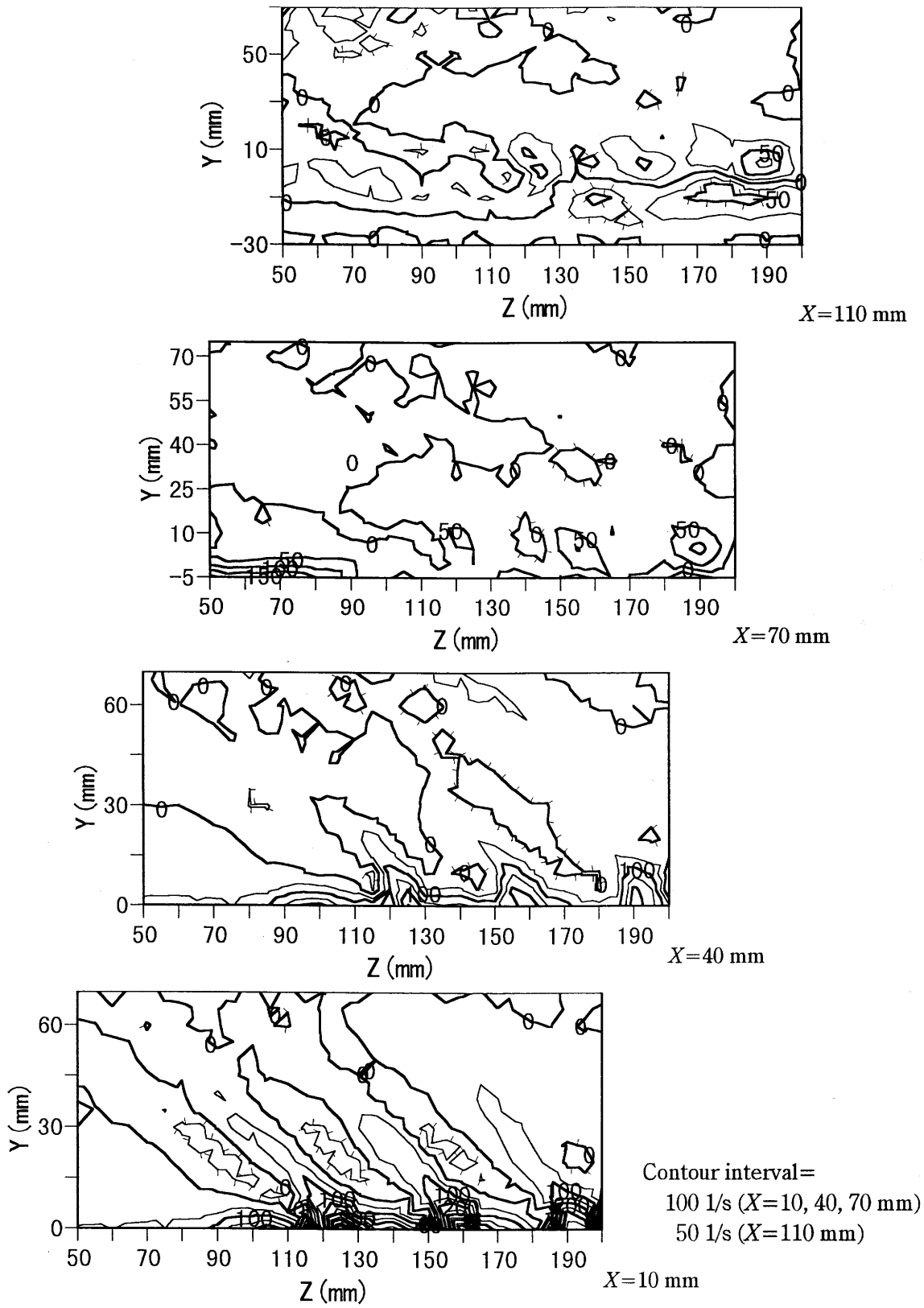

Figure 5.16 Contours of streamwise vorticity. Decorated lines denote negative vorticity (U_0=6.5 m/s, VR=5.6, f_p=20 Hz, α=30 deg).

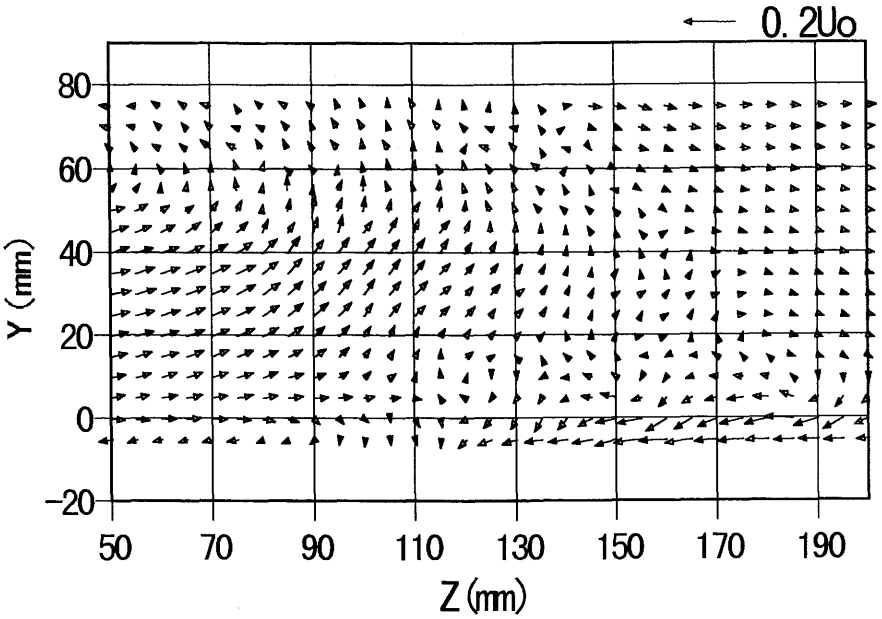

(a) X=70 mm

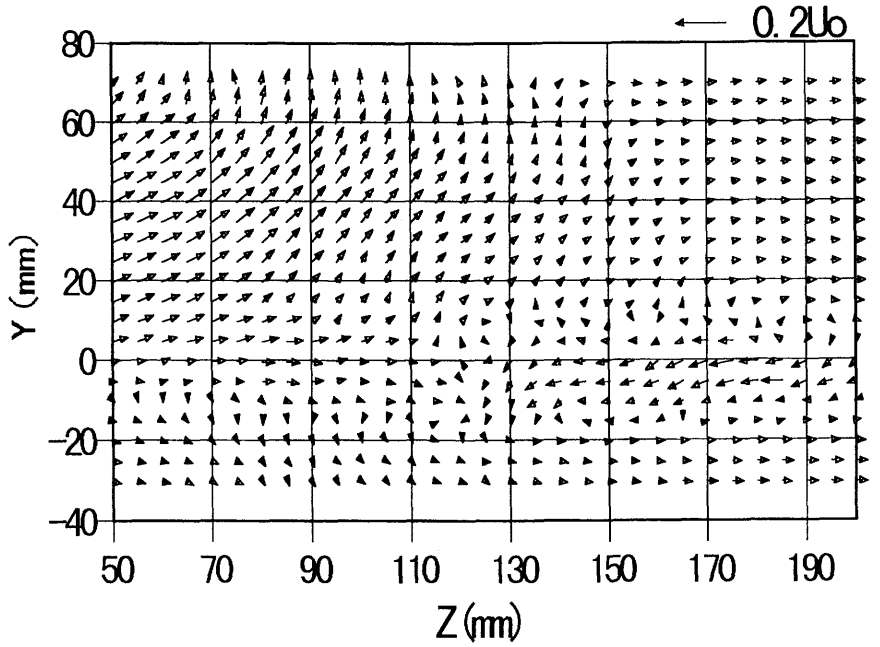

(b) X=110 mm

Figure 5.17 Secondary flow vectors (U_0=6.5 m/s, VR=5.6, f_p=20 Hz, α =30 deg).

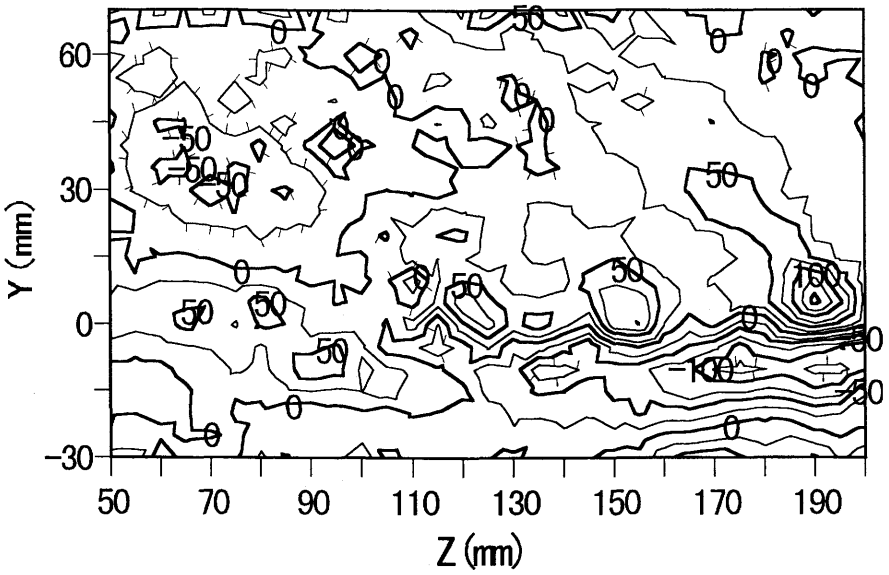

(a) Contours of streamwise vorticity (Decorated lines denote negative vorticity, Contour interval =25 1/s)

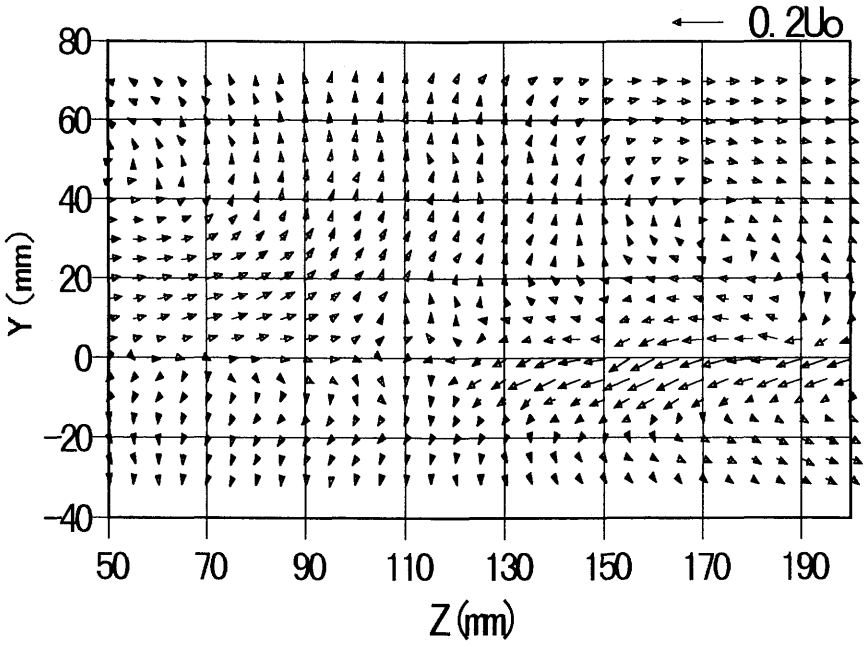

(b) Secondary flow vectors

Figure 5.18 Flow situation at X=110 mm (U_0=11.1 m/s, VR=5.6, f_p=20 Hz, α =30 deg).

6. GENERATING MECHANISM OF LONGITUDINAL VORTICES USING PULSED JETS

In Chapter 5, the mechanism for suppressing flow separation was investigated by making a comparison between steady and pulsed jets. It was clarified that the shape and the downstream development of vortices for the pulsed jet case were different from those for the steady jet case. However, the reasons why the vortices for the steady jet case behave in a manner different from those for the pulsed jet case are unknown. In this chapter, in order to understand these reasons velocity measurements in a *Y-Z* plane over various phases of pulsed jets are carried out.

6.1 Experimental Method

Figure 3.12 indicates the vortex generator jet device. The pulsed jet flow was produced by passing or shutting off the secondary air from a compressor using a rotor disk of the vortex generator jet device. The revolutions per minute of the rotor were measured by using a non-contact type revolution indicator. A reflector was set on a coupling which connects the rotor with a driving motor of the vortex generator jet device. The revolutions per minute were determined from the time interval for which the signal was detected. The velocity measurements were carried out in response to the signal detection of the revolution indicator in order to know the flow field in a fixed phase of the pulsed jet. Varying the position of the reflector on the coupling, we changed the phase.

6.2 Results and Discussion

6.2.1 Longitudinal Vortices in Various Phases of Pulsed Jets

Figure 6.1 shows various rotor positions relative to the flow pass of the secondary air of the vortex generator jet device. Phase NT is just out of phase to the pass. Phase 3 corresponds to the phase where the hole in the rotor disk coincides with the flow pass. In this phase, the maximum issuing jet rate is attained. Phase 1 corresponds to the phase just before jets are issuing. Phase 5 corresponds to that just after issuing. Phase 2 and phase 4 correspond to the intermediate phase between phase 1 and phase 3, and that between phase 3 and phase 5, respectively. Furthermore, phase 7 indicates a phase delayed by a quarter cycle to phase 3 and phase 6 is in the intermediate between phase 5 and phase 7.

Figure 6.2 shows the contours of streamwise vorticity for the pulsed and steady jet cases. For the pulsed jet case the streamwise vorticity is calculated by averaging data over a whole phase. It is seen from Fig. 6.2 that for the steady jet case the vorticity contours are circular in shape and the negative vortices exist on the upwash side of the positive vortices. The counter-rotating vortex pairs of nearly equal strength are formed. On the other hand, for the pulsed jet case the vorticity contours are not circular but appear to have vertical elongation and the longitudinal vortices exist close to the lower wall.

Figure 6.3 shows longitudinal vortices in various phases of the pulsed jets. In phase NT, longitudinal vortices are not observed in the flow field because the jets are not issued. The longitudinal vortices are generated near the lower wall in phase 1 or 1a corresponding to the instant at which the jets begin to be issued. Phase 1a indicates the intermediate phase between phase 1 and phase 2. In phase 2, the longitudinal vortices grow in the vertical direction. In phase 3, the vorticity contours have the maximum vertical elongation at a pitch angle of 45 degrees. When the phase changes from phase 4 to 6, the longitudinal vortices have no spreading but they move gradually toward the lower wall. Furthermore, after phase 6 the longitudinal vortices are not observed in the flow field. For the

reasons mentioned above, the different feature of longitudinal vortices between the steady and pulsed jets can be explained by considering the vortex behavior in each phase of pulsed jets.

6.2.2 Downstream Development of Longitudinal Vortices

Figures 5.9 and 5.12 show the downstream development of longitudinal vortices for the pulsed jet case and the steady jet case, respectively. For the steady jet case longitudinal vortices form counter-rotating vortex pairs and are lifted away from the lower wall in the downstream direction due to the velocity induced by a pair of vortices. On the other hand, for the pulsed jet case longitudinal vortices develop in the downstream direction without forming a vortex pair and exist close to the lower wall. In order to investigate this phenomenon the downstream development of longitudinal vortices was examined in fixed phases of issuing pulsed jets.

Figure 6.4 shows the downstream development of longitudinal vortices in phase 3 which corresponds to the maximum issuing jet rate. At $X=5$ mm, the vorticity contours are strongly elongated in the vertical direction. The longitudinal vortices have the strong influence of the jet pitch angle and therefore are elongated in the vertical direction in comparison with the steady jet case. At $X=20$ mm, the positive vorticity contours begin to split out in the vertical direction. In other words, for the pulsed jet case the positive vortex is affected by the adjacent negative vortex in contrast to the steady jet case, and therefore the positive vortex develops downstream in such a way that the vorticity contours are split out in the vertical direction. At $X=22$ or 26 mm, the split positive vortices exist above the negative vortices because the positive vorticity contours have the vertical elongation. At $X=30$ mm, the vertical positions of the positive vortices are different from those of the negative ones for three vortex pairs. At $X=40$ and 44 mm, the negative vortices collapse in shape, since the positive vortices exist above the negative vortices. At $X=49$ mm, the negative vortices do not keep their circular shape and become weaker. For the reason given above, we see that the negative vorticity decays more rapidly than the positive one. For pulsed jets

the interaction between adjacent positive and negative vortices is promoted by the jet pitch angle and as a result any strong counter-rotating vortex pairs are not produced. Therefore, the upward movement of longitudinal vortices is suppressed in the downstream direction.

Figure 6.5 shows the downstream development of longitudinal vortices for issuing a single jet. This case corresponds to phase 3, i.e., the maximum issuing jet rate. It is seen that the downstream development of longitudinal vortices is similar to the three-jet case. It is clear that for the single-jet case the positive vortex is split out vertically into two pieces by the interaction with the opposite sign vortex at $X=20$ mm. At $X=40$ mm, the split positive vortex exists above the negative vortex and a counter-rotating vortex pair is produced. The longitudinal vortices disappear at $X=60$ mm. This phenomenon in which the positive vortex is split out by the interaction with the negative vortex is not affected by the interaction with the adjacent vortex pairs but by the jet pitch angle.

The downstream development of longitudinal vortices in the phase delayed by a quarter cycle to phase 3 (phase 7) is shown in Fig. 6.6. Longitudinal vortices are not observed at $X=5$ mm. It is seen that the longitudinal vortices are attaching to the lower wall at $X=20$ mm. However, they do not attach to the lower wall at $X=30$ mm and exist apart from the lower wall at $X=50$ mm. The vorticity becomes stronger in the downstream direction and the trailing edge of longitudinal vortex exists near $X=20$ mm. Longitudinal vortices produced by issuing jets develop in the downstream in such a way that the trailing edge of vortices attaches to the lower wall.

6.2.3 Upward Development of Longitudinal Vortices

In Fig. 6.4, at $X=30$ mm three pairs of vortices exist at nearly equal vertical positions. However, at $X=49$ mm the vortex pair on the left side edge of the figure is placed at the higher vertical position in comparison with the other vertex pairs. The negative vortex which exists at the center or on the right side edge of Fig. 6.4 exists between the positive vortices. The vorticity becomes weaker under the influence of the interaction between the opposite sign vortices on both sides. On the other hand, no negative vortex on the left side edge exists between

the positive vortices. The negative vortex on left side edge is maintained further downstream compared with the other negative vortices because a positive vortex exists only on either side. Therefore, the vortex pair at the left side edge has the strong influence of the velocity induced by the vortex pair and thus exists at the higher vertical position than the other vortex pairs. Figure 6.7 shows the upward development of longitudinal vortices for the case of large *VR* due to a single jet in phase 3. The vorticity is strong and therefore persists further downstream because the jet speed is faster. The vorticity contours are strongly elongated in the vertical direction at $X=5$ mm and are circular at $X=110$ mm. The pair of vortices have an upward movement at $X=130$ and 160 mm. The upward movement is brought about by the velocity induced by the vortex pair.

Suppression of flow separation is achieved by the secondary flow of longitudinal vortices which can transport high momentum fluid of the freestream to the boundary layer. In the sense of performing effective separation control it is important that vortices are strong and keep their positions near the lower wall where the secondary flow toward the lower wall is effective (*cf.* Chapter 5). For this reason, the upward movement of longitudinal vortices is not desirable. For the vortex generator jet method it is important to choose properly the jet spacing and also the jet pitch angle which can make the interaction between adjacent vortices. In other words, the suppression of the upward movement of vortices is achieved by the interaction between adjacent vortices under the influence of the jet pitch angle and the effective jet spacing.

6.3 Conclusions

From the study on the generating mechanism of longitudinal vortices due to pulsed jets, the following conclusions were drawn:

1. As the phase of pulsed jets proceeds from the phase of non-issuing jets, longitudinal vortices produced from the lower wall grow in the vertical direction and the vorticity contours have vertical elongation in the phase with the maximum issuing jet rate due to the jet pitch angle. After that time, the longitudinal vortices move toward the lower wall, as the phase

changes to the jet-off situation.

2. For pulsed jets longitudinal vortices have the stronger influence of the jet pitch angle in comparison with the steady jet case.

3. For pulsed jets a positive vortex is split out in the vertical direction by the influence of the neighboring negative vortex and the split positive vortex covers the negative vortex. This means that the attenuation of negative vorticity is promoted and therefore the generation of a vortex pair is suppressed. This leads to the suppression of the upward movement of vortices.

4. For the vortex generator jets with multi-jet orifices, it is desirable that the jet spacing which can make the interaction between adjacent vortices is selected.

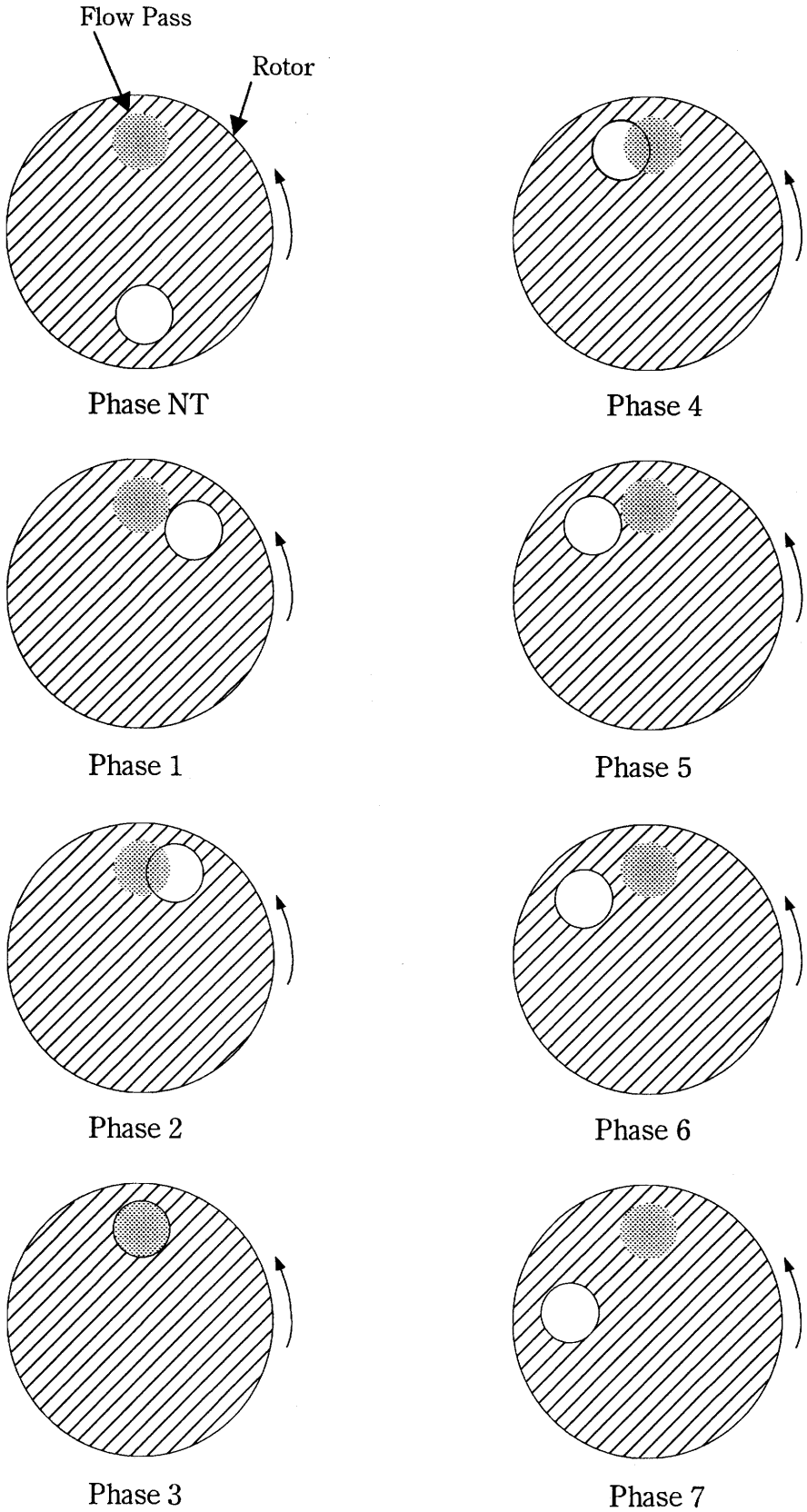

Figure 6.1 Various rotor positions relative to flow pass of secondary air.

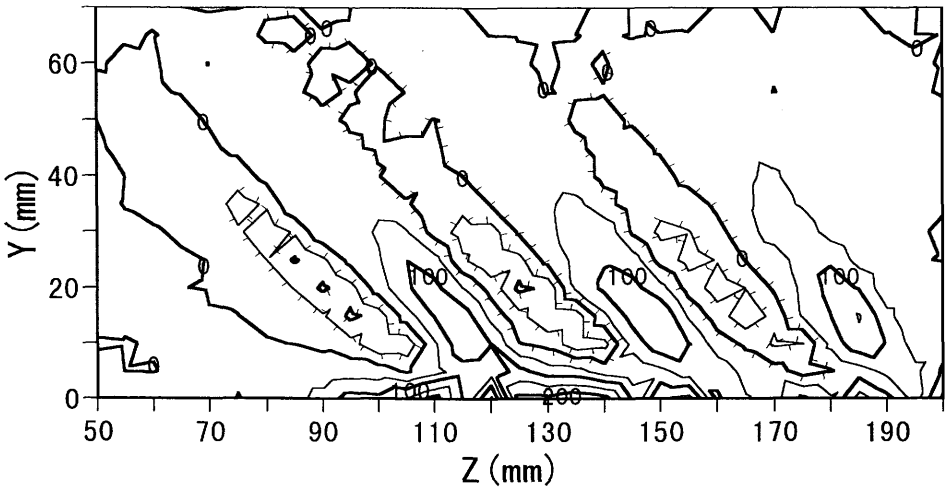

(a) Pulsed jets (VR=5.6, f_p=10 Hz, Contour interval =50 1/s)

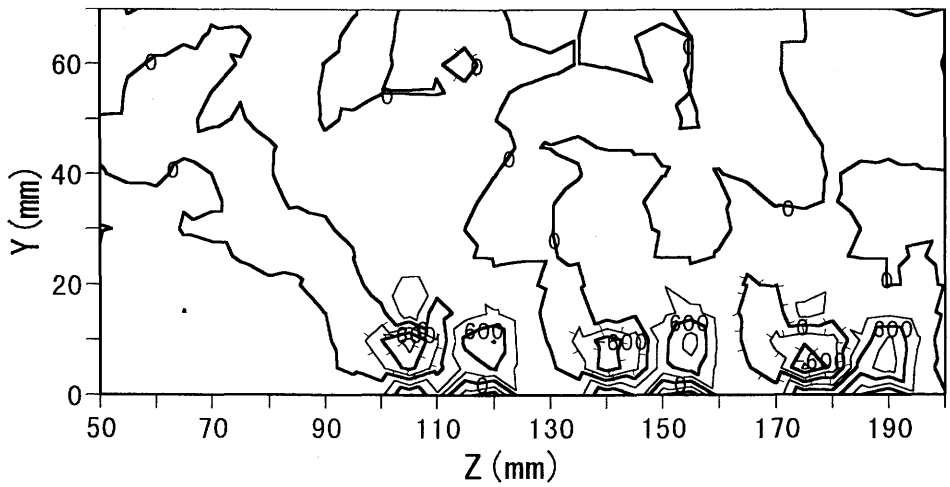

(b) Steady jets (VR=9.5, Contour interval =300 1/s)

Figure 6.2 Contours of streamwise vorticity at X=10 mm. Decorated lines denote negative vorticity (U_0=6.5 m/s).

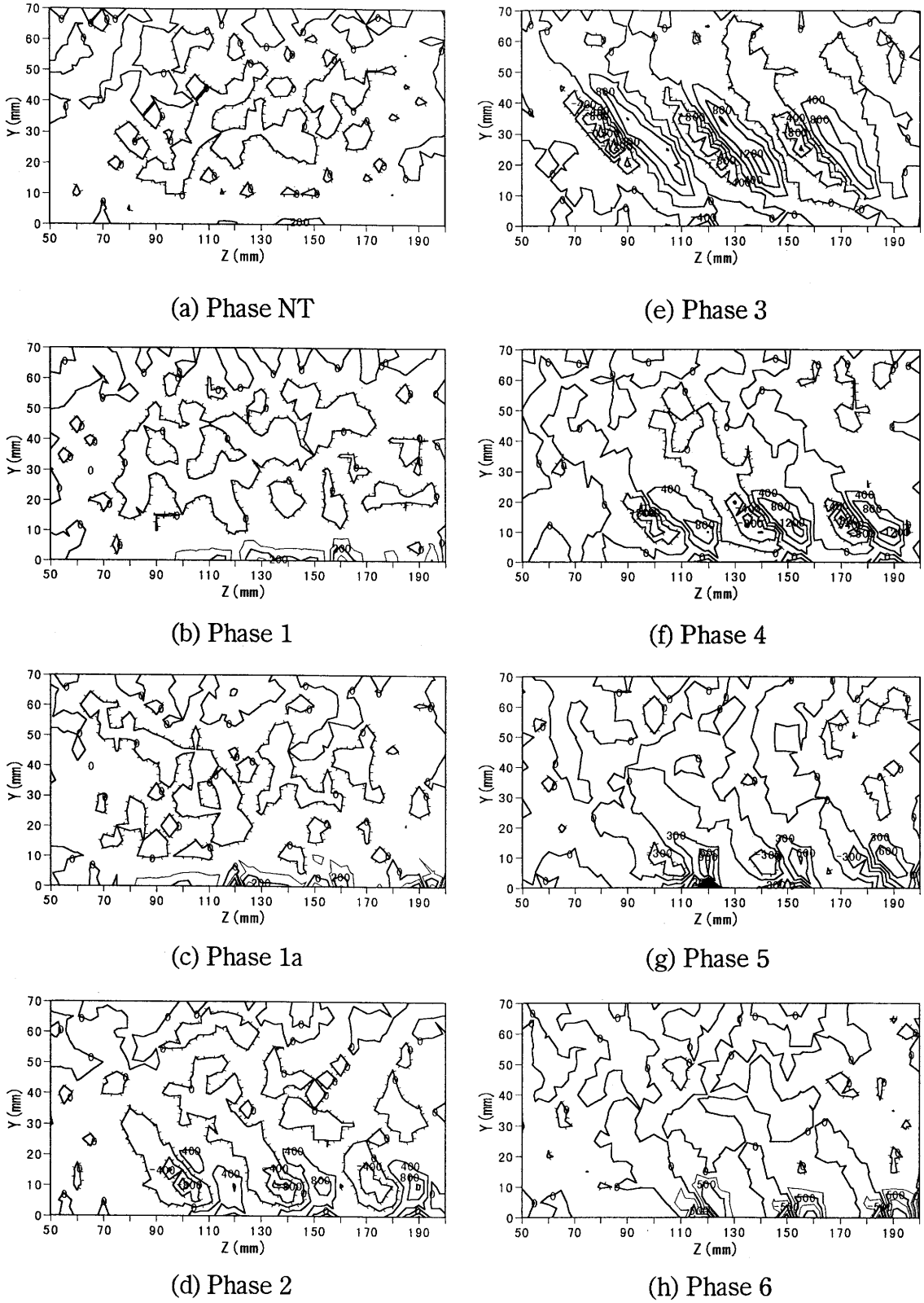

(a) Phase NT

(e) Phase 3

(b) Phase 1

(f) Phase 4

(c) Phase 1a

(g) Phase 5

(d) Phase 2

(h) Phase 6

Figure 6.3 Situation of longitudinal vortices in various phases (X=5 mm, U_0= 6.5 m/s, VR=5.6, f_p=10 Hz).

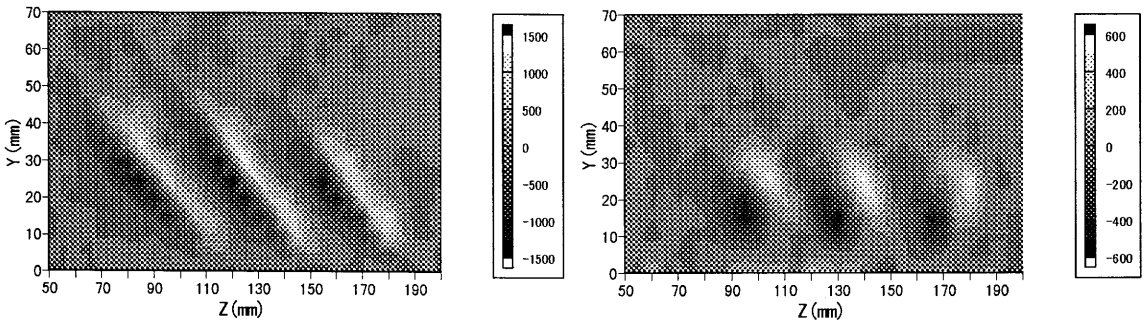

(a) X=5 mm

(e) X=30 mm

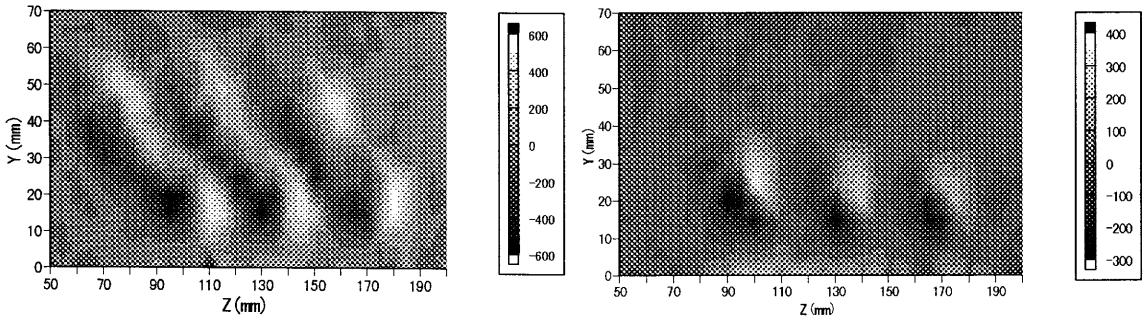

(b) X=20 mm

(f) X=40 mm

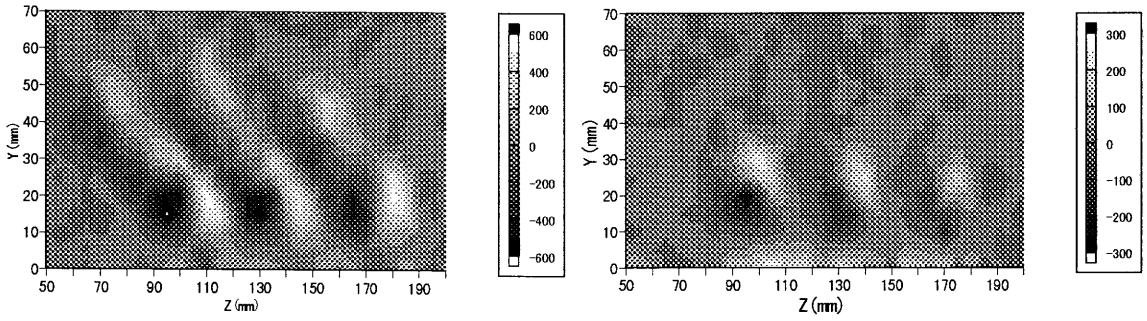

(c) X=22 mm

(g) X=44 mm

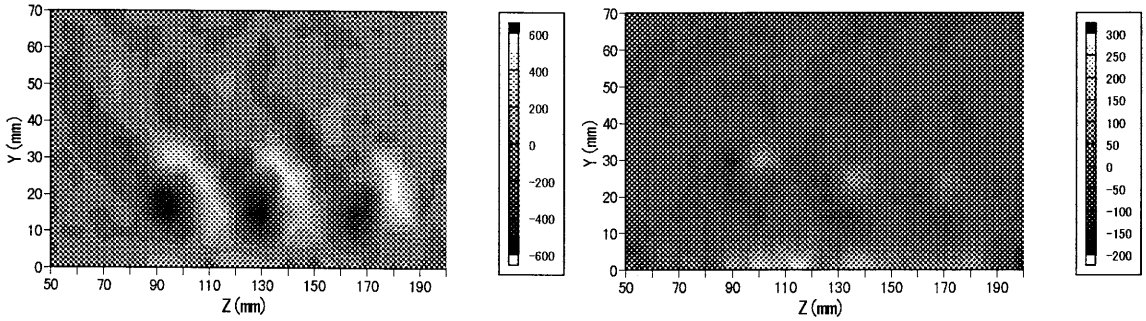

(d) X=26 mm

(h) X=49 mm

Figure 6.4 Downstream development of longitudinal vortices in phase 3 (U_0= 6.5 m/s, VR=5.6, f_p=20 Hz).

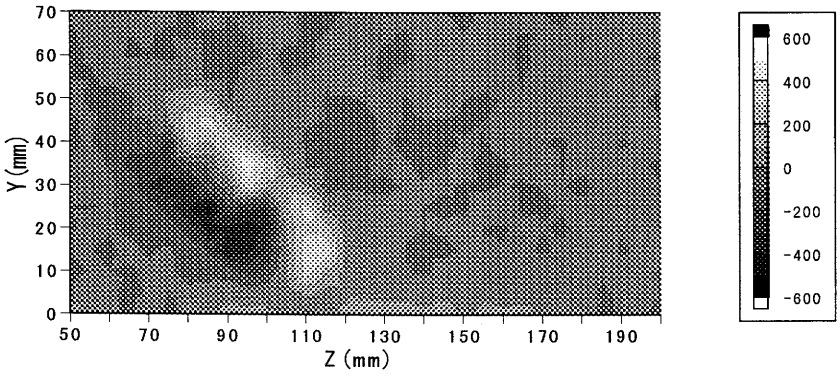

(a) X=20 mm

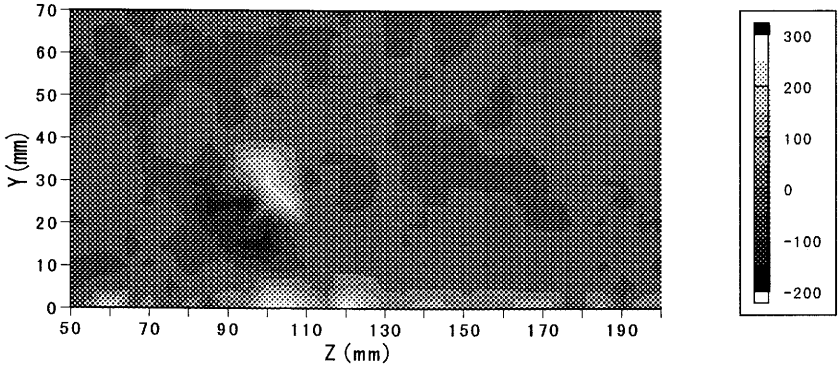

(b) X=40 mm

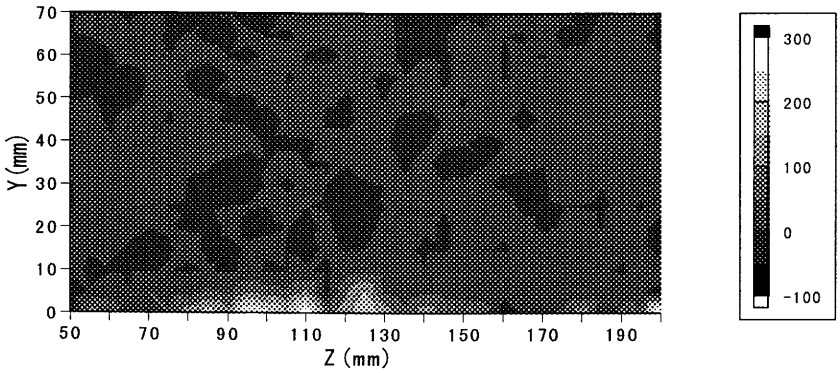

(c) X=60 mm

Figure 6.5 Downstream development of longitudinal vortices (U_0=6.5 m/s, VR=7, f_p=20 Hz).

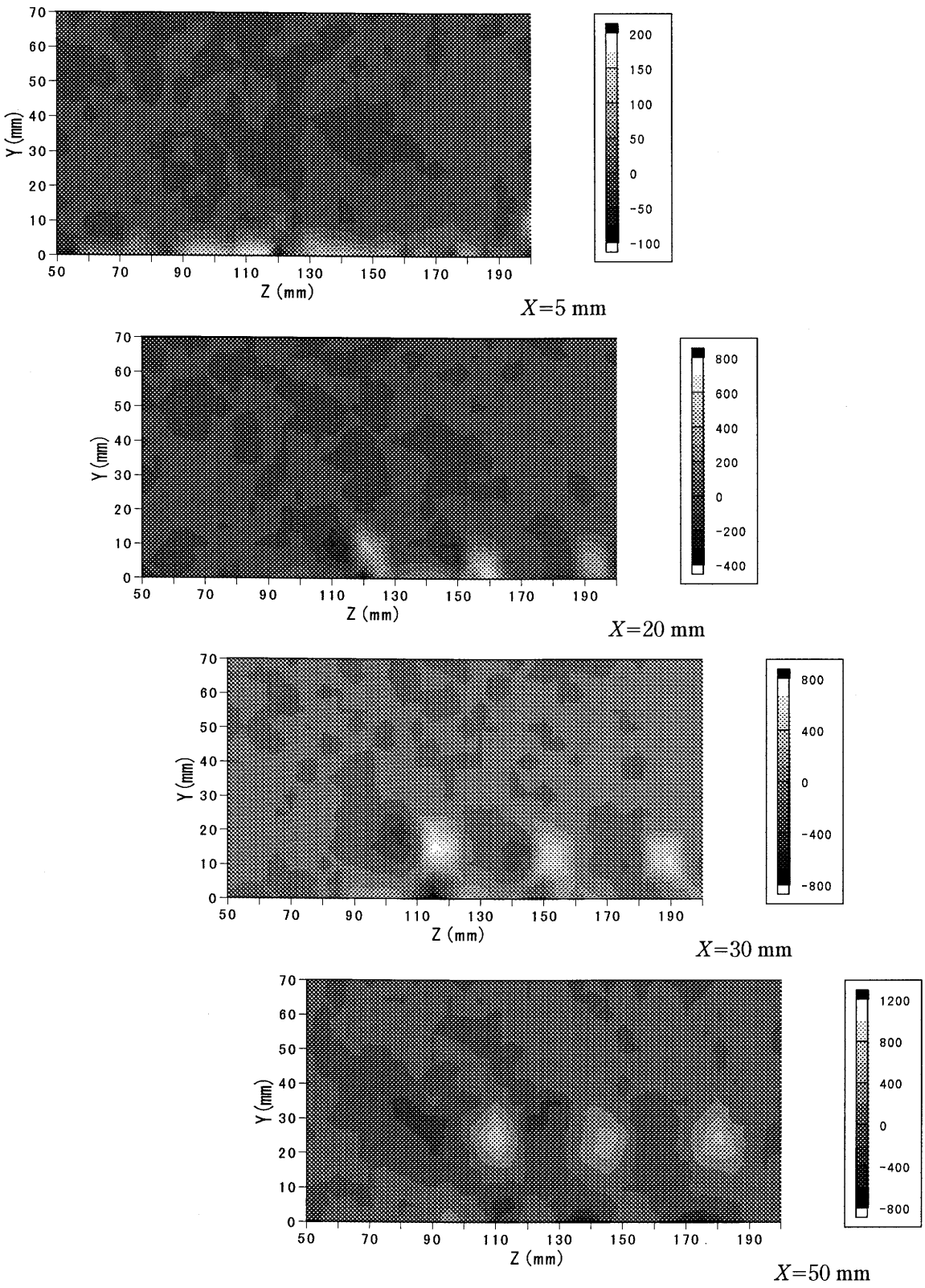

Figure 6.6 Downstream development of longitudinal vortices in phase 7 (U_0= 6.5 m/s, VR=5.6, f_p=20 Hz).

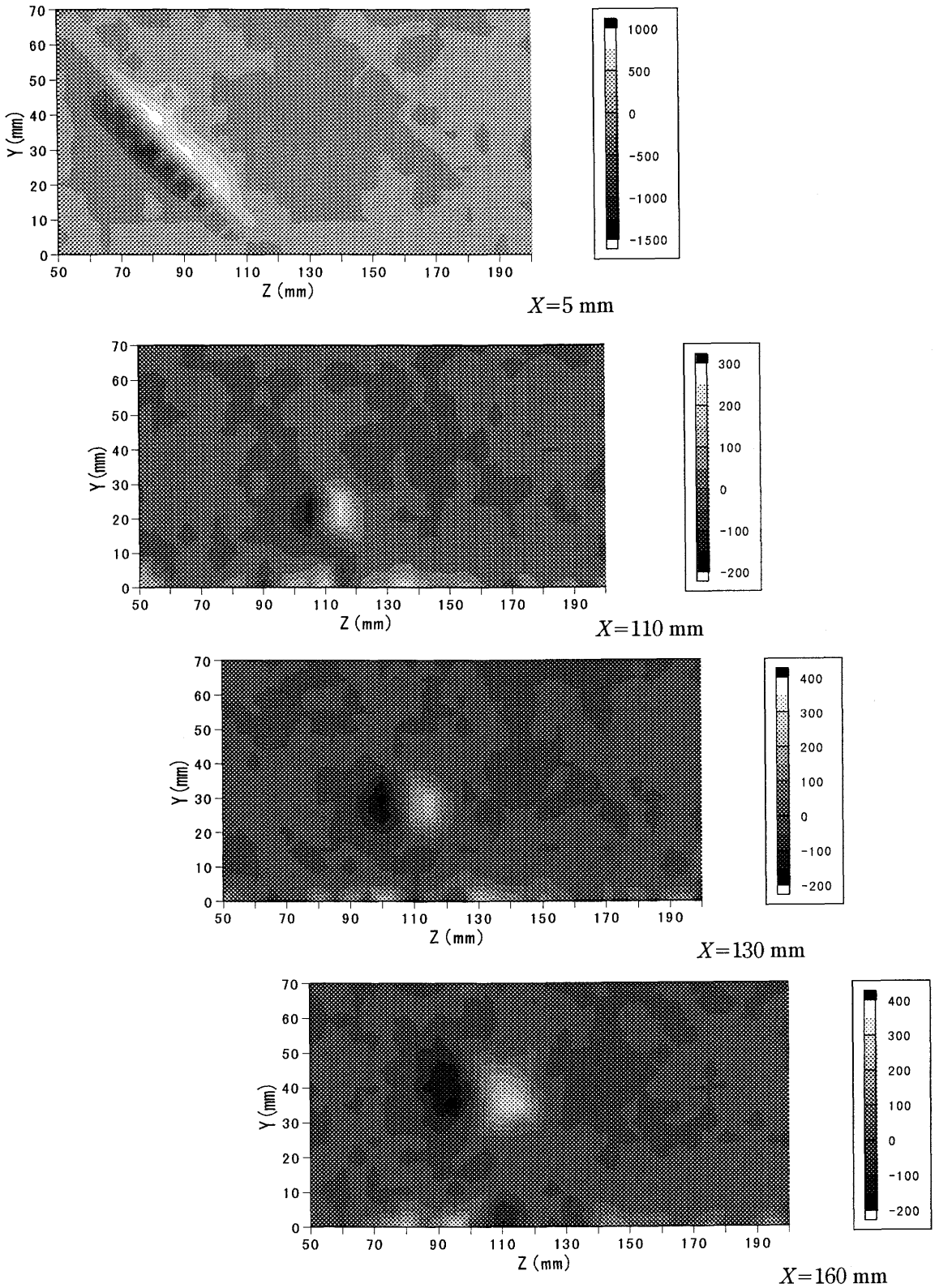

Figure 6.7 Downstream development of longitudinal vortices in phase 3 (U_0= 5 m/s, VR=14, f_p=20 Hz).

7. EFFECT OF JET PITCH ANGLE ON SUPPRESSING FLOW SEPARATION

Compton and Johnston [15] investigated the strength and decay rate of a longitudinal vortex for seven cases of jet skew angle with a pitch angle of 45 degrees. They concluded that an optimal jet skew angle to strengthen the vorticity might be between 45 and 90 degrees to the downstream direction. However, a fixed pitch angle of 45 degrees was examined in their study. Therefore the effect of jet pitch angle on separation control and the subsequent downstream development of longitudinal vortices for various pitch angles were unknown. It is necessary that engineering design data (e.g., jet skew and pitch angles) should be provided for effective utilization because the beneficial effect of separation control is obtained only if the jets are pitched to a wall and skewed with respect to the freestream direction. In this chapter, we investigate the effect of jet pitch angle on suppressing flow separation and the downstream development of longitudinal vortices in three cases of jet pitch angles.

7.1 Experimental Method

Two freestream velocities U_0=6.5 and 11.1 m/s were investigated. The diffuser's divergence angle was set at 20 degrees. Figure 3.3 shows the configuration of jets and the coordinate system used to describe the flowfield. Three jets 2 mm in diameter were placed at the upstream of the divergent lower wall and their orifices were configured on the right side of the lower wall in the test section (viewed from upstream). The jets in this study were skewed at 90 degrees (θ =90 degrees) to the freestream direction (0 degree being downstream). The effect of jet pitch angle on suppressing flow separation was studied experimentally in three cases with the pitch angle set at 30, 45, and 60 degrees.

The jet pitch angle can be changed by replacing the jet orifice unit shown in Fig. 3.4. Velocity measurements were carried out using an X-array hot wire probe. The hot wire probe was supported by a three-axis computer-controlled traverse unit. Streamwise velocity profiles were measured at $Z=110$ mm to avoid the effect of jet orifices and the downstream locations were chosen at $X=40$, 70, and 110 mm. The velocity measurements in a Y-Z plane were carried out at equal spaces of 5 mm, in the X and Y directions. Pressure recovery in the diffuser C_p was made in reference to the static pressure at two measurement points, in the upstream of the divergent portion (unstalled region) and in the divergent portion. Static pressure measurements were carried out at several stations in the divergent portion (see Fig. 3.13) using a differential pressure transducer which had the ability to measure very small differential pressure (0.01 mmAq).

7.2 Results and Discussion

7.2.1 Flow Visualization Results

The surface tuft method was used as the diagnostic technique to observe the effect of jet pitch angle of vortex generator jets on separation control. Tufts were put on the lower wall of the test section at every interval of 15 mm in the downstream direction at $Z=125$ and 140 mm. Figure 7.1 shows the surface flow in the divergent portion of the test section. The air flows from left to right of Fig. 7.1. For an unforced case flow separation is observed near the inlet of the divergent portion. It is seen from Fig. 7.1 that the separation point moves downstream by issuing jets. A pitch angle of 30 degrees or 45 degrees makes separation control more effective than the 60-deg case in the downstream direction.

7.2.2 Velocity Measurements in a Y-Z Plane

Streamwise vorticity of longitudinal vortices produced by the interaction

between the jets and the freestream is shown in Fig. 7.2. In this study, we define the positive vortices in a Y-Z plane for vortices of clockwise-rotation when we view from upstream. For the 30-deg case negative vorticity due to the counter-rotating vortices produced on the upwash side of the longitudinal vortices are weaker than the positive vorticity at $X=10$ mm and therefore a pair of vortices of nearly equal strength does not exist at the measurement planes. In particular, the strength of negative vorticity is very weak compared with that of positive vorticity at $X=70$ and 110 mm. For the 45-deg case three pairs of vortices of nearly equal strength exist at $X=10$ mm. However, at $X=70$ and 110 mm a pair of vortices of nearly equal strength exits near $Z=110$ mm alone. Issuing jets at a pitch angle of 60 degrees have a tendency to produce strong counter-rotating vortices and consequently three pairs of vortices are maintained at the longer downstream location in comparison with the other cases. They move apart more rapidly from the lower wall than the other cases because of the velocity induced by a pair of vortices. In three cases of the jet pitch angle, the 30-deg case can keep the vortices at the location nearest to the lower wall in the downstream direction. The downstream development of longitudinal vortices for $U_0=6.5$ m/s is shown in Fig. 7.3. Comparing Fig. 7.2 with Fig. 7.3, we can see that the downstream development of longitudinal vortices in three cases of the jet pitch angle is quite similar to the $U_0=11.1$ m/s case. However, the vorticity for $U_0=6.5$ m/s decreases more rapidly in the streamwise direction than that for $U_0=11.1$ m/s because the longitudinal vortices are weaker than the $U_0=11.1$ m/s case.

For the 60-deg case three pairs of vortices have similarly upward movements in the downstream direction. On the contrary, for the 45-deg and 30-deg cases the longitudinal vortex of positive vorticity on the left-side edge of Fig. 7.2 or 7.3 at $X=110$ mm is lifted away from the lower wall in comparison with the other vortices. For the 60-deg case longitudinal vortices keep their circular shape. However, for the 45-deg and 30-deg cases positive vortices do not keep their circular shape but rather become wider in the spanwise direction as they grow. Therefore, for the 45-deg and 30-deg cases the spanwise distance between two positive vortices becomes narrow and the negative vortices which exist between two positive vortices are split out in the vertical direction due to the interaction with the positive vortices on both sides. The negative vorticity decreases in the downstream direction and disappears at the longer streamwise distance. The upward movement of the positive vortex is suppressed because the split negative

vortex exists above the positive vortex and no vortex pair is formed. The relationship between the vertical positions of the positive and negative vortices is also seen from Fig. 7.4 which shows the mean vorticity in the spanwise direction. For the 60-deg case the peak positive vorticity has the nearly equal vertical position of the peak negative vorticity. On the contrary, for the 45-deg and 30-deg cases the position of the peak negative vorticity in the vertical direction is higher than that of the peak positive vorticity. The positive vorticity on the left-side edge of Fig. 7.2 or 7.3 forms a vortex pair by the influence of negative vorticity which has not been split out. The positive vortex on the left-side edge of Fig. 7.2 or 7.3 exists at the higher vertical location in comparison with the other positive vortices due to the vortex pair. The movement of a vortex pair coincides with the results about the interaction between a vortex pair and a turbulent boundary layer shown by Pauley and Eaton [9].

Figures 7.5 and 7.6 show secondary flow velocities of longitudinal vortices. The secondary velocities toward the lower wall for the 60-deg case become weaker than those for the other cases because longitudinal vortices are lifted away from the lower wall. On the contrary, for the 30-deg and 45-deg cases the secondary flow toward the lower wall is observed near $Y=-20$ mm, and as a result the effective suppression can be achieved (see Fig. 7.1). The suppression results from keeping longitudinal vortices near the lower wall and therefore the 60-deg case is inferior to the others regarding the control of boundary layer separation. In other words, it is desirable that longitudinal vortices are controlled in keeping their position near the lower wall. However, for the 45-deg case an upwash region is produced in a narrow spanwise region by a vortex pair at $Z=110$ mm (see Fig. 7.5(b) or 7.6(b)). The upwash makes ineffective the secondary flow toward the lower wall.

7.2.3 Separation Effect versus Jet Pitch Angle

The pressure recovery from an unforced case $C_{p_{df}}$ is defined as

$$C_{pdf} = C_{p\,VR} - C_{puf} \ , \tag{7.1}$$

where C_p is expressed in Eq. (2.6), subscript *uf* and *VR* indicate the unforced case

and issuing jet case, respectively. Figure 7.7 shows the distribution of pressure recovery along the wall static pressure holes. It is seen from Fig. 7.7 that the effective pressure recovery is obtained in order of a pitch angle of 30, 45, and 60 degrees for the same VR. In particular, comparing the 30-deg case with the 45-deg case for VR=5.6 at X=110 mm, the high pressure recovery is obtained for the 30-deg case. Figure 7.8 shows the downstream decay of the maximum positive vorticity. The vorticity is strong in order of a pitch angle of 30, 45, and 60 degrees at X=10 mm. However, the vorticity for the 60-deg case is stronger than that for the 45-deg case at X=110 mm. This means that considerable things for separation control are not the strength of longitudinal vortices solely. As mentioned above, for the effective separation control it is necessary that longitudinal vortices exist near the lower wall and the secondary flow which can transport high momentum fluid of the freestream toward the lower wall is produced. For the 30-deg case longitudinal vortices are strong and can keep their positions near the lower wall. Therefore, for the 30-deg case the effective separation control can be achieved in lower VR in comparison with the 45-deg and 60-deg cases.

Figure 7.9 shows the streamwise velocity profiles at X=110 mm. For the 30-deg and 60-deg cases the near-wall velocity increase in the divergent portion is observed. The near-wall velocity increase for the 30-deg case is larger than that for the 60-deg case because the strong secondary flow toward the lower wall is produced by the longitudinal vortices which exist near the lower wall in comparison with the 60-deg case (see Fig. 7.2 or 7.3). On the other hand, for the 45-deg case near-wall velocity increase is not observed. This is because the streamwise velocity measurements are carried out just at the plane where the upwash occurs (see Fig. 7.9).

7.2.4 Suppression Effect in the Downstream Direction

Figure 7.10 shows flow visualization results at X=200 mm for the 30-deg and 45-deg cases. The visualization images indicate that the suppression effect for the 45-deg case persists further downstream and wider in the spanwise direction than that for the 30-deg case. Figure 7.11 shows the distribution of pressure recovery

in the divergent portion. The value of $C_{p_{df}}$ for the 30-deg case is higher than that for the 45-deg case at $X=110$ and 160 mm. However, the value of $C_{p_{df}}$ for the 45-deg case is higher than that for the 30-deg case at $X=200$ and 250 mm. This means that the effective pressure recovery for the 45-deg case is obtained over a longer downstream distance in comparison with that for the 30-deg case.

Figures 7.12 and 7.13 show vorticity contours and secondary flow vectors measured at $X=200$ mm, respectively. Comparing Fig. 7.12(a) with Fig. 7.12(b), we see that the downstream development of longitudinal vortices for a pitch angle of 45 degrees is different from that for a pitch angle of 30 degrees. For the 30-deg case three pairs of vortices become a single vortex. On the other hand, for the 45-deg case three pairs of vortices are degenerated to a counter-rotating vortex pair in the downstream direction. Because for the 45-deg case the negative vortex of nearly equal strength to the positive one is produced near the injection point of the jet flow. On the contrary, for the 30-deg case the negative vortex is weaker than the positive one near the same location. Comparing Fig. 7.13(a) with Fig. 7.13(b), we can see that the secondary velocities for the 30-deg case become stronger in the spanwise direction than in the vertical direction at the region between $Z=120$ mm and $Z=140$ mm. On the other hand, for the 45-deg case the secondary velocities toward the lower wall are strong at the same spanwise region under the influence of a pair of vortices. This is because the secondary flow of the positive vortex in the spanwise direction is interrupted by the secondary flow of the negative vortex at the upper and slant location of the positive vortex and the flow in the spanwise direction is directed toward the lower wall.

Accordingly, in the 30-deg case separation control is made effectively because longitudinal vortices keep their location near the lower wall and become stronger than in the other cases. However, the secondary velocities toward the lower wall become weaker over a longer streamwise distance due to the existence of a single vortex, and as a result the spanwise region in which the suppression effect can be obtained decreases at the longer streamwise direction. On the contrary, for a pitch angle of 45 degrees longitudinal vortices are degenerated to a counter-rotating vortex pair and the suppression effect persists further downstream.

7.3 Conclusions

From the present experimental study for discussing the effect of jet pitch angle of vortex generator jets on separation control, the following conclusions were drawn:

1. The effective separation control using vortex generator jets is accomplished by keeping the location of longitudinal vortices near the lower wall.

2. For a pitch angle of 60 degrees, longitudinal vortices move apart more rapidly from the lower wall than the other cases, and hence the 60-deg case is inferior to the others regarding the control of boundary layer separation.

3. For the 45-deg case, three pairs of vortices are degenerated to a counter-rotating vortex pair in the downstream direction, and as a result the secondary velocities toward the lower wall become strong and the suppression effect persists further downstream. However, if an upwash occurs at the spanwise location, the suppression effect of flow separation could not be achieved in the upwash region.

4. In the 30-deg case, separation control is made effectively because longitudinal vortices become stronger than in the other cases and keep their location near the lower wall. In other words, this case enables us to perform separation control at a lower jet flow rate. However, the region in the spanwise direction which gives suppression effect decreases in the downstream direction in comparison with the 45-deg case because three pairs of longitudinal vortices become a single vortex over a longer streamwise distance and the downward secondary flow becomes weaker near the lower wall.

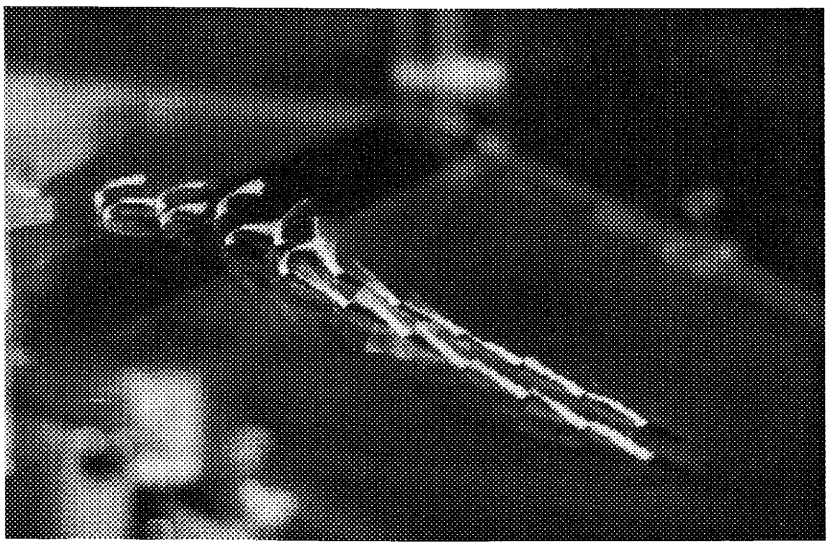

(a) Unforced

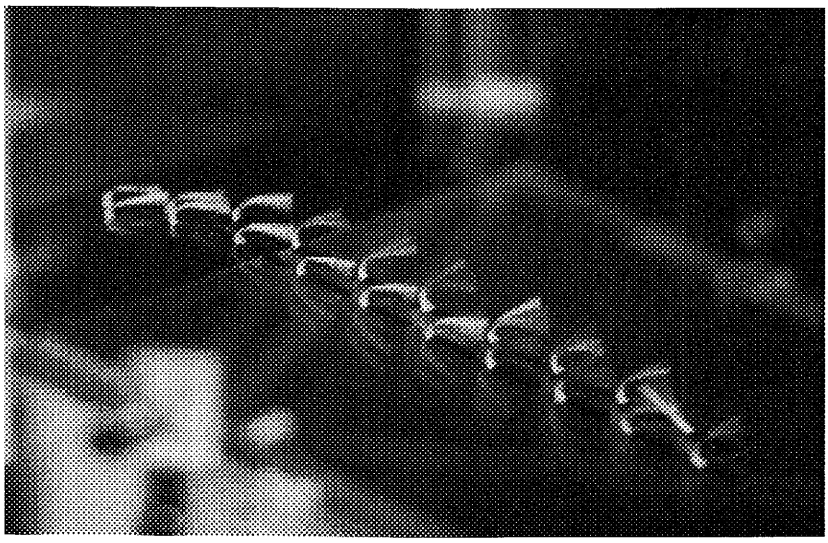

(b) ϕ =30 deg

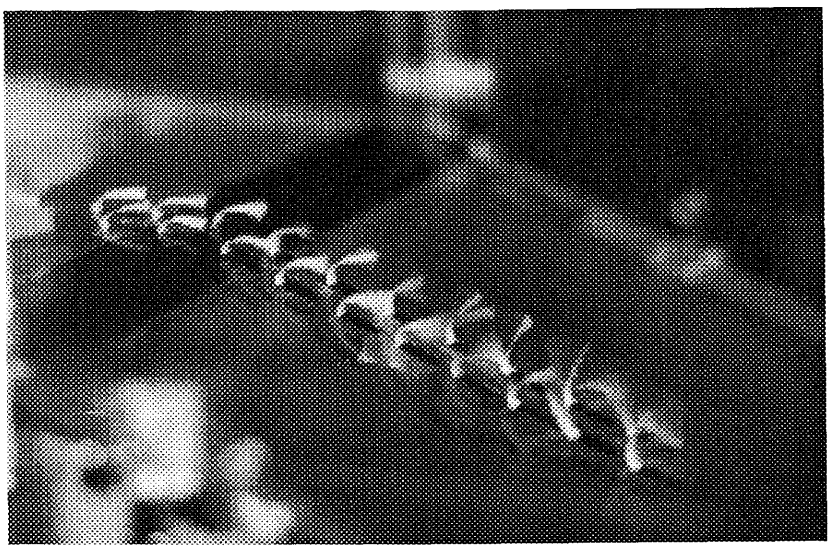

(c) ϕ =45 deg

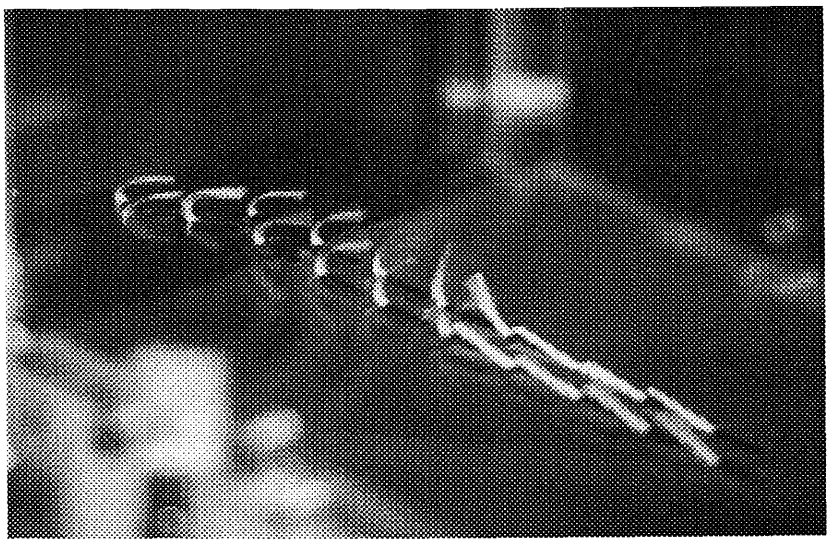

(d) ϕ =60 deg

Figure 7.1 Surface flow in divergent portion of the test section (U_0=11.1 m/s, VR=9.5).

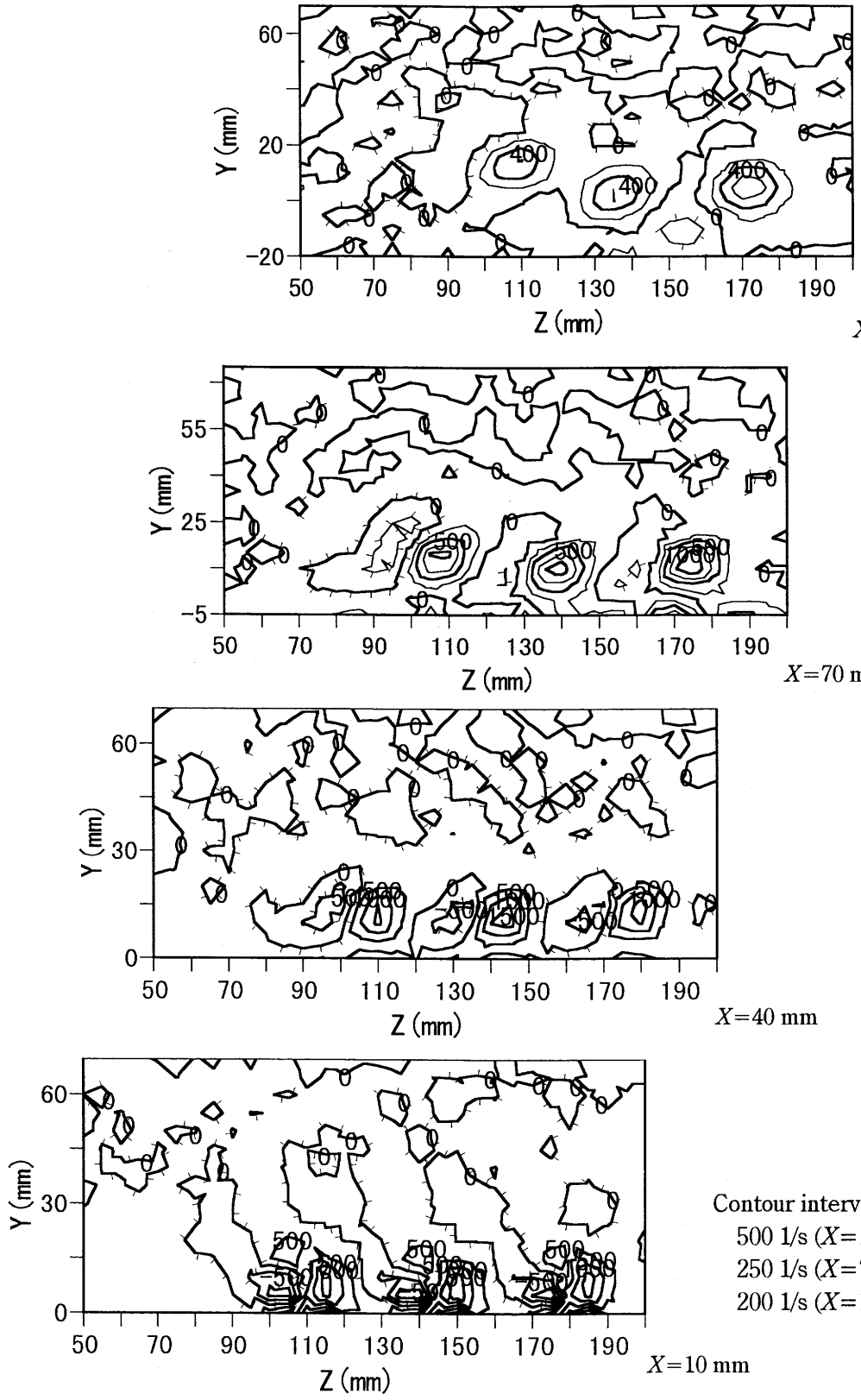
Y (mm)
Z (mm)
X=110 mm
X=70 mm
X=40 mm
X=10 mm
Contour interval=
500 1/s (X=10, 40 mm)
250 1/s (X=70 mm)
200 1/s (X=110 mm)

(a) ϕ =30 deg

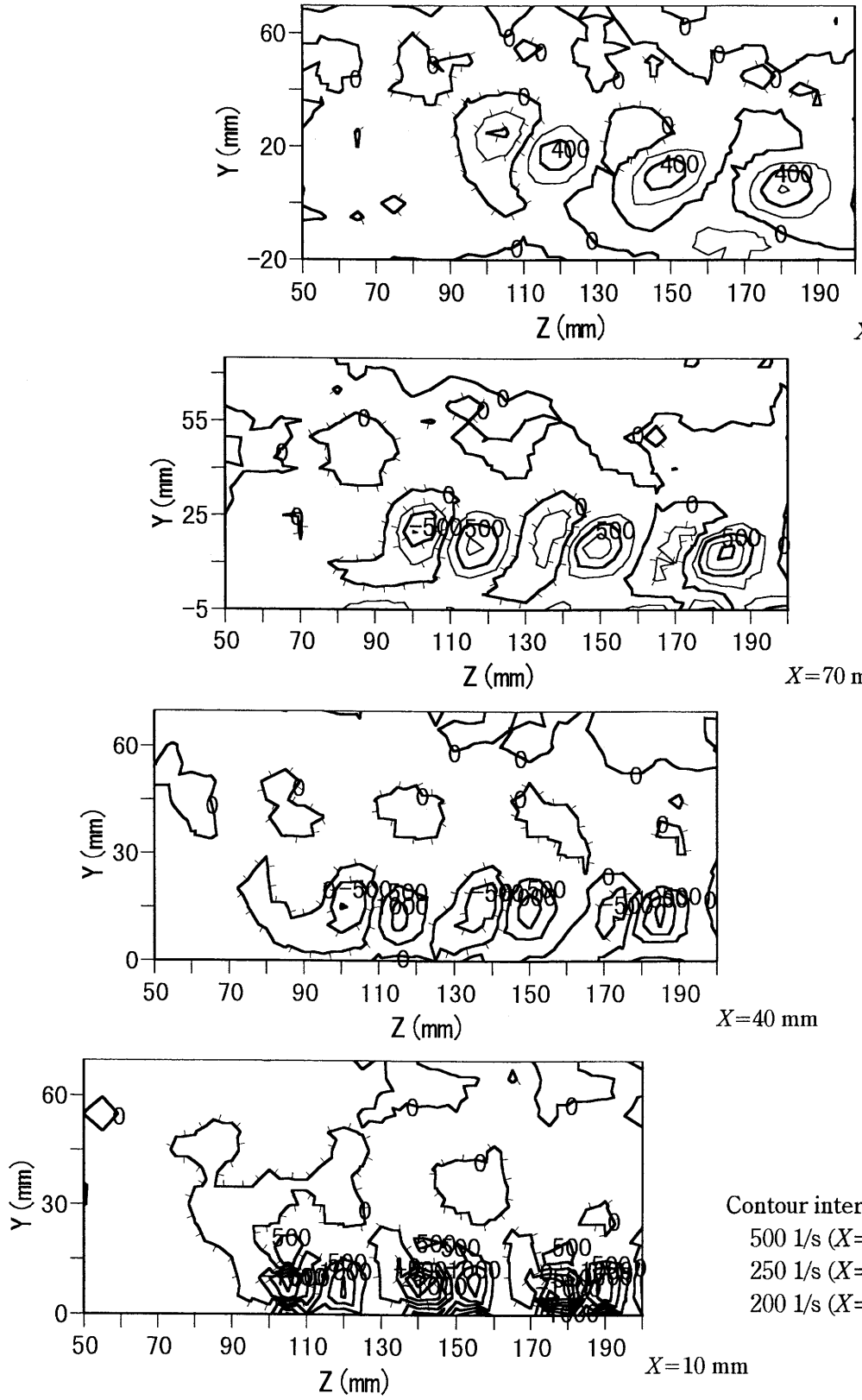
60
20
-20
Y (mm)
50 70 90 110 130 150 170 190
Z (mm)
400
X=110 mm
55
25
-5
Y (mm)
50 70 90 110 130 150 170 190
Z (mm)
500
X=70 mm
60
30
0
Y (mm)
50 70 90 110 130 150 170 190
Z (mm)
X=40 mm
60
30
0
Y (mm)
50 70 90 110 130 150 170 190
Z (mm)
X=10 mm
Contour interval=
500 1/s (X=10, 40 mm)
250 1/s (X=70 mm)
200 1/s (X=110 mm)

(b) ϕ =45 deg

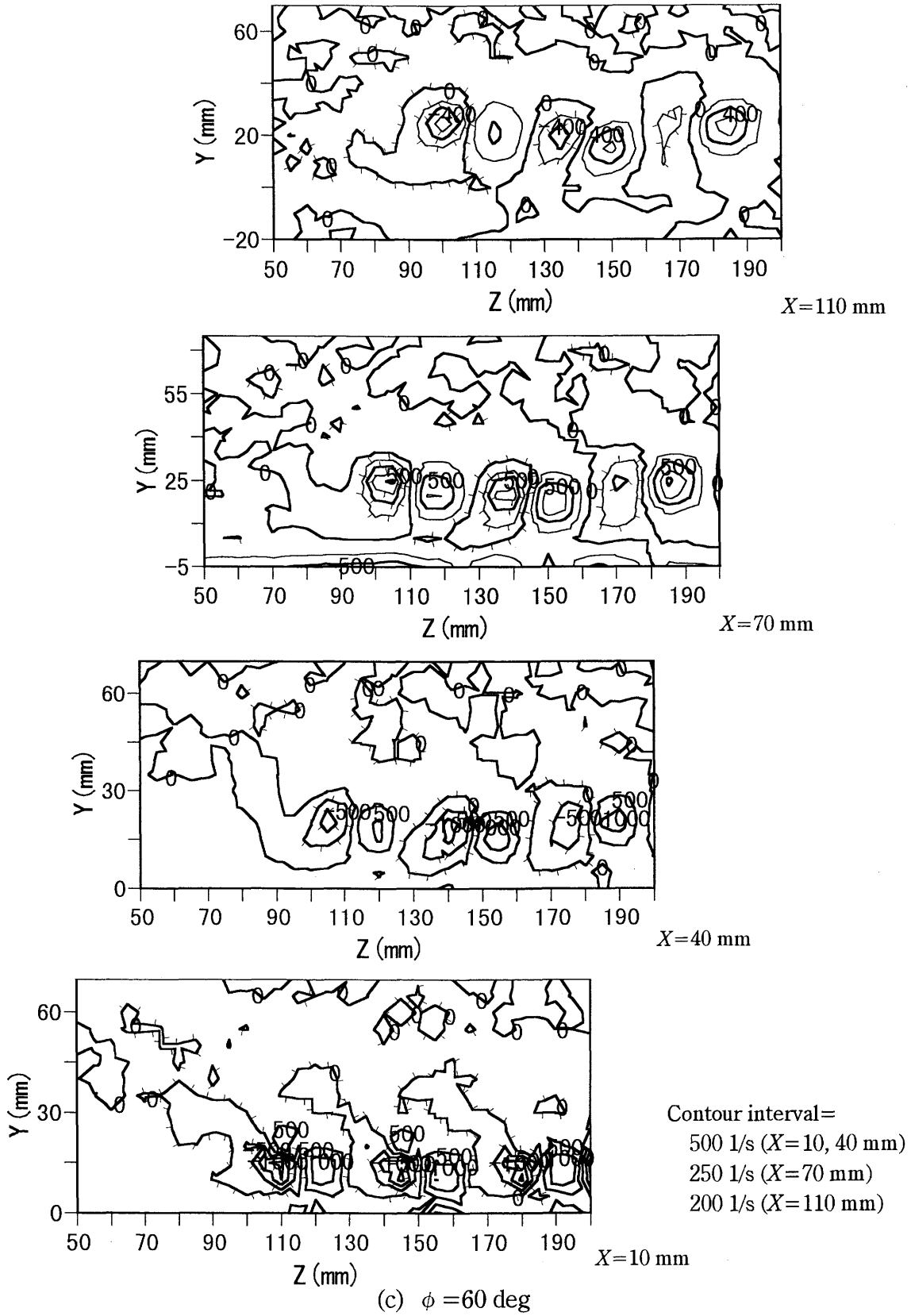

(c) ϕ =60 deg

Figure 7.2 Contours of streamwise vorticity (U_0=11.1 m/s, VR=9.5). Decorated lines denote negative vorticity.

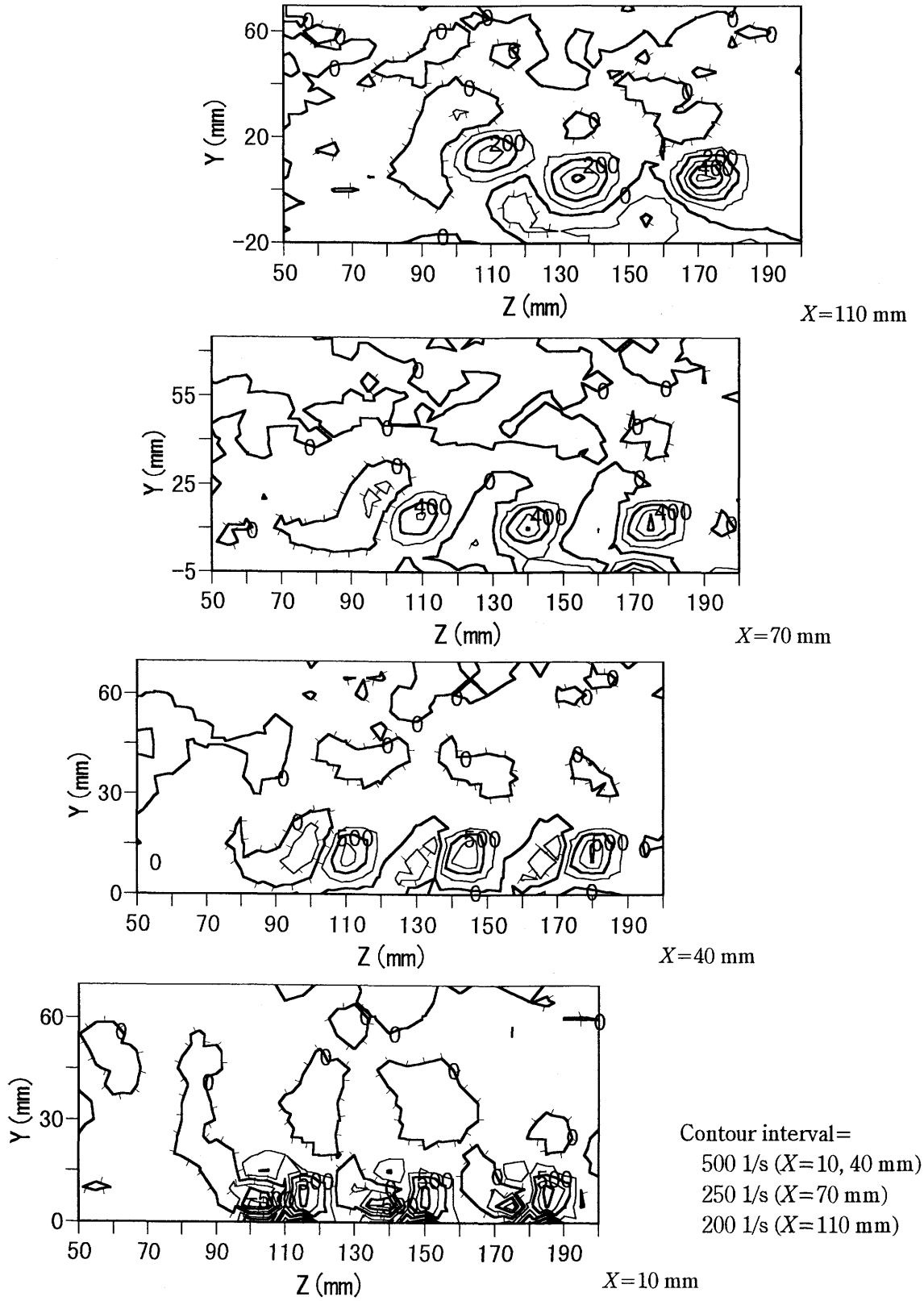
Y (mm)
Z (mm)
X=110 mm
X=70 mm
X=40 mm
X=10 mm
Contour interval=
500 1/s (X=10, 40 mm)
250 1/s (X=70 mm)
200 1/s (X=110 mm)

(a) ϕ =30 deg

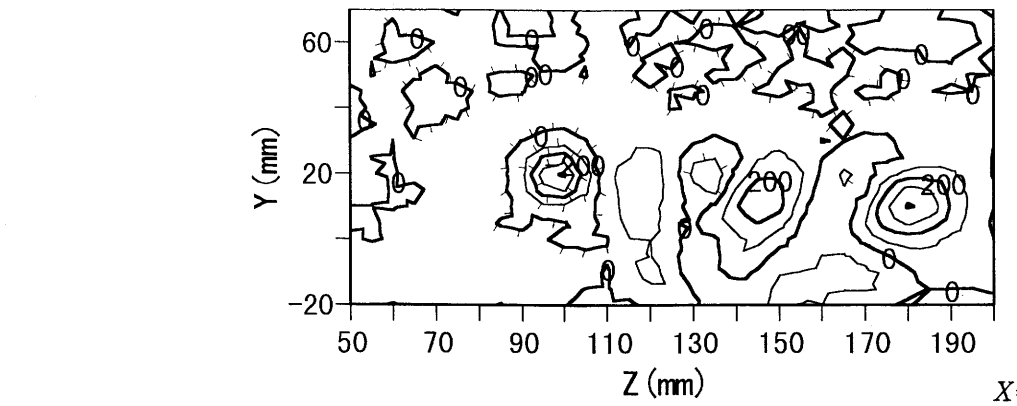

X=110 mm

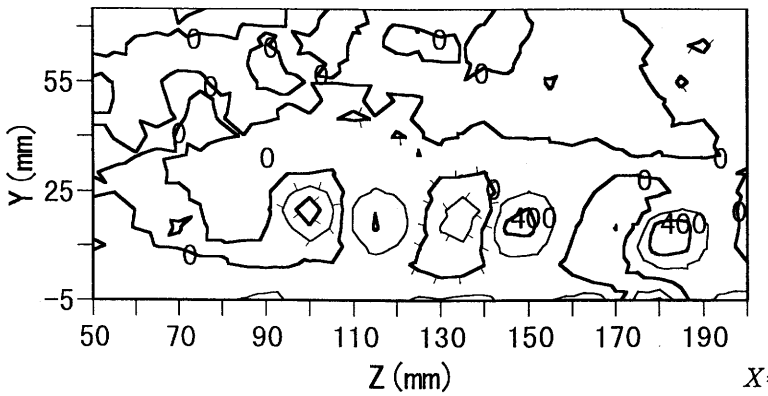

X=70 mm

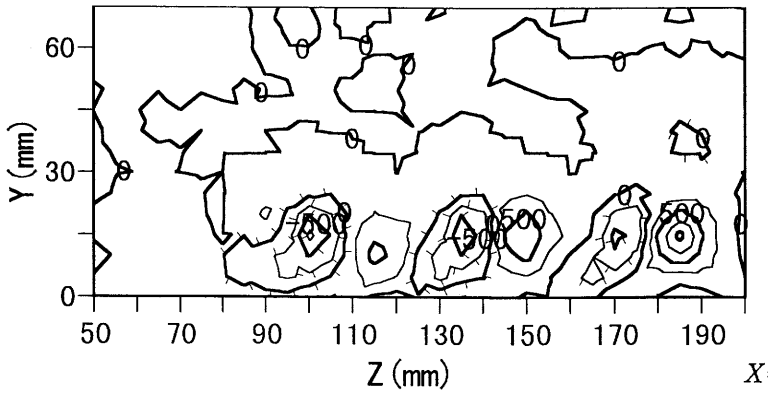

X=40 mm

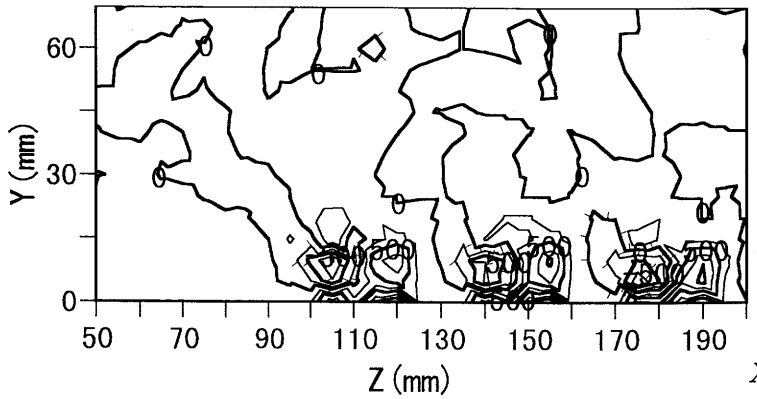

Contour interval=
500 1/s (X=10, 40 mm)
250 1/s (X=70 mm)
200 1/s (X=110 mm)

X=10 mm

(b) ϕ =45 deg

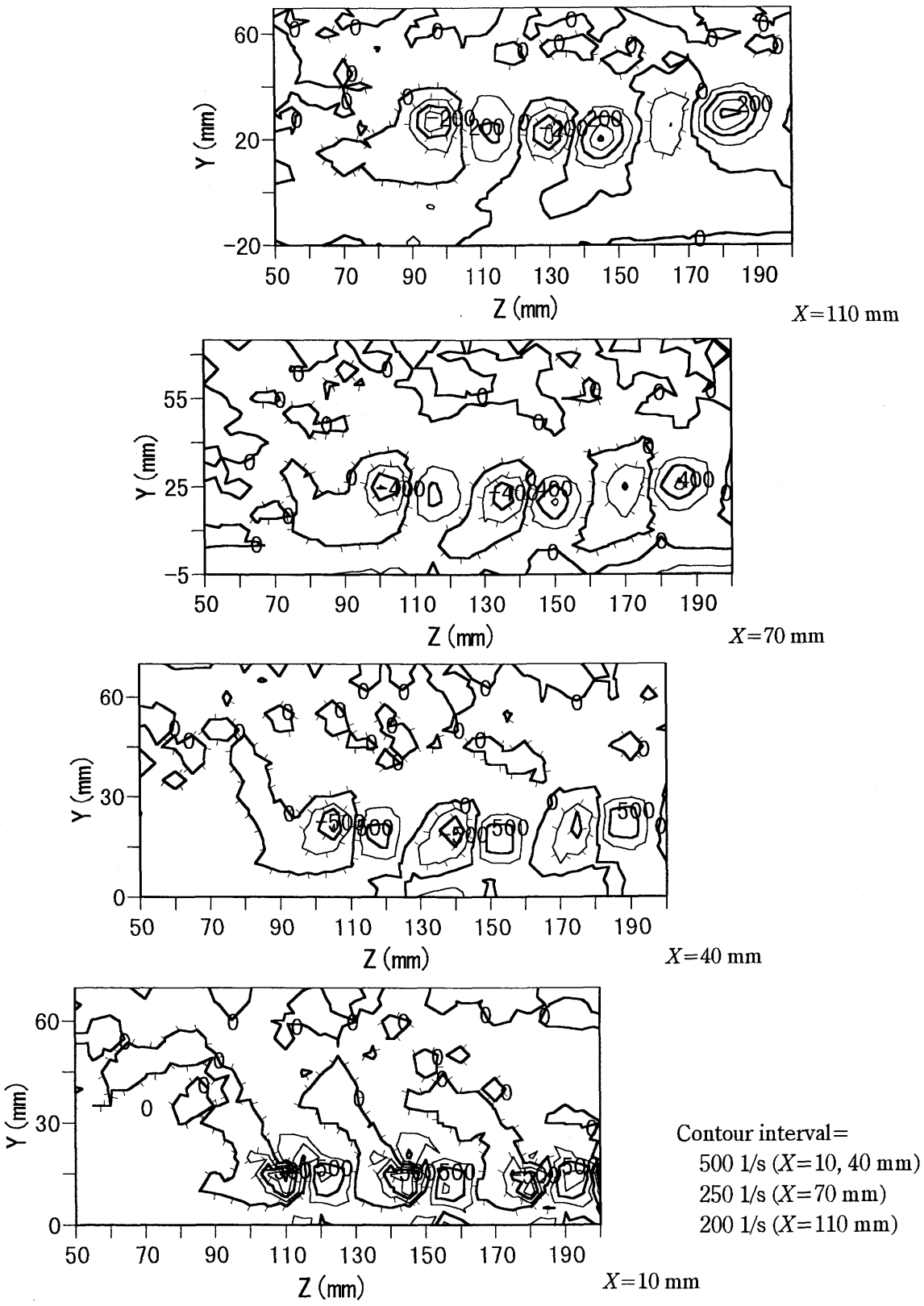

(c) ϕ =60 deg

Figure 7.3 Contours of streamwise vorticity (U_0=6.5 m/s, VR=9.5). Decorated lines denote negative vorticity.

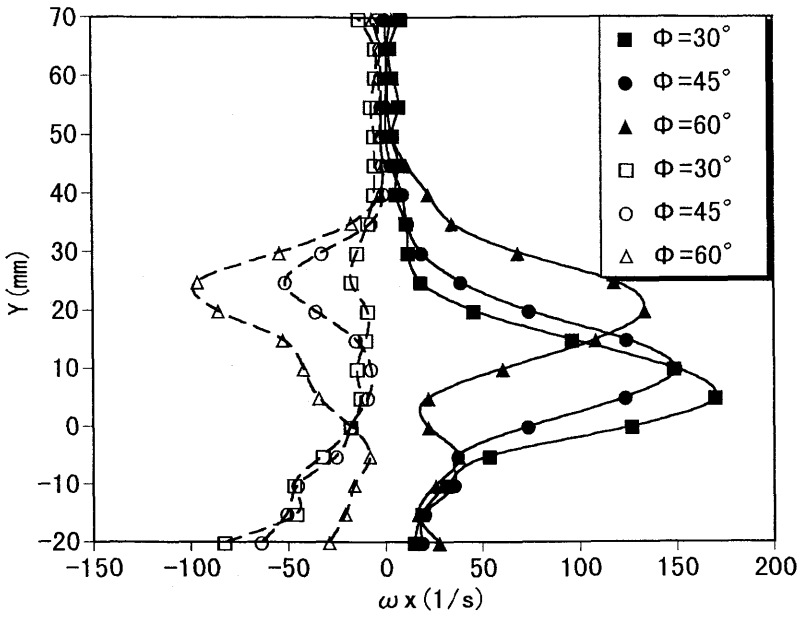

(a) U_0=11.1 m/s, VR=9.5

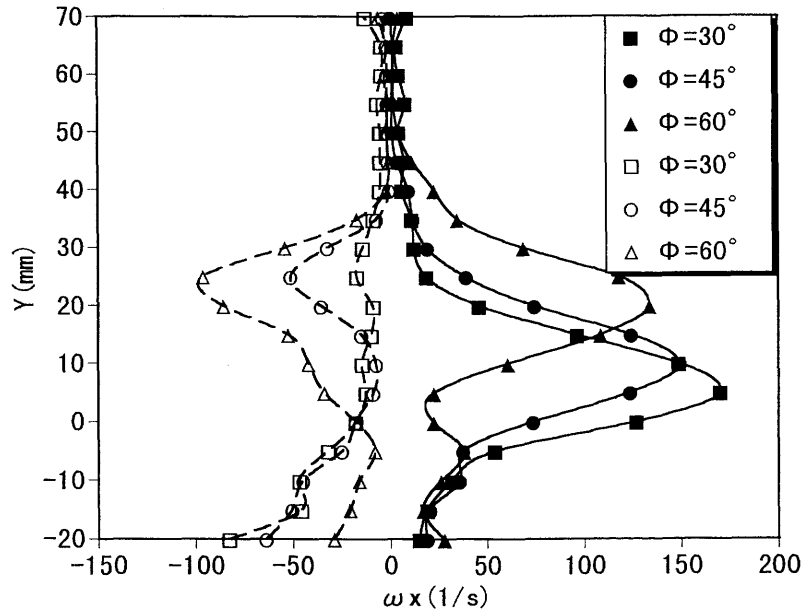

(b) U_0=6.5 m/s, VR=9.5

Figure 7.4 Mean vorticity in spanwise direction at X=110 mm. Open symbols denote negative vorticity.

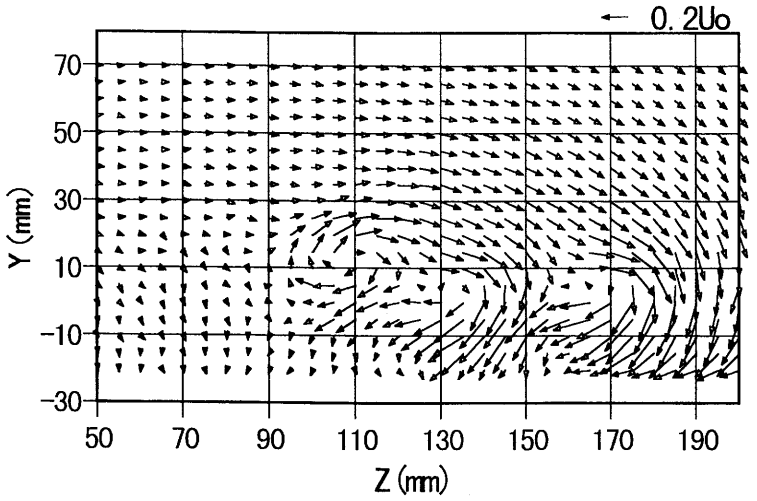

(a) ϕ =30 deg

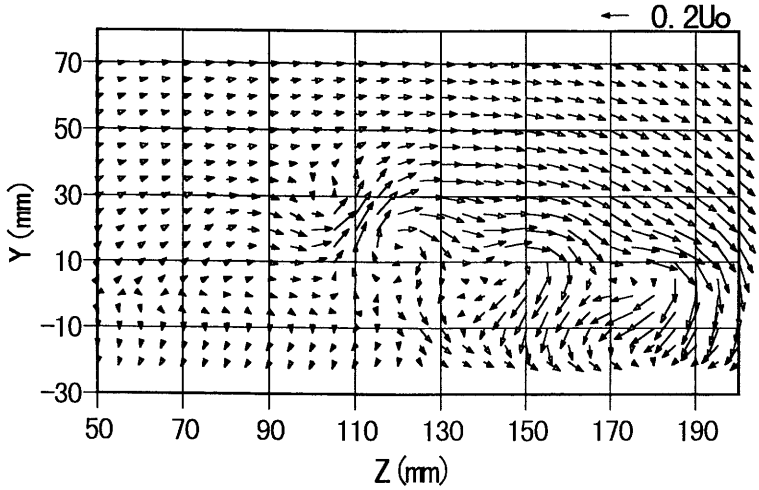

(b) ϕ =45 deg

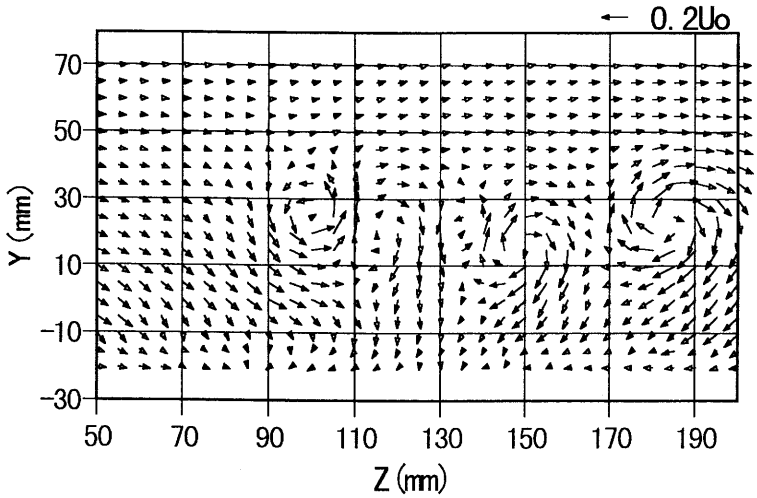

(c) ϕ =60 deg

Figure 7.5 Secondary flow vectors at X=110 mm (U_0=11.1 m/s, VR=9.5).

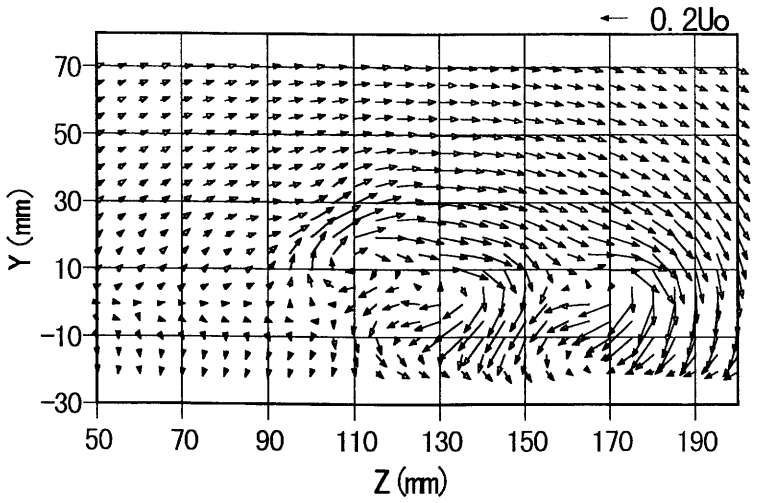

(a) ϕ =30 deg

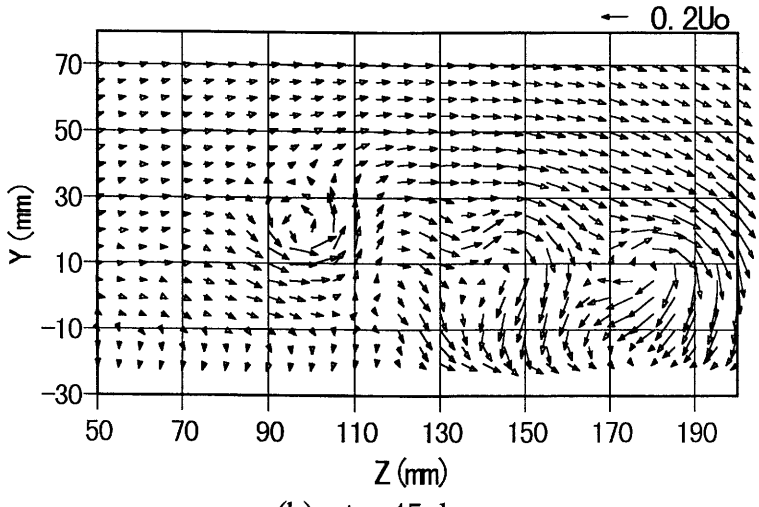

(b) ϕ =45 deg

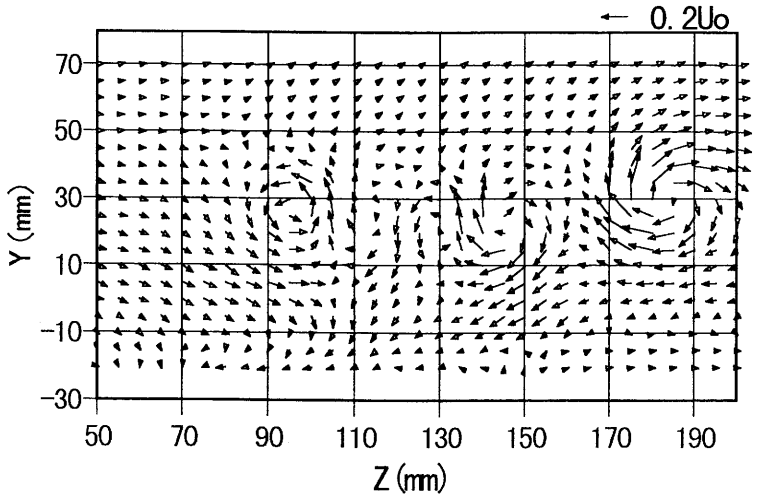

(c) ϕ =60 deg

Figure 7.6 Secondary flow vectors at X=110 mm (U_0=6.5 m/s, VR=9.5).

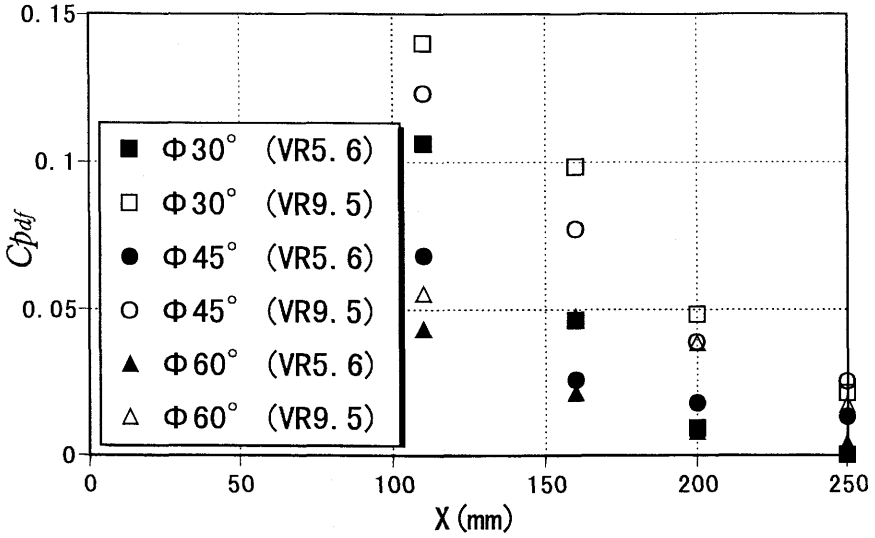

Figure 7.7 Distribution of pressure recovery along the wall static pressure holes of divergent portion (U_0=11.1 m/s).

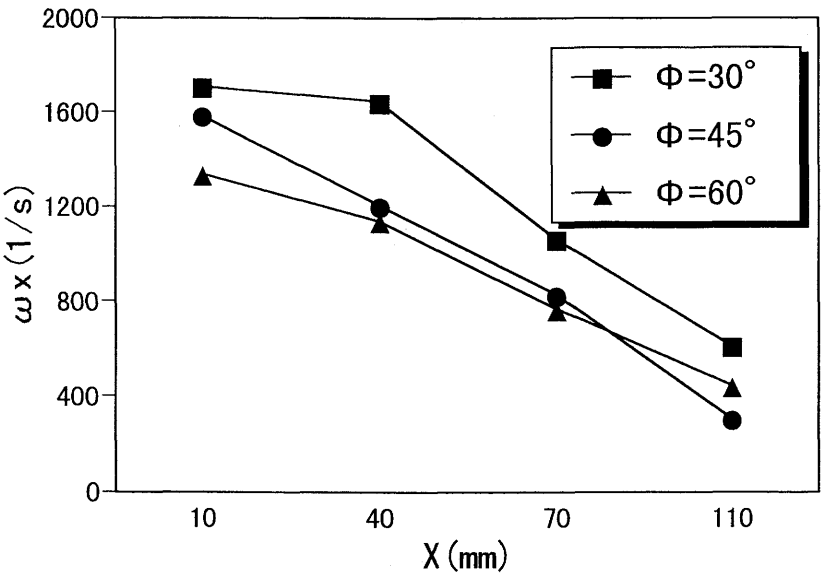

Figure 7.8 Effect of pitch angle on the downstream decay of maximum positive vorticity (U_0=11.1 m/s, VR=9.5).

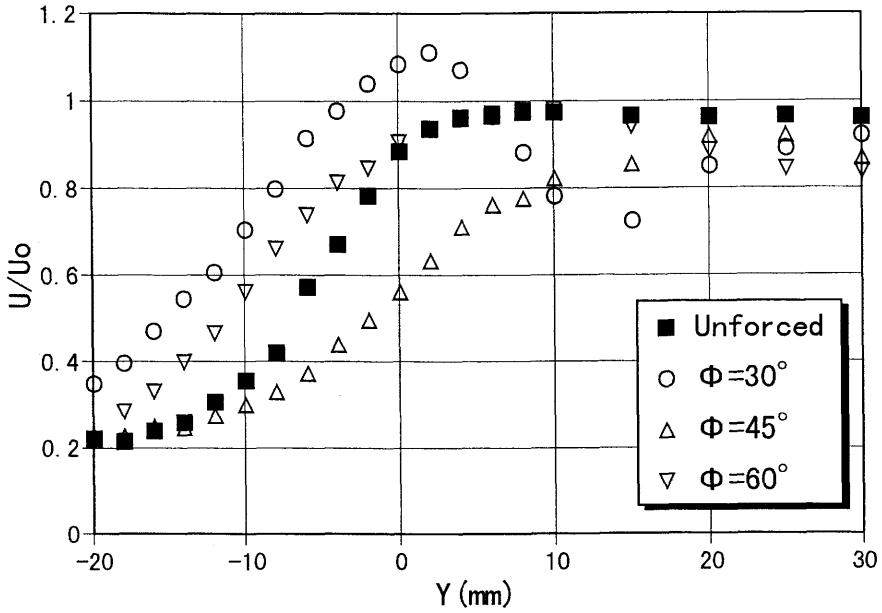

(a) U_0=11.1 m/s, VR=9.5

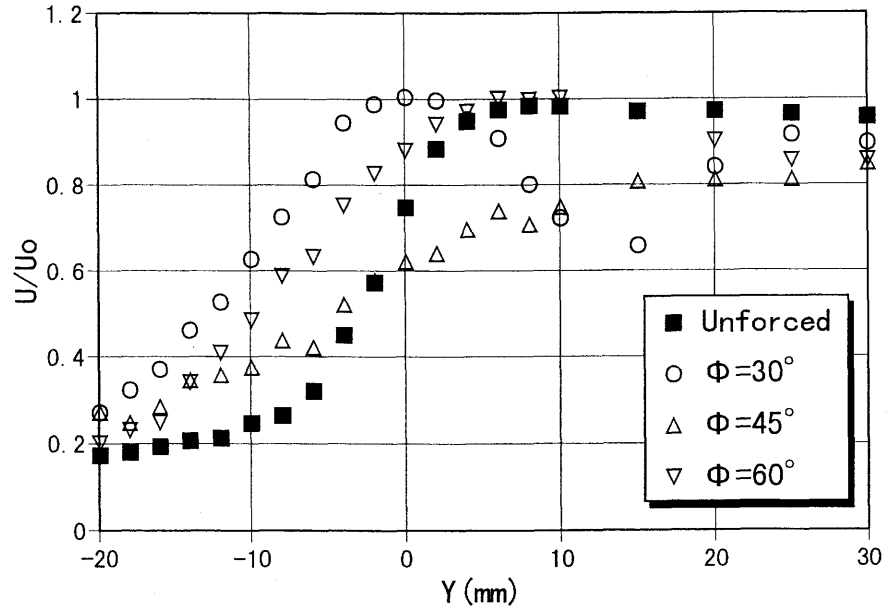

(b) U_0=6.5 m/s, VR=9.5

Figure 7.9 Streamwise velocity profiles at X=110 mm.

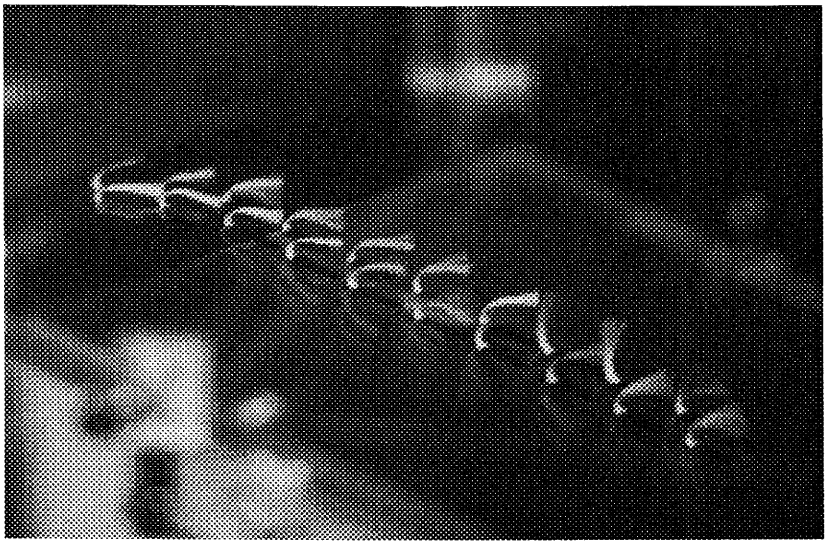

(a) ϕ =30 deg

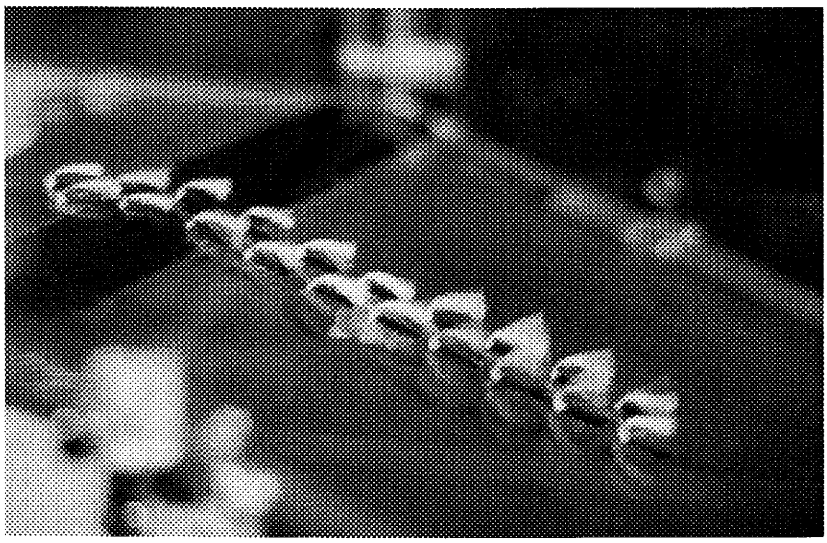

(b) ϕ =45 deg

Figure 7.10 Surface flow in divergent portion of the test section (U_0=11.1 m/s, VR=14).

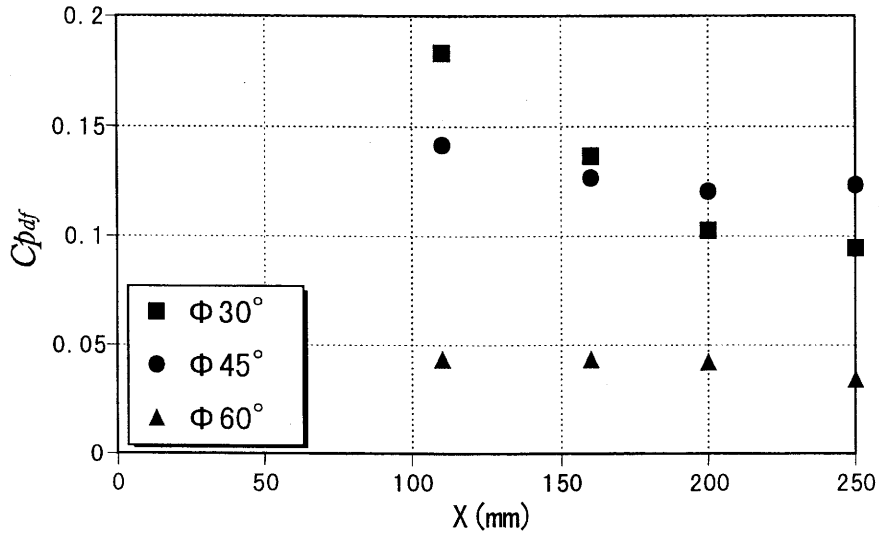

Figure 7.11 Distribution of pressure recovery along the wall static pressure holes of divergent portion (U_0=11.1 m/s, VR=14).

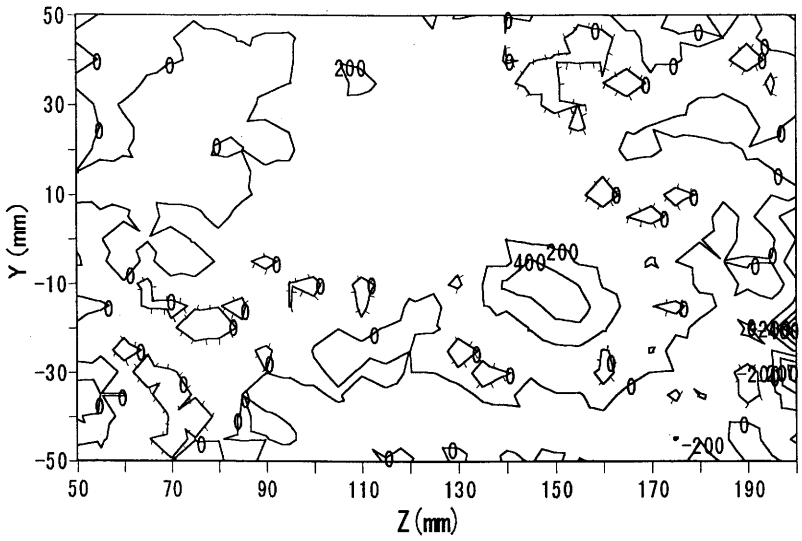

(a) ϕ =30 deg (Contour interval=200 1/s)

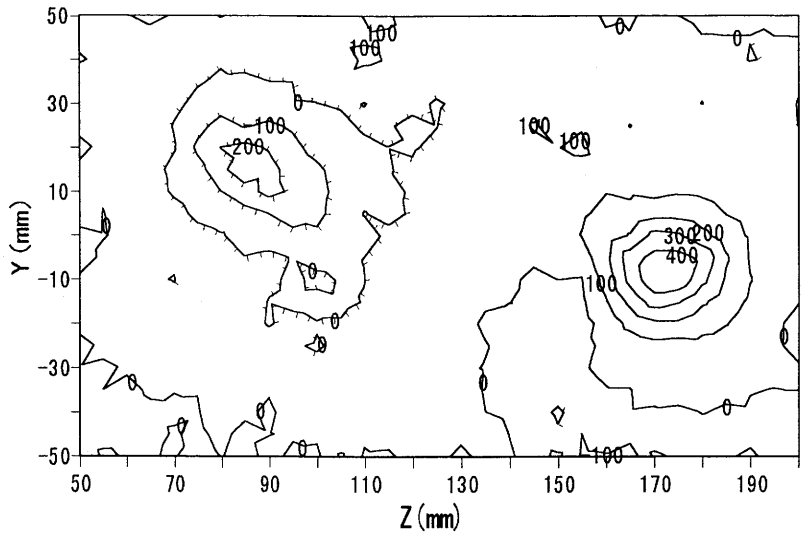

(b) ϕ =45 deg (Contour interval=100 1/s)

Figure 7.12 Contours of streamwise vorticity at X=200 mm (U_0=11.1 m/s, VR=14). Decorated lines denote negative vorticity.

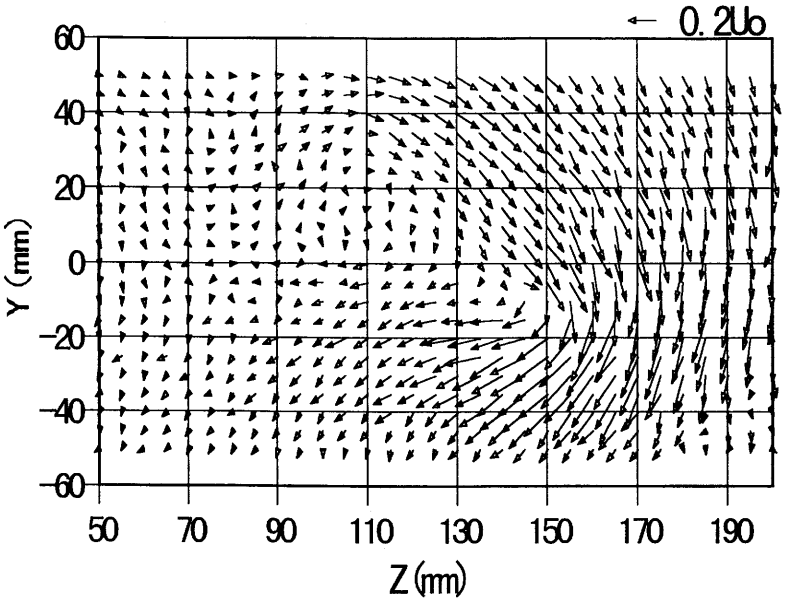

(a) ϕ =30 deg

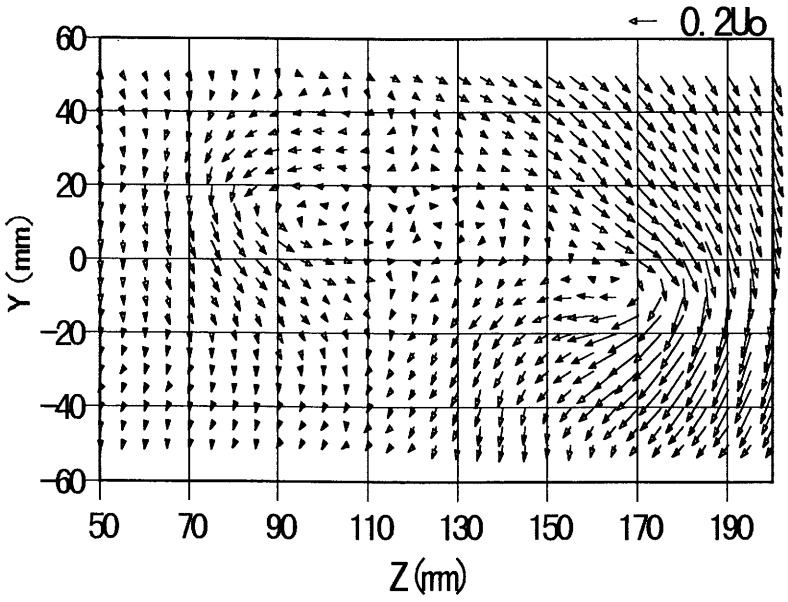

(b) ϕ =45 deg

Figure 7.13 Secondary flow vectors at X=200 mm (U_0=11.1 m/s, VR=14).

8. DEVELOPMENT OF ACTIVE SEPARATION CONTROL FEEDBACK SYSTEM

The vortex generator jet method has been studied since the first examination in the 1950's. In recent years, for the vortex generator jet method the effects of various parameters and longitudinal vortices on separation control begun to be understood gradually. However, any applications of vortex generator jets, which have the ability to control adaptively various flow conditions, to time-varying flow fields have never been reported. In this chapter, an active separation control feedback system is developed in utilizing the results of earlier chapters and is practically applied to flow separation control of a diffuser.

8.1 Experimental Method

Experiments were conducted in a low speed wind tunnel. A schematic diagram of the wind tunnel is shown in Fig. 3.1. The test section had the function of a variable diffuser which could adjust the divergence angle between 0 and 45 degrees. In the present experimental system, flow does not separate at the divergence angle between 0 and 10 degrees. A detailed diagram of the test section is shown in Fig. 3.2. Jet flow was delivered through a metering valve after accumulating the air to a tank by using a compressor. A rotameter was placed downstream of the metering valve. Three jet orifices were placed at the upstream of the divergent lower wall and they were configured on the right-hand side of the lower wall in the test section (see Fig. 3.3). The jets were skewed at 90 degrees (θ =90 degrees) with respect to the freestream direction (0 degree being downstream). If we do not mention particularly, we set the divergence angle of the test section, the jet pitch angle and the jet orifice diameter as α =20 degrees, ϕ =45 degrees and D_j=3 mm, respectively.

Velocity measurements were carried out using an X-array hot wire probe. The hot wire probe was supported by a three-axis computer-controlled traverse unit. The active separation control feedback system was practically applied to time-varying flow fields. In this study, the flow conditions could be changed by varying the freestream velocity and the divergence angle of the test section. Separation control was made in reference to the static pressure at two measurement points, in the upstream of the divergent portion (X=-150 mm, unstalled region) and in the divergent portion (X=110 mm). Static pressure measurements were carried out at several stations in the downstream direction (see Fig. 3.13) using a differential pressure transducer which had the ability to measure very small differential pressure (0.01 mmAq). The pressure value was converted from the output voltage of the differential pressure transducer. For the vortex generator jet method the strength of longitudinal vortices could be adjusted by varying the jet speed and therefore separation control corresponding to the degree of separation became possible by adjusting the jet speed. Figure 8.1 shows the flow chart of this system (Active Separation Control System Using Vortex Generator Jets: ASCSVGJ) and Fig. 8.2 shows the schematic diagram. This system mainly consists of a differential pressure transducer, a valve with controller, and a personal computer. The valve was actuated by an electric signal from the personal computer. In this system, a differential pressure between two points, the upstream of divergent portion and the measurement station in the diffuser, which judge the initial flow situation were measured initially. If a flow separation was detected, the vortex generator jet device operates and controls the jet speed to suppress the separation.

8.2 Results and Discussion

8.2.1 Control System of ASCSVGJ

The variable *dif* denotes the state value of this system for judging the flow situation, defined by

$$dif = \frac{dpv - dpv_{int}}{dpv_{uf} - dpv_{int}}, \tag{8.1}$$

where dpv is the output voltage of the differential pressure transducer and the subscript *int* indicates the initial voltage when no wind blows and *uf* indicates the situation before issuing jets. A control reference SV, which was used as a judging parameter of the suppression of flow separation, was determined by using a state value of this system *dif*. Concretely speaking, SV is the state value of the system when the suppression of flow separation is achieved. Whether separation occurs or not is judged in reference to the flow visualization results. Therefore, if the system achieves the pressure recovery sufficiently above the control reference, the system judges the attainment of the control. Figure 8.3 shows the pressure recovery of the diffuser along the flow direction for two cases of control reference. For the case of SV-Case 1 the value of SV was set to 0.7. SV-Case 1 is provided for the purpose of attaining the suppression at X = 110 mm. For SV-Case 2 the value of SV was determined to maintain the suppression effect even in the further downstream. For both cases this system measures the static pressure at the same position in a diffuser (X=110 mm). It can be seen from Fig. 8.3 that at X=250 mm SV-case 2 has a more effective pressure recovery in comparison with SV-Case 1. In other words, this system has the ability to select basic (suppression up to the measurement position) and extended (suppression persisting further downstream) control by setting up the control reference SV. In this paper, SV-Case 1 is reported.

Figure 8.4 shows the differential pressure variation after this system began to suppress flow separation in three freestream velocities. Figure 8.4 indicates that effective pressure recovery can be achieved by operating the system for each freestream velocity. This system continues to control after attaining the suppression of flow separation. In the control process, varying the freestream velocity causes change in the differential pressure. However, this system has the ability to correct the differential pressure change by including dpv_{uf} in the state value *dif*. In other words, this system enables us to judge the suppression effect using the same SV for different freestreams. In order to approach the state value *dif* to control reference SV, the jet speed is adjusted. The control variable q is defined as the jet flow rate per control step and is set to be constant. However, only for the situation in which *dif* approaches SV, the value of q is decreased and the overshooting of the target value is prevented.

8.2.2 Control Effect of ASCSVGJ

Figure 8.5 shows the flow visualization in the divergent portion of the test section for U_0=6.5 m/s. The surface tuft method was used as a diagnostic technique to observe the effect of the active separation control system on separated flows. Tufts were put on the lower wall of the test section at Z=140 mm. In Fig. 8.5, the air flows from left to right and the tuft of the downstream side of this figure is at X=110 mm. It is seen that this control system can suppress flow separation.

If the rate of pressure recovery of the diffuser is defined near the center axis of the wind tunnel, pressure losses may be neglected. Then from Eq. (2.10), the local pressure recovery coefficient C_{p_L} for U_i and U_e is given by

$$C_{p_L} = \Delta p / \frac{1}{2}\rho U_i^2 \; ; \quad \Delta p \approx \frac{1}{2}\rho(U_i^2 - U_e^2) \tag{8.2}$$

where subscript i and e indicate the inlet and outlet of the diffuser, respectively. In this study, U_i was measured at X=-10 mm and U_e at X=250 mm. Those two measurement stations are the movable limits of the traverse unit. For the case of U_0=6.5, 8.5 and 11.1 m/s, diffuser effectiveness ($\eta = C_{p_L}/C_{p_{th}}$) was 0.6, 0.5, and 0.4, respectively. The diffuser effectiveness for U_0=11.1 m/s was lower than that for the other cases, because the effective suppression of flow separation was not achieved over a longer streamwise distance. For the same VR the vorticity of the longitudinal vortex became stronger as the freestream velocity became faster. The suppression of flow separation was achieved with low VR at X=110 mm for U_0=11.1 m/s in comparison with the other cases of U_0=6.5 and 8.5 m/s. Therefore, for U_0=11.1 m/s the suppression is not maintained in the downstream direction. From Fig. 8.3, it is clear that the effective pressure recovery in the downstream of X=200 mm is not achieved for SV-Case 1.

Using an X-array hot wire probe, we tried to measure the back-flow behavior in order to clarify the effectiveness of this system in separation control. The measurements were carried out by applying the manner shown by Nishi et al. [20]. As shown in Fig. 8.6, an X-array hot wire probe with an L-type support was inserted in the divergent portion of the test section so as to be perpendicular to the freestream direction. The increment of output of channel 2 is greater than that of channel 1 due to the blocked effect of the longer prong, if the flow is in the forward

or downstream direction. On the other hand, under the back-flow condition the increment of output of channel 1 becomes greater than that of channel 2 because the longer prong does not affect the output. Making use of this character of X-array hot wire probe, the comparison of back-flow behavior between the cases in control and without control of this system was made. The output of X-array hot wire probe is shown in Fig. 8.7. It is seen that the output of the channel 1 decreases considerably in control and that of the channel 2 increases in control. Therefore, it can be said that the flow in the downstream direction increases for the case in control.

8.2.3 Applications of ASCSVGJ to the Separated Flow

In order to adaptively suppress flow separation, this system was applied to time-varying flow fields caused by change in the freestream velocity or that of the divergence angle of the test section. Figures 8.8 and 8.9 show the time variation of differential pressure under control for the flow field which causes flow separation. In these figures, point "A" is just when the separation control is attained by operating the system. Point "B" indicates the point at which the flow condition is changed and point "C" is when the system senses change in the flow conditions and restarts to suppress the flow separation.

Figure 8.8(a) shows the differential pressure plotted against the control time for the situation in which flow separation occurs due to change in the freestream velocity after the suppression of flow separation has been attained. In this example, the flow is separated initially. The system tries to suppress flow separation and attains suppression at point "A". Beyond point "A", the system keeps the jet speed constant. When the freestream velocity is changed at point "B", the flow separation can not be suppressed by the given jet speed and therefore the differential pressure decreases. The system restarts to suppress flow separation at point "C" and as a result the suppression is attained at point "A". After that time, the system keeps the jet speed constant.

Figure 8.8(b) shows the time variation of the differential pressure for the situation in which no flow separation occurs, though the freestream velocity changes. The system initially tries to suppress flow separation for the separated

flow field and attains the suppression at point "A". Beyond point "A", the system maintains constant jet speed. The freestream velocity changes at point "B", but the flow does not separate and the differential pressure increases. The system restarts at point "C" and decreases the jet speed. The differential pressure begins to decrease, and beyond point "A" the system keeps the jet speed constant. The system can decrease the jet speed in order to optimize performance or to avoid secondary air loss for issuing jets.

Figure 8.9(a) shows the case in which flow separation occurs due to change in the divergence angle of the test section. In this case, the flow is not separated initially because the divergence angle is small ($\alpha = 10$ degrees). The system senses to be unstalled and cuts off the jets completely at point "A". Separation is suppressed without jet flow issuing (jet-off situation) at point "A". Flow separation is caused by change in the divergence angle of the test section at point "B". The system restarts to suppress the separation at point "C" and suppresses it. The system keeps the jet speed constant beyond point "A".

Figure 8.9(b) shows the case in which no flow separation occurs even with change in the divergence angle. The system maintains the jet speed after suppression of the flow separation is once attained at point "A". When the divergence angle is changed at point "B", the flow condition indicates the unstalled flow field. Therefore, the system restarts to optimize the performance at point "C" and finally attains the optimal condition at point "A", which is in the jet-off situation.

8.2.4 Control Time of ASCSVGJ

The control time which is necessary to attain separation control is related to the response speed against the change of flow field. In other words, the more quickly flow situations are responsible to the system, the faster separation control can be performed. For the case of the jet pitch angle of 30 degrees, time variation of differential pressure under control is shown in Fig. 8.10. Comparing the 30-deg case with the 45-deg case (see Fig. 8.4), the 30-deg case attains the control target more rapidly than that for the 45-deg case among the three cases of freestream velocity. Figure 8.11 indicates the mean vorticity distribution over the spanwise

direction at $X=110$ mm. For the 30-deg case, the vorticity is stronger and the vortices are lower in comparison with the 45-deg case. Therefore, the case of a pitch angle of 30 degrees makes effective the pressure recovery and also the suppression of flow separation at $X=110$ mm, where the differential pressure is measured (*cf.* Chapter 7). This result means that the system could attain the control quickly, if the difference between the differential pressures of stalled and unstalled flow fields is large. In other words, the system can be operated stably and controlled more quickly, if pressure fluctuations can be neglected in comparison with a large pressure recovery.

In these experiments, the jet flow rate per control step is kept constant for various flow situations. However, if the jet flow rate is variable in attaining the control target, a faster response system can be developed. In the next section, we will explain the improved system (Improved ASCSVGJ: IASCSVGJ) which is the faster response system compared with the original system.

8.2.5 Improved ASCSVGJ by Considering Control Time

In order to attain a faster response, ASCSVGJ is improved. The alteration points from ASCSVGJ to IACSCVGJ are that 1) the jet pitch angle is set at 30 degrees in order to make effective the pressure recovery and also the separation control at $X=110$ mm, where the differential pressure are measured (*cf.* Chapter 7), 2) the jet flow rate per control step varies adaptively for various flow situations, and 3) the jet orifice is 2 mm in diameter. The alteration point 1) or 2) is useful to decrease the number of sampling data and the control step because pressure fluctuations in the system can be reduced by a large pressure recovery and therefore the system attains a faster response. The alteration point 3) is used for the purpose of avoiding secondary air loss for issuing jets. For the $D_j=3$ and 2 mm cases the comparison between the streamwise vorticity contours is shown in Fig. 8.12. Comparing the case of $D_j=3$ mm with that of $D_j=2$ mm, we see that the $D_j=3$ mm case gives broad longitudinal vortices in the spanwise direction because jet orifices become wider in the spanwise direction due to the jet pitch angle. This means that the controlled region is spread in the spanwise direction and make more effective separation control in comparison with the $D_j=2$ mm case. Therefore, the

D_j=3 mm case gives small VR for the control target. However, the D_j=3 mm case gives lager jet flow rate than the D_j=2 mm case. For example, the jet flow rate and VR are Q_j=25 l/min and VR=7, respectively, for D_j=2 mm and ϕ =30 degrees (corresponding to the improved system). In addition, the jet flow rate and VR are Q_j=48 l/min and VR=6, respectively, for D_j=3 mm and ϕ =45 degrees (corresponding to the original system). Table 8.1 gives the values of the jet flow rate and VR for three different freestream velocities when the system attains the control. The D_j=2 mm case for a pitch angle of 30 degrees can avoid the jet flow loss because the jet flow rate is the only control variable in this system.

For the improved system time variation of differential pressure under control is shown in Fig. 8.13. Comparing Fig. 8.13 with Fig. 8.4, it is seen that the control time of the improved system is shorter than that of the original system for each freestream velocity.

Figures 8.14 and 8.15 show the time variation of differential pressure under control for time-varying flow fields caused by change in the freestream velocity and the divergence angle of the test section. Points "A", "B", and "C" in these figures indicate the same meaning as those in Fig. 8.8 or 8.9. Figure 8.14 shows the differential pressure plotted against the control time for the situation in which flow separation occurs due to change in the divergence angle of the test section for each freestream velocity. Figure 8.15 shows the case in which flow separation occurs due to change in the divergence angle and the freestream velocity. We can see from Fig. 8.14 or 8.15 that this improved system can adapt flow situation continuously and can achieve faster separation control in comparison with the original system.

8.3 Conclusions

An active separation control system using vortex generator jets which can adapt to various flow conditions was developed. We conclude that our active separation control system can adaptively suppress flow separation for flow fields caused by some changes in freestream velocity and the divergence angle of the test section. Furthermore, for the control time which is important in the design of actual system, data for developing the system with a quick response were obtained.

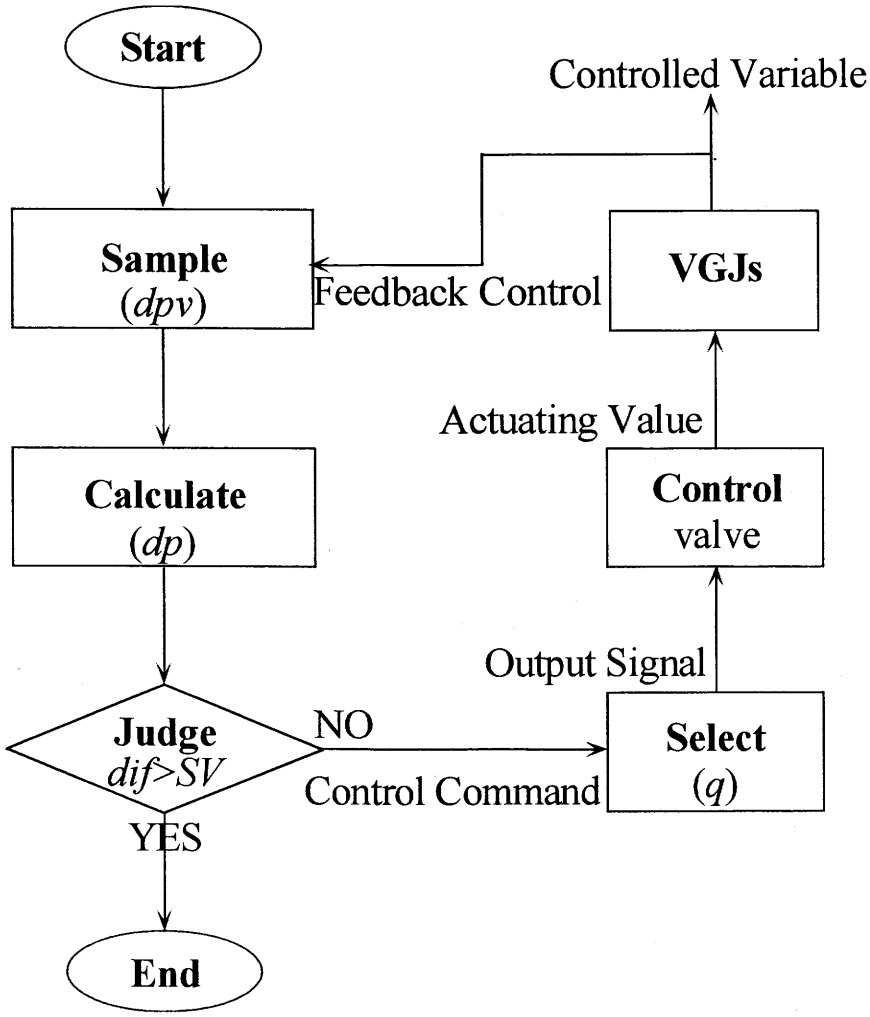

Figure 8.1 Flow chart of ASCSVGJ.

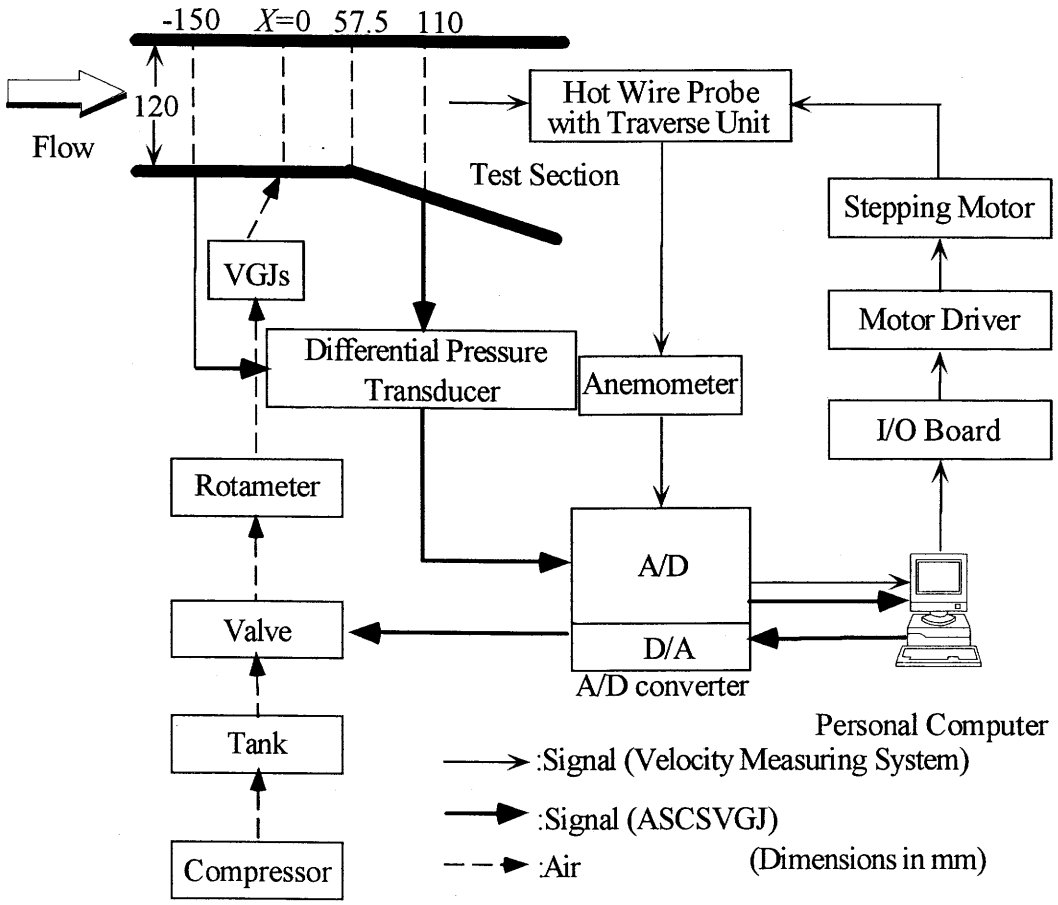

Figure 8.2 Schematic diagram of ASCSVGJ.

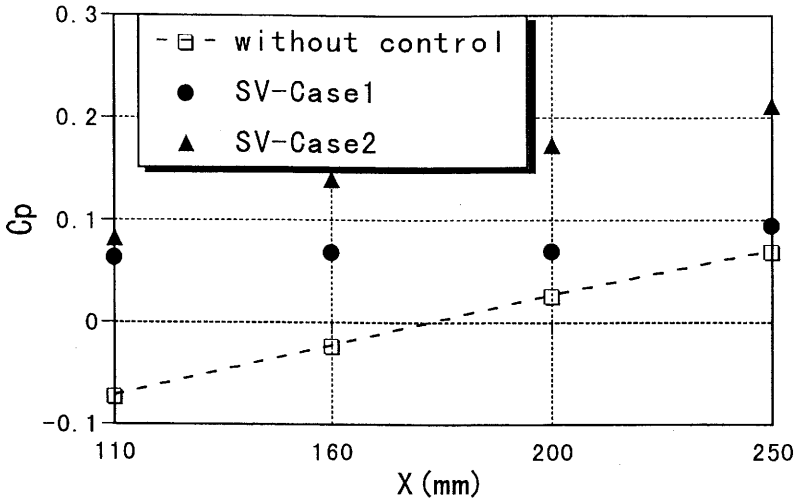

(a) U_0=6.5 m/s

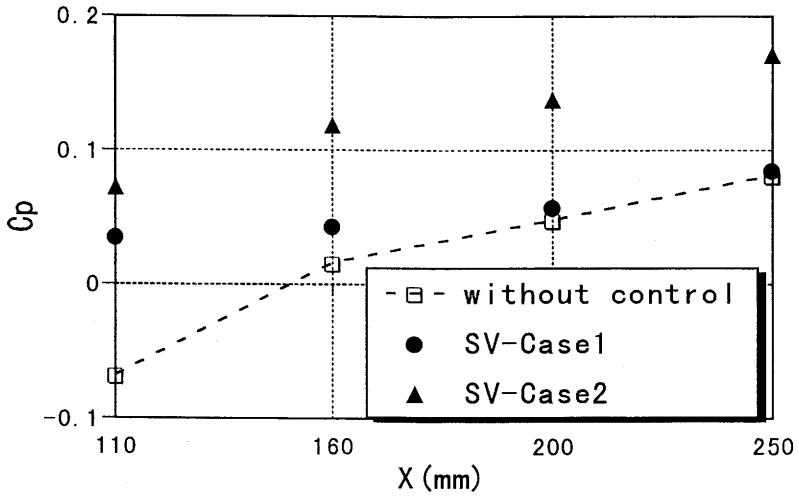

(b) U_0=8.5 m/s

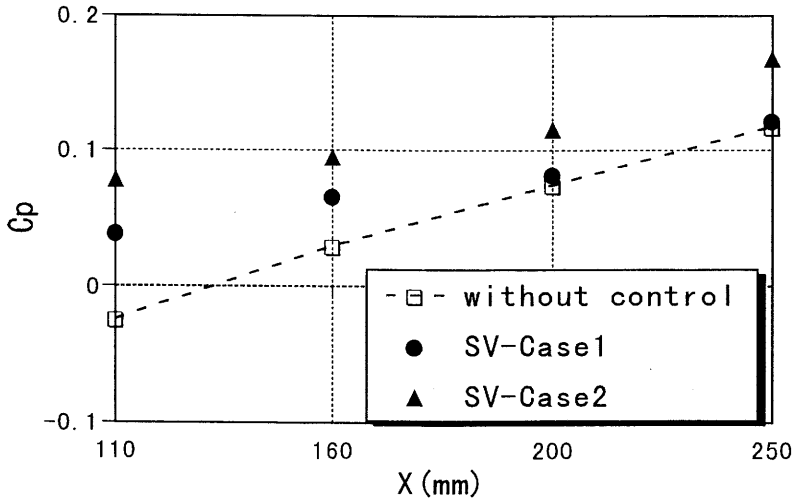

(c) U_0=11.1 m/s

Figure 8.3 Pressure distribution in the downstream direction.

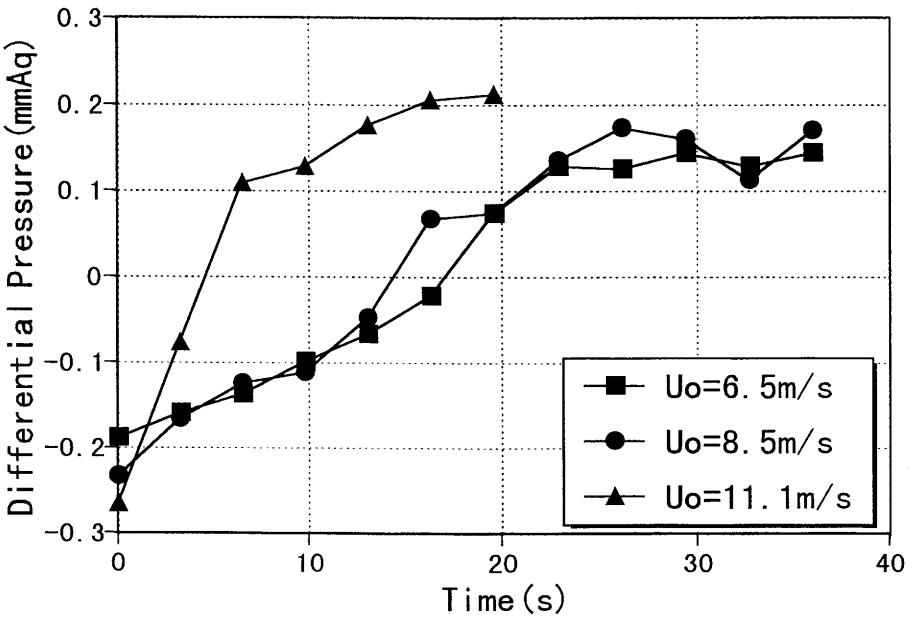

Figure 8.4 Variation of differential pressure under control.

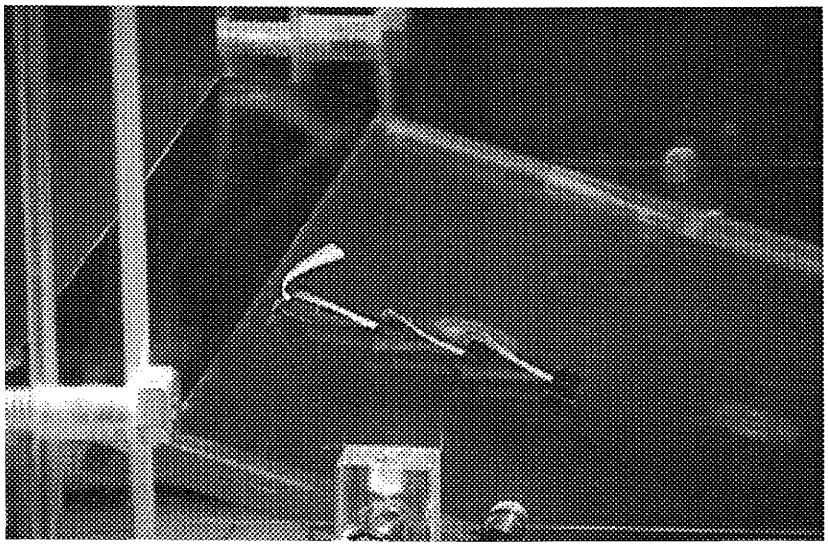

(a) Without control

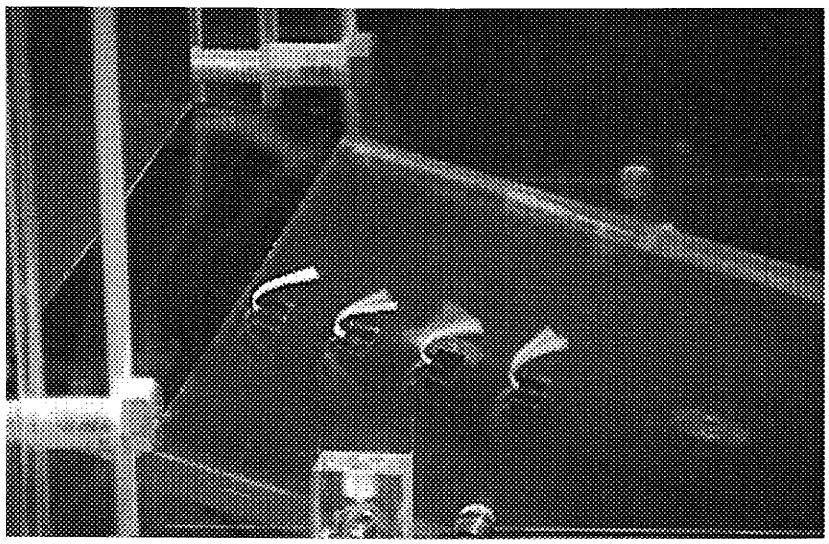

(b) With control

Figure 8.5 Surface flow in divergent portion of the test section (U_0=6.5 m/s).

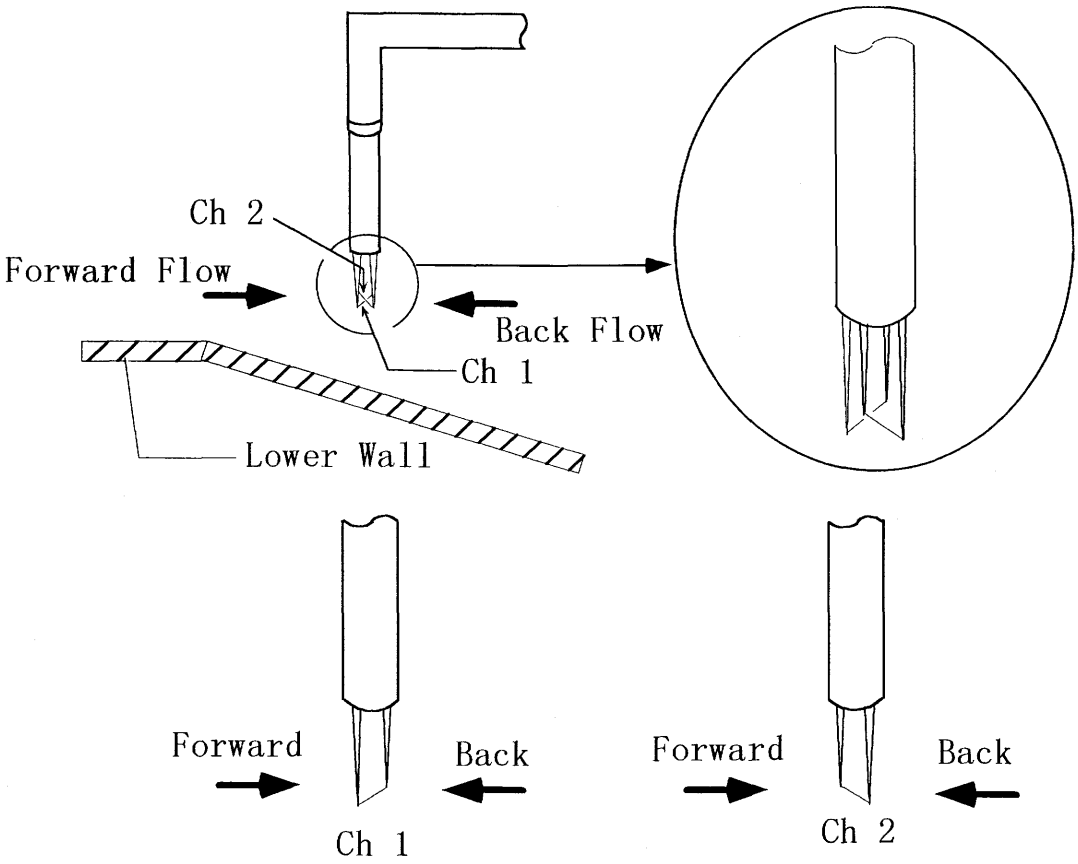

Figure 8.6 Channel 1 or 2 position of X-array hot wire probe.

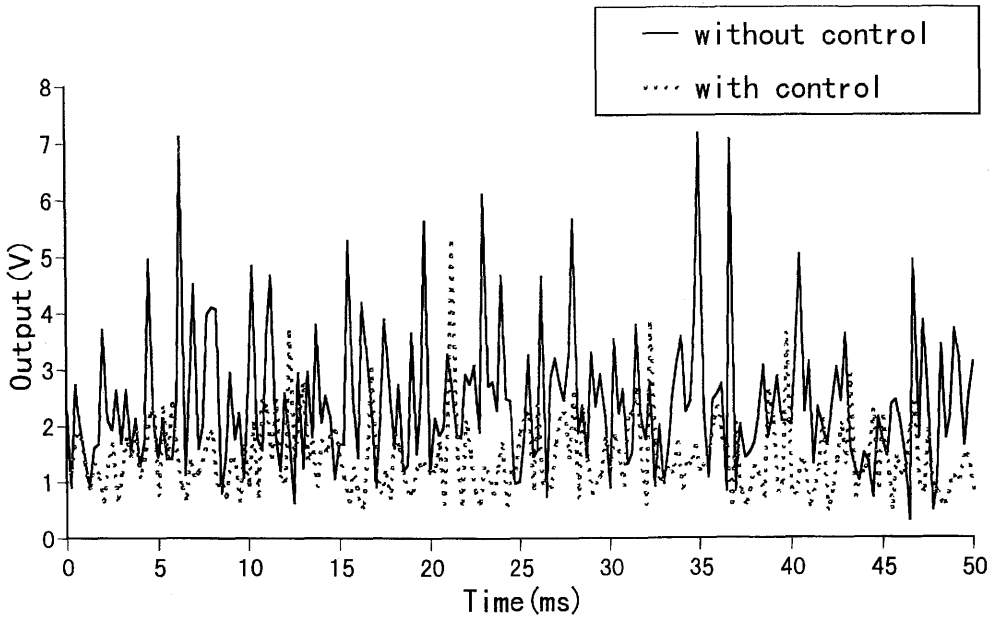

(a) Channel 1 output

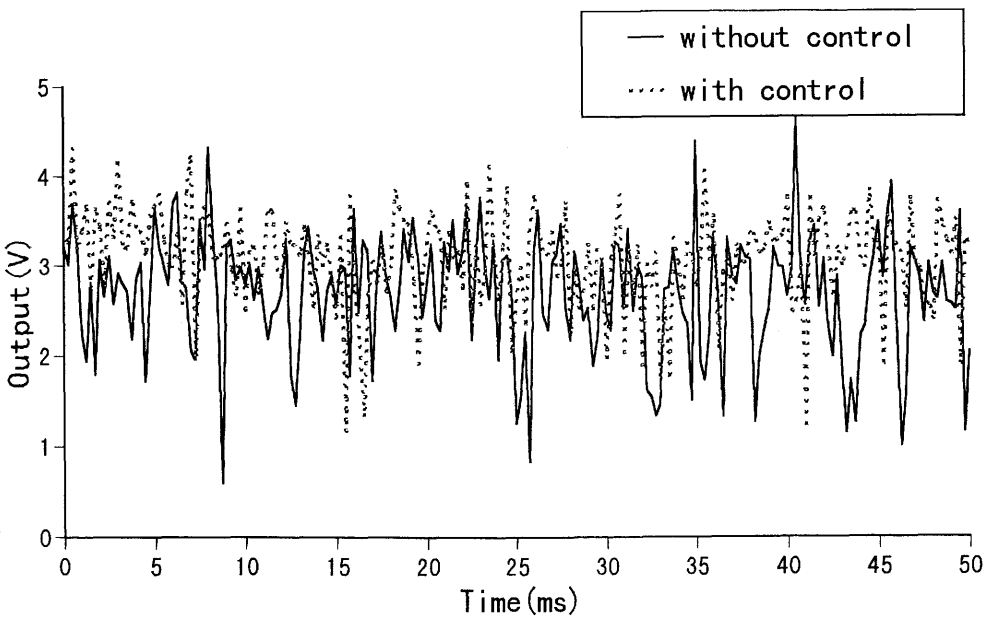

(b) Channel 2 output

Figure 8.7 Output of velocity signals at X=110 mm, Y=-4 mm, Z=160 mm (U_0=6.5 m/s).

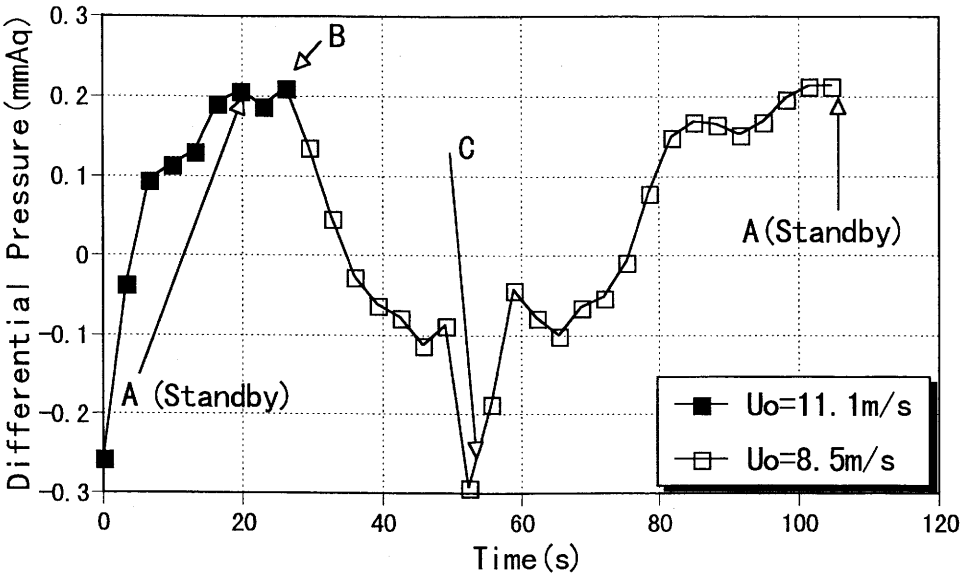

(a) U_0=11.1 m/s → 8.5 m/s

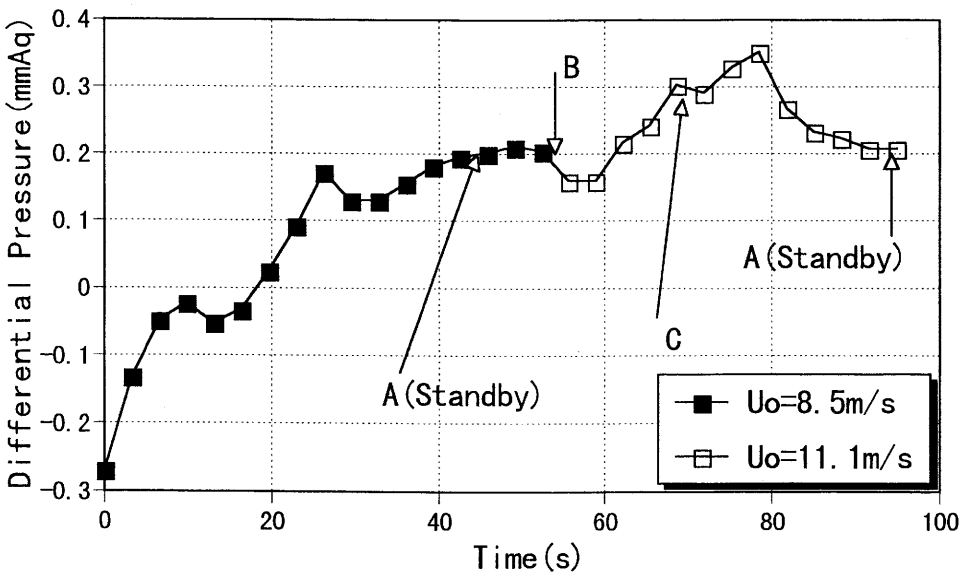

(b) U_0=8.5 m/s → 11.1 m/s

Figure 8.8 Variation of differential pressure under control.

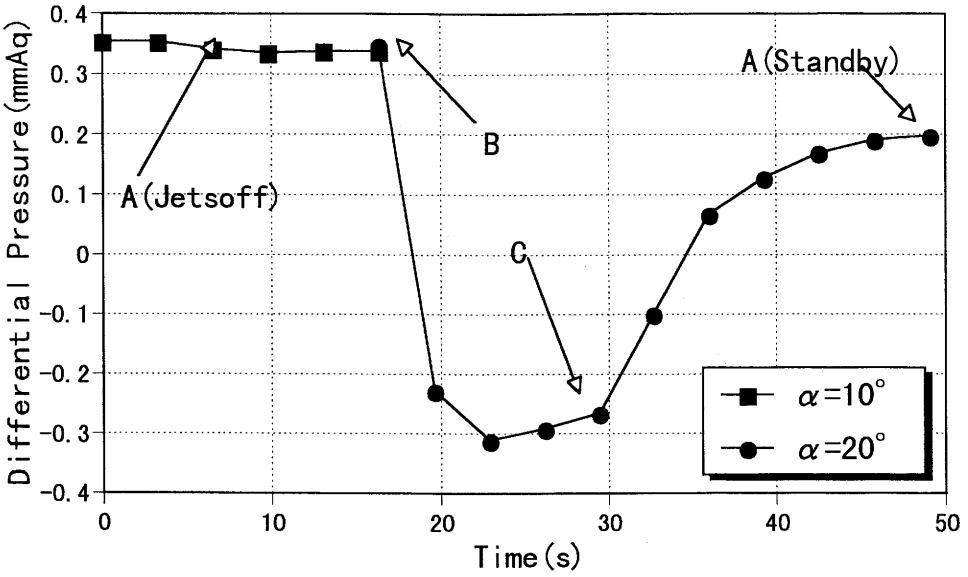

(a) $\alpha = 10$ deg $\rightarrow$ 20 deg

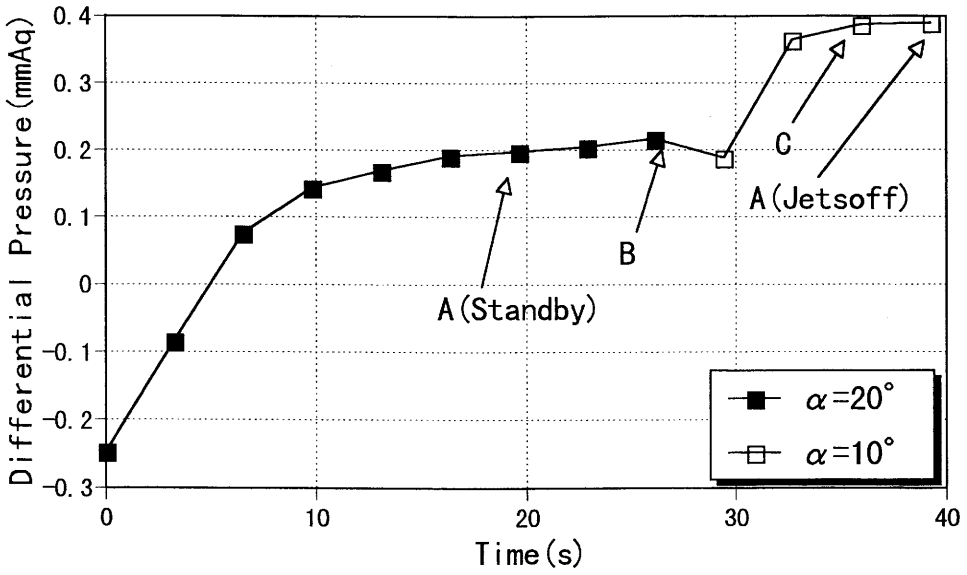

(b) $\alpha = 20$ deg $\rightarrow$ 10 deg

Figure 8.9 Variation of differential pressure under control (U_0=11.1 m/s).

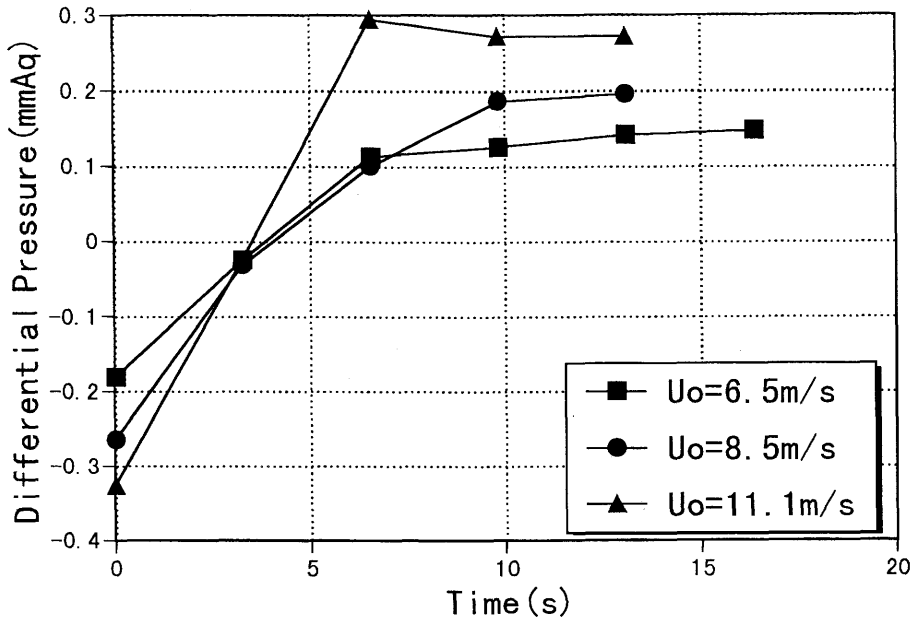

Figure 8.10 Variation of differential pressure under control (ϕ =30 deg, D_j=2 mm).

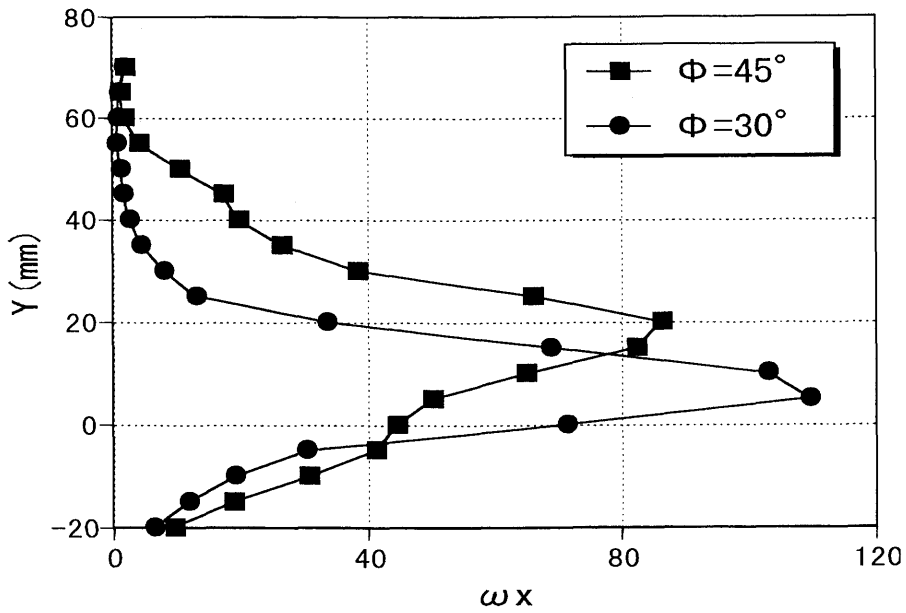

Figure 8.11 Mean vorticity in spanwise direction at X=110 mm (U_0=6.5 m/s, VR=9.5, D_j=2 mm).

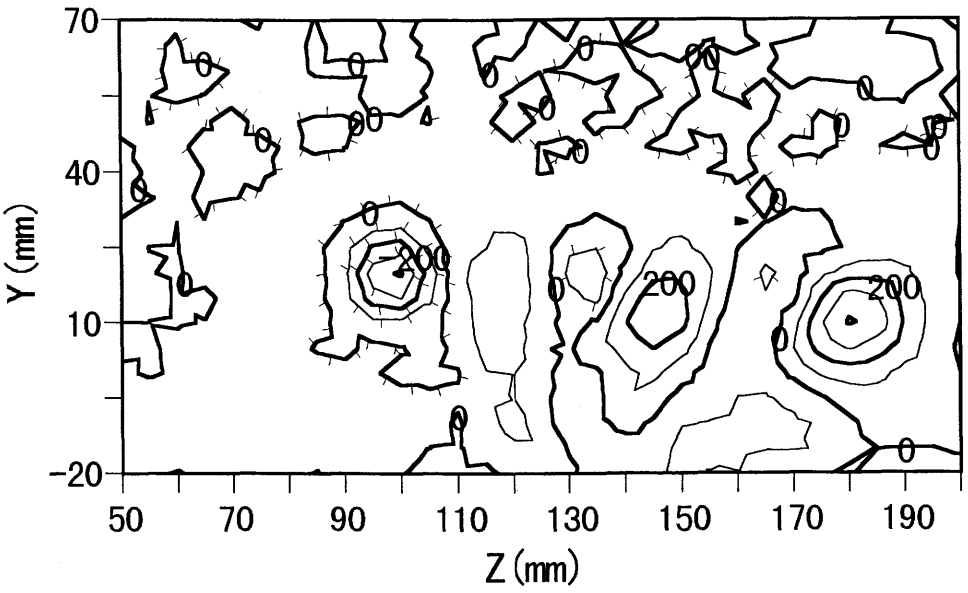

(a) D_j=2 mm

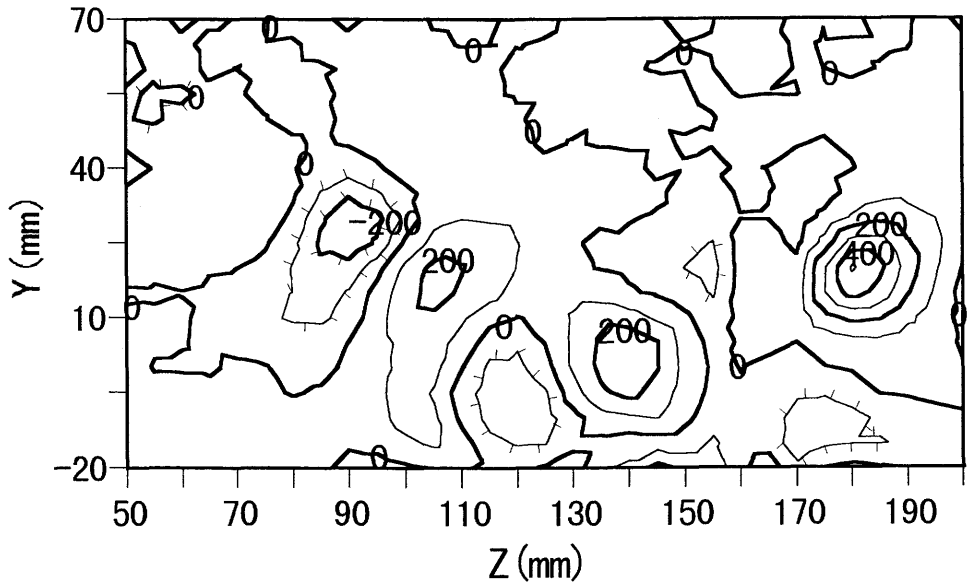

(b) D_j=3 mm

Figure 8.12 Contours of streamwise vorticity at X=110 mm (U_0=6.5 m/s, VR =9.5). Decorated lines denote negative vorticity. Contour interval =100 1/s.

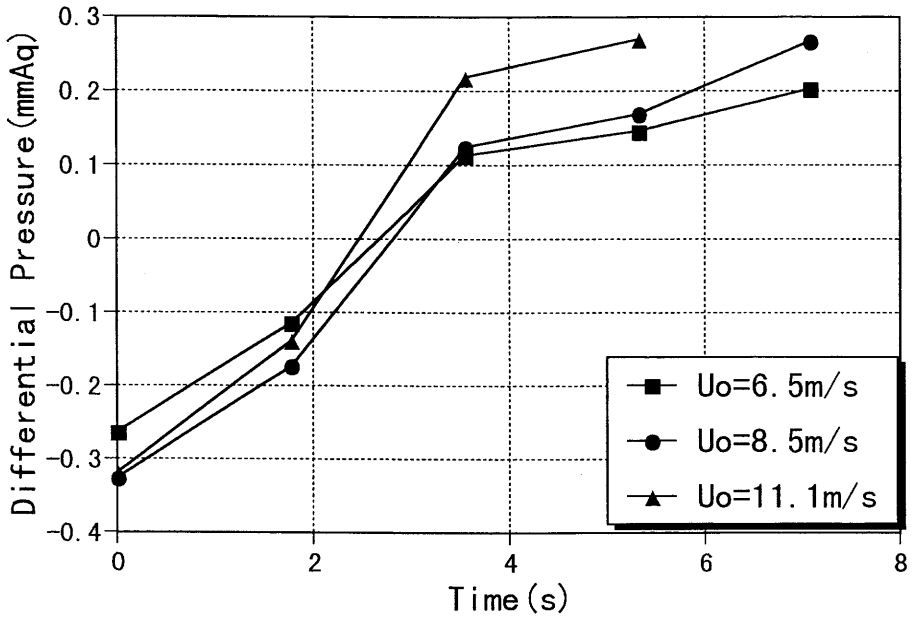

Figure 8.13 Variation of differential pressure under control with IASCSVGJ.

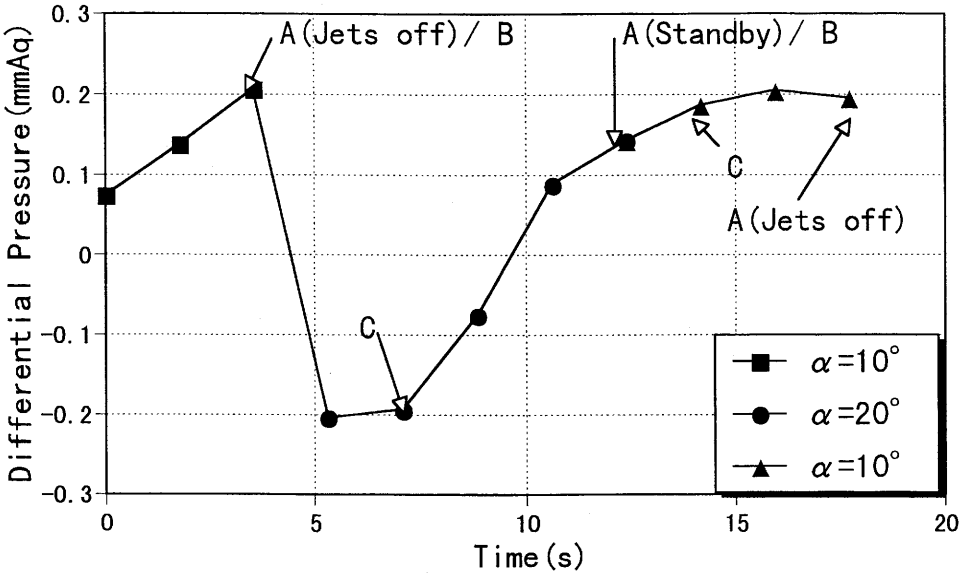

(a) α =10 deg → 20 deg → 10 deg (U_0=6.5 m/s)

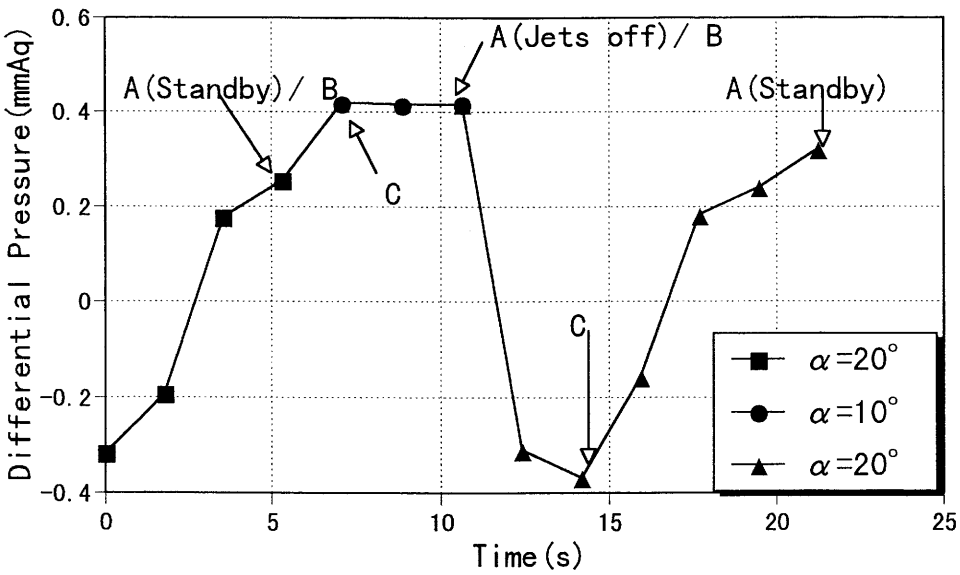

(b) α =20 deg → 10 deg → 20 deg (U_0=11.1 m/s)

Figure 8.14 Variation of differential pressure under control with IASCSVGJ.

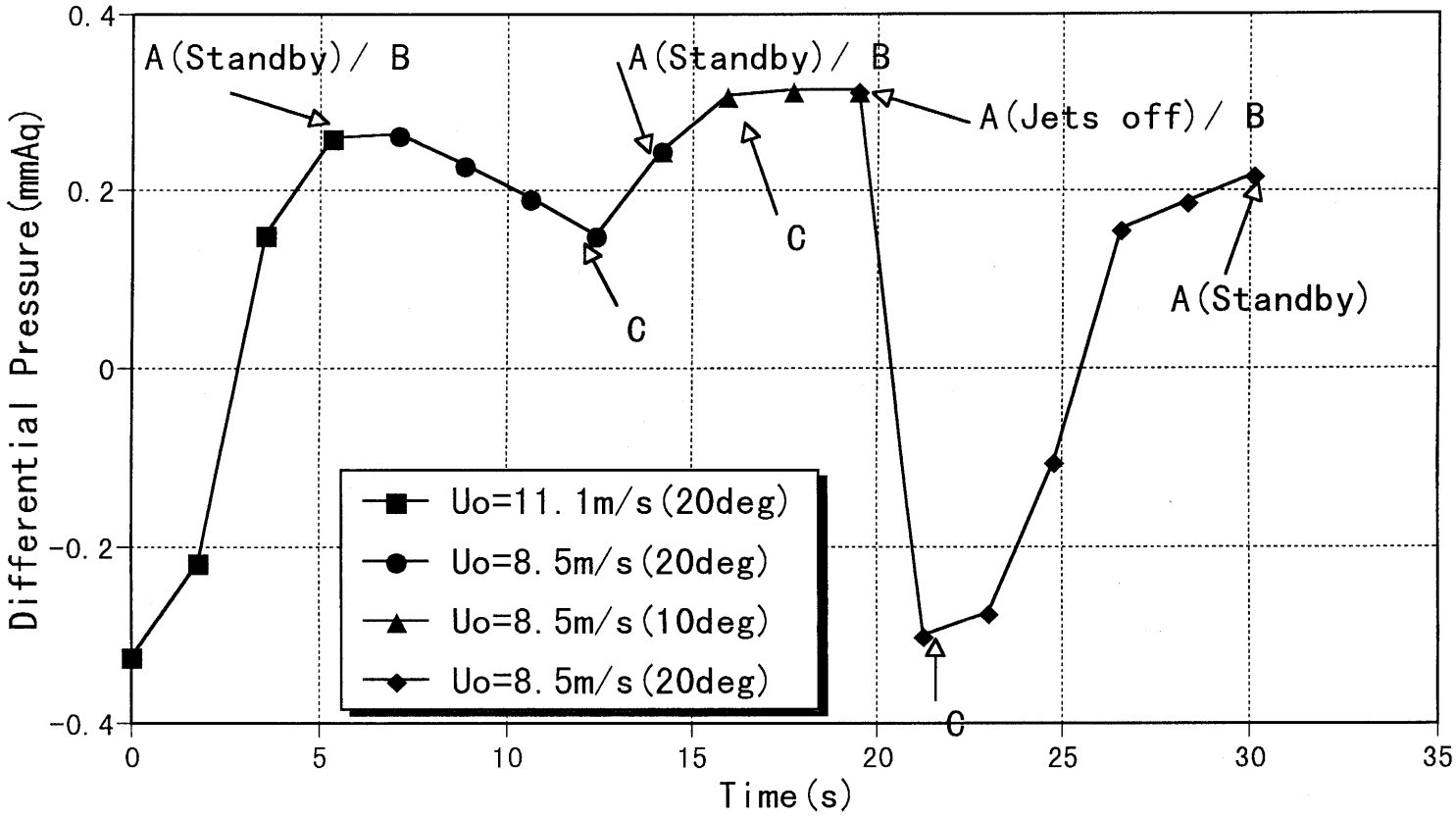

Figure 8.15 Variation of differential pressure under control with IASCSVGJ.

Table 8.1 Values of jet flow rate and VR when the system attains control

Jet Orifice Diameter D_j (mm)	Pitch Angle ϕ (degree)	Freestream Velocity U_0 (m/s)	Jet Flow Rate Q_j (l/min)	VR
2	30	6.5	25	7
3	45	6.5	48	6
2	30	8.5	29	6
3	45	8.5	45	4
2	30	11.1	21	3
3	45	11.1	28	2

9. SUMMARY AND RECOMMENDATIONS

9.1 Summary of Results and Conclusions

An experimental study about an active separation control using vortex generator jets was conducted. The interaction of wall-jet flows with a freestream generates longitudinal vortices that persist further downstream and enhance mixing between a boundary layer and the freestream. For the flow field derived longitudinal vortices, the streamwise velocity, streamwise vorticity, and pressure recovery were measured. Moreover, flow visualization was used as a diagnostic technique to observe the flow condition. These data sets were used to investigate the effect of boundary layer condition and a jet pitch angle on separation control, and the mechanism for suppressing flow separation. Furthermore, we tried to develop an active separation control feedback system utilizing these results. Summarizing our results on the active separation control using vortex generator jets, the following conclusions could be drawn:

1. For the vortex generator jet method, separation control can be achieved without surveying boundary layer conditions before jets are issued.

2. The suppression of flow separation is achieved by the secondary flow of longitudinal vortices which transports high momentum fluid of the freestream toward the lower wall. The effective separation control is accomplished by keeping the location of longitudinal vortices near the lower wall.

3. In order to suppress the upward movement of longitudinal vortices, it is desirable to produce no counter-rotating vortex pair of nearly equal strength.

4. For the suppression of generating the counter-rotating vortex pair of nearly equal strength, it is available 1) to derive the pulsed jet flow and 2) to adjust the jet pitch angle.
   These promote the interaction between positive and negative vortices, and as a results the generation of a vortex pair is prevented to be produced in the downstream direction.

5. Both the strength and the vertical position of longitudinal vortices are affected by a jet pitch angle and an optimal jet pitch angle may be less than 60 degrees.

6. If we can issue jets near the location where the flow separation occurs, the pulsed jet method is desirable. Longitudinal vortices generated by pulsed jets make effective separation control because the boundary layer thickness is not distorted in the spanwise direction. However, it should be noted that longitudinal vortices do not persist further downstream in comparison with the steady jet case.

7. If we cannot issue jets near the location where the flow separation occurs, the steady jet method is desirable. Longitudinal vortices generated by steady jets persist further downstream because the vorticity becomes stronger in comparison with the pulsed jet case. However, it should be noted that the boundary layer thickness is strongly distorted in the spanwise direction at some downstream locations.

8. An active separation control feedback system which has the ability to control adaptively the flow field of a diffuser caused by the change of flow situation (e.g., freestream velocity and diffuser's divergence angle) is developed. Separation control of this system was made in reference to the static pressure only at two measurement points, in the upstream of the divergent portion and in the divergent portion.

9.2 Recommendations for Future Work

Several observations made in this study could be more fully justified with measurements extending them to a region closer to the wall. In particular it would be helpful that the vortices in the boundary layer are investigated. These measurements would help in gaining a better understanding of the suppression mechanism of longitudinal vortices.

Our active separation control system is justified to be useful for suppressing flow separation in our wind tunnel tests. However, for the actual use of this system it is necessary to apply our system to a different freestream velocity range.

Lastly, it is greatly to be hoped that computational studies for finding the relationship between various parameters of vortex generator jets and the characteristics of longitudinal vortices (e.g., strength and downstream development) will be pursued.

REFERENCES

[1] Wallis, R. A., "A Preliminary Note on a Modified Type of Air Jet for Boundary Layer Control," Aeronautical Research Council, Current Paper No.513, Australia, 1956.

[2] Taylor, H. D., "Application of Vortex Generator Mixing Principle to Diffusers," United Aircraft Corp., Rept. R-15064-5, 1950.

[3] Schubauer, G. B., and W. G. Spangenberg, "Forced Mixing in Boundary Layer," *Journal of Fluid Mechanics*, Vol. 8, 1960, pp. 10-31.

[4] Mehta, R. D., "An Experimental Study of a Vortex/Mixing Layer Interaction," AIAA Paper 84-1543, 1984.

[5] Mehta, R. D., "Effect of a Longitudinal Vortex on a Separated Turbulent Boundary Layer," AIAA Paper 85-0530, 1985.

[6] Mehta, R. D., "A Study of Vortex/Separated Boundary Layer Interactions at Transonic Mach Numbers," AIAA Paper 86-0346, 1986.

[7] Cutler, A. D., and P. Bradshaw, "The Interaction Between a Strong Longitudinal Vortex and a Turbulent Boundary Layer," AIAA Paper 86-1071, 1986.

[8] Mehta, R. D., I. M. M. A. Shabaka, A. Shibl, and P. Bradshaw, "Longitudinal Vortices Imbedded in Turbulent Boundary Layers," AIAA Paper 83-0378, 1983.

[9] Shabaka, I. M. M. A., R. D. Mehta, and P. Bradshaw, "Longitudinal Vortices Imbedded in Turbulent Boundary Layers. Part 1. Single Vortex," *Journal of Fluid Mechanics*, Vol. 155, 1985, pp. 37-57.

[10] Mehta, R. D., "Interaction Between a Longitudinal Vortex and a Shock-Induced Turbulent Boundary Layer Separation," AIAA Paper 86-0346, 1986.

[11] Mehta, R. D., and P. Bradshaw, "Longitudinal Vortices Imbedded in Turbulent Boundary Layers. Part 2. Vortex Pair with 'Common Flow' Upwards," *Journal of Fluid Mechanics*, Vol. 188, 1988, pp. 529-546.

[12] Pauley, W. R., and J. K. Eaton, "Experimental Study of the Development of Longitudinal Vortex Pairs Embedded in a Turbulent Boundary Layer," *AIAA Journal*, Vol. 26, No. 7, 1988, pp. 816-823.

[13] Shizawa, T., and K. Eaton, "Turbulent Measurements for a Longitudinal Vortex Interacting with a Three-Dimensional Turbulent Boundary Layer,"

AIAA Journal, Vol. 30, No. 1, 1992, pp. 49-55.

[14] Matsumoto, A., "Turbulent Boundary Layer Perturbed by Streamwise Vortices," *Journal of the Japan Society for Aeronautical and Space Sciences*, Vol. 34, No. 386, 1986, pp. 141-152 (in Japanese).

[15] Wallis, R. A., and C. M. Stuart, "On the Control of Shock-Induced Boundary-Layer Separation with Discrete Air Jets," Aeronautical Research Council, Current Paper No. 595, Australia, 1958.

[16] Ball, W. H., "Test of Wall Blowing Concepts for Diffuser Boundary Layer Control," AIAA Paper 84-1276, 1984.

[17] Johnston, J. P., and M. Nishi, "Vortex Generator Jets-Means for Flow Separation Control," *AIAA Journal*, Vol. 28, No. 6, 1990, pp. 989-994.

[18] Compton, D. A., and J. P. Johnston, "Streamwise Vortex Production by Pitched and Skewed Jets in a Turbulent Boundary Layer," *AIAA Journal*, Vol. 30, No. 3, 1992, pp. 640-647.

[19] McManus, K. R., H. H. Legner, and S. J. Davis, "Pulsed Vortex Generator Jets for Active Control of Flow Separation," AIAA Paper 94-2218, 1994.

[20] Nishi, M., Y. Shibata, M. Nakamura, and M. Okamoto, "Application of Vortex Generator Jets to Control the Flow from Separating in a Conical Diffuser," ASME FED-Vol. 217, *Separated and Complex Flows*, 1995, pp. 27-34.

[21] Nishi, M., K. Yoshida, and K. Morimitsu, "Control of Separation in a Conical Diffuser by Vortex Generator Jets," *Proceedings of the International Conference on Fluid Engineering* (Tokyo, Japan), JSME ICFE-97-1203, 1997, pp. 333-338.

[22] Selby, G. V., J. C. Lin, and F. G. Howard, "Control of Low-Speed Turbulent Separated Flow Using Jet Vortex Generators," *Experiments in Fluids*, Vol. 12, No. 6, 1992, pp. 394-400.

[23] Zhang, X., "Computational Analysis of Co- and Contra-Rotating Streamwise Vortices in a Turbulent Boundary Layer," AIAA Paper 93-3035, 1993.

[24] Honami, S., T. Shizawa, and A. Uchiyama, "Behavior of the Laterally Injected Jet in Film Cooling: Measurements of Surface Temperature and Velocity/Temperature Field Within the Jet," *Transactions of the ASME, Journal of Turbomachinery*, Vol. 116, 1994, pp. 106-112.

[25] Zhang, X., and M. W. Collins, "Flow and Heat Transfer in a Turbulent Boundary Layer Through Skewed and Pitched Jets," *AIAA Journal*, Vol. 31, No. 9, 1993, pp. 1590-1599.

[26] Leylek, J. H., and R. D. Zerkle, "Discrete-Jet Film Cooling: A Comparison of Computational Results With Experiments," *Transactions of the ASME, Journal of Turbomachinery*, Vol. 116, 1994, pp. 358-368.

[27] Goldstein, R. J., and E. R. G. Eckert, "Effect of Hole Geometry and Density on Three-Dimensional Film Cooling," *Journal of Heat Mass Transfer*, Vol. 17, 1974, pp. 595-607.

[28] Johnston, J. P., and Z. Khan, "The Origins of the Dominant Vortex From a Pitched and Skewed Jets," *Proceedings of the International Conference on Fluid Engineering* (Tokyo, Japan), JSME ICFE-97-1201, 1997, pp. 321-325.

[29] Hasegawa, H., and K. Matsuuchi, "The Mechanism of Active Boundary Layer Control Using Vortex Generator Jets," *Transactions of JSME*, Vol. B-64, No. 617, 1998, pp. 92-99 (in Japanese).

[30] Hasegawa, H., and K. Matsuuchi, "The Mechanism of Active Boundary Layer Control Using Vortex Generator Jets," *Proceedings of the 21st Congress of the International Council of the Aeronautical Sciences* (Melbourne, Australia), ICAS-98-3, 4, 3, 1998.

[31] Hasegawa, H., and K. Matsuuchi, "Effect of Jet Pitch Angle of Vortex Generator Jets on Suppressing Flow Separation," *Transactions of JSME*, Vol. B-64, No. 627, 1998, pp. 164-170 (in Japanese).

[32] Hasegawa, H., and K. Matsuuchi, "Effect of Jet Pitch Angle of Vortex Generator Jets on Separation Control," *Proceedings of the Third International Conference on Fluid Mechanics* (Beijing, China), 1998, pp. 526-531.

[33] Hasegawa, H., K. Matsuuchi, and J. Tanaka, "Development of an Active Separation Control Feedback System Using Vortex Generator Jets," *Turbomachinery*, Vol. 26, No. 12, 1998, pp. 746-753 (in Japanese).

[34] Schlichting, H., "Boundary-Layer Theory," McGraw-Hill, 1979.

[35] Ikui, T., and M. Inoue, "Viscous Fluid Dynamics," Rikougakusya, 1995 (in Japanese).

[36] Ito, H., and M. Honda, "Fluid Dynamics," Maruzen, 1982 (in Japanese).

[37] Milne-Thomson, L., M., "Theoretical Hydrodynamics," Macmillan Education, 1968.

[38] Gad-el-Hak, M., and D. M. Bushnell, "Separation Control: Review," *Transactions of the ASME, Journal of Fluid Engineering*, Vol. 113, 1991, pp. 5-30.

[39] Tani, I., A. Kohashi, and H. Sato, "Experimental Method of Fluid Dynamics," Iwanami, 1977 (in Japanese).

[40] Lomas, C. G., "Fundamental of Hot Wire Anemometry," Cambridge University Press, 1985.

APPENDIX A: LIST OF USED SYMBOLS

It was found necessary to use the same symbol to denote different quantities in order not to depart too drastically from the conventions normally employed in general papers. For example, α denotes the modified coefficient of kinetic energy and the diffuser's divergence angle.

The following is a list of symbols used in this paper.

A.1 General Symbols

a, b, n = King's law constants
A = sectional area of diffuser
AR = W_e/W_i = area ratio
E = output voltage of hot wire anemometer
C_p = pressure recovery coefficient
C_{p_L} = local pressure recovery coefficient
$C_{p_{th}}$ = ideal pressure recovery coefficient
H_{12} = δ_1/δ_2 = shape factor
p = pressure (force per unit area)
$\widetilde{p_l}$ = pressure loss of diffuser
u, v = velocity components
V_{eff} = effective cooling velocity of hot wire
U_c = streamwise velocity near the center axis of diffuser
U_L = local streamwise velocity
$\overline{u}$ = mean streamwise velocity over the cross section
W_e, W_i = width of inlet or exit of diffuser
x, y, z = cartesian coordinates
α = modified coefficient of kinetic energy
δ = boundary layer thickness

δ_1 = displacement thickness

δ_2 = momentum thickness

η = diffuser effectiveness

ρ = density (mass per unit volume)

μ = viscosity

$\nu = \mu / \rho$ = kinematic viscosity

ω_x = streamwise component of mean vorticity

A.2 Symbols in This Experiment

$C_{pdf} = C_{p_{VR}} - C_{pwf}$ = pressure recovery from unforced case

D_j = jet hole diameter

D_t = tripping wire diameter

dif = state value of system

dp = differential pressure

dpv = output voltage of pressure transducer

Δp = differential pressure between inlet and outlet of diffuser

q = control variable (jet flow rate per control step)

f_p = pulse frequency

Q_j = jet flow rate

SV = control reference

U = mean velocity in X direction

U_0 = freestream velocity

V = mean velocity in Y direction

V_j = jet mean speed

VR = ratio, V_j/U_0

W = mean velocity in Z direction

X = streamwise coordinate (measure from jet hole)

Y = vertical coordinate (measure from lower wall)

Z = spanwise coordinate (measured from left wall viewed from upstream)

α = divergence angle of diffuser

ϕ = jet pitch angle

θ = jet skew angle

Subscript

e = diffuser outlet X=250 mm

i = diffuser inlet X=-10 mm

int = initial situation

uf = non-jet situation

VR = issuing jet situation

APPENDIX B: LIST OF EXPRIMENTAL INSTRUMENTS

Table B.1 Experimental instruments

Instruments	Model	Mfg. Co.
Blower	SFJ-304-IV- I	SWIDEN
Electric Valve	2AF5-10	CKD
Rotameter	J-2693	RIKASEIKI KOGYO
Personal Computer	SRV 4100-500	SORD
Interface Board (A/D, D/A Converter)	AD12-16(PC)E	CONTEC
X-Array Hot Wire Probe	0252R-T5	NIHON KAGAKU KOGYO
Hot Wire Anemometer (CTA System Anemometer)	MODEL 1010	NIHON KAGAKU KOGYO
Single-Wire Probe	9055P0141	DANTEC
Linearizer	MODEL 1013	NIHON KAGAKU KOGYO
Temperature Measurement Unit / Probe	MODEL 1020	NIHON KAGAKU KOGYO
Stepping Motor	KP6M2-005	JAPAN SERVO
Stepping Motor Driver	SMD-301	JAPAN SERVO
Interface Board (Stepping Motor Control Unit)	SMC-3(PC)	CONTEC
Electric Motor	M6100-201K	ORIENTAL MOTOR
Revolution Indicator	MODEL 00204	ONO SOKKI
Differential Pressure Transducer	3051CD1A52A1 AB4D9D3Q4	FISHER-ROSEMOUNT

APPENDIX C: JET SPEED MEASUREMENTS

Jet speed measurements were carried out by using an X-array hot wire probe. Each channel of the X-array hot wire probe was individually used for the measurements because the probe diameter was not sufficiently small in comparison with the jet orifice diameter. Figure C.1 shows a schematic diagram of the jet speed measurements. The hot wire probe was traversed at equal interval of 0.3 mm in the transverse direction of the jet orifice because the jet orifice became wider in the spanwise direction due to the jet pitch angle. Figure C.2 shows the distribution of the jet speed along the center axis of the jet orifice. Table C.1 gives the jet speed for Fig. C.2. The jet mean speed is calculated by integrating along the center axis of the jet orifice from traversing distance equals -1 mm to 1 mm (corresponding to the D_j=2 mm case). For the steady jet case (f_p=0 Hz) this result coincides with the result calculated from the continuity equation (conservation of mass). Figure C.3 shows the jet speed versus the jet flow rate. From Fig. C.3, for the pulsed jet case the relationship between the jet mean speed and the jet flow rate is given by

$$V_j = 0.95 \times Q_j , \tag{C.1}$$

or

$$V_j = 1.03 \times Q_j . \tag{C.2}$$

Equations (C.1) and (C.2) correspond to f_p=10 Hz and f_p=20 Hz, respectively. For the steady jet case the jet mean speed are calculated from the continuity equation, for D_j=2 mm and D_j=3 mm, as

$$Q_j = 0.565 \times V_j , \tag{C.3}$$

and

$$Q_j = 1.272 \times V_j , \tag{C.4}$$

respectively.

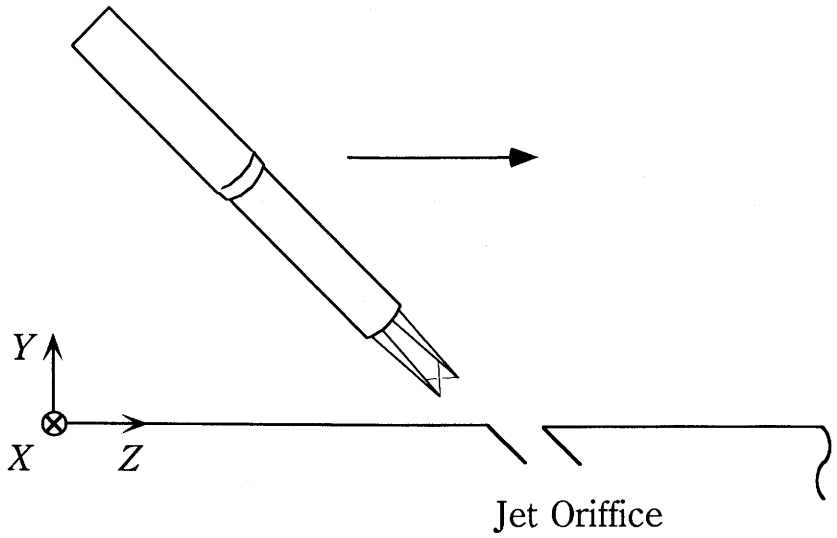

(a) Viewed from upstream

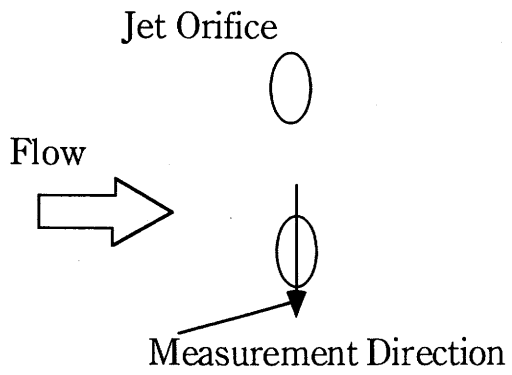

(b) Viewed from top

Figure C.1 Schematic diagram of jet speed measurements.

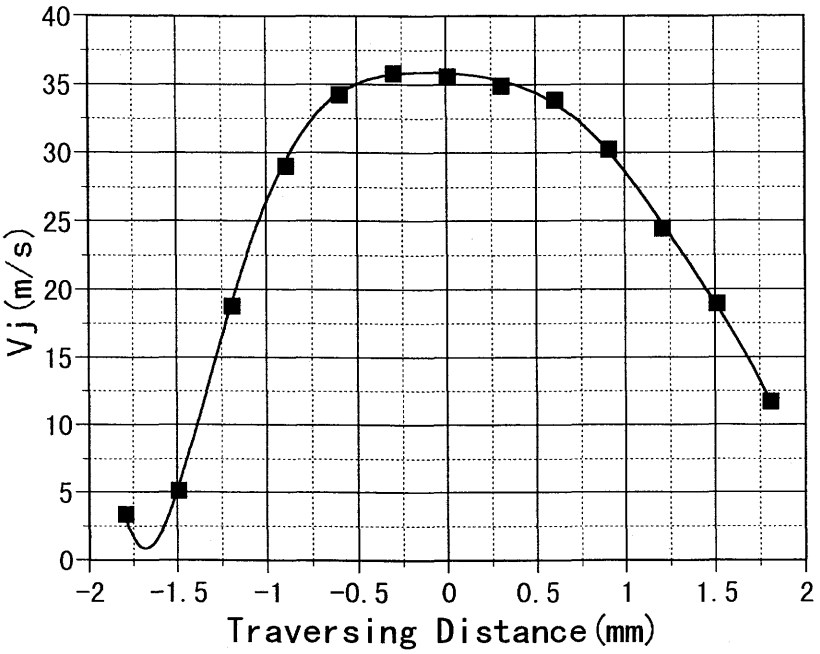

(a) f_p=0 Hz, Q_j=16 l/min

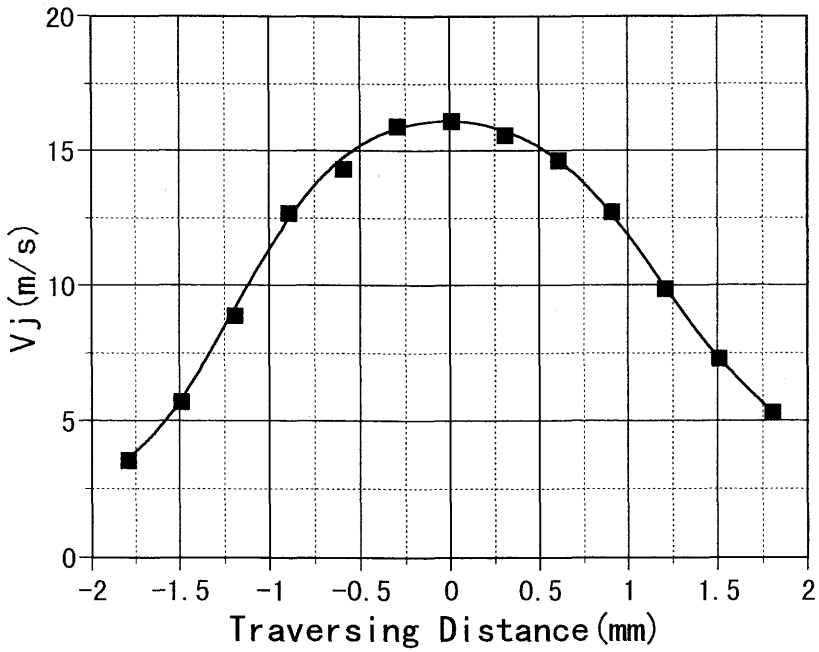

(b) f_p=10 Hz, Q_j=16 l/min

Figure C.2 Distribution of jet speed along the center axis of jet orifice.

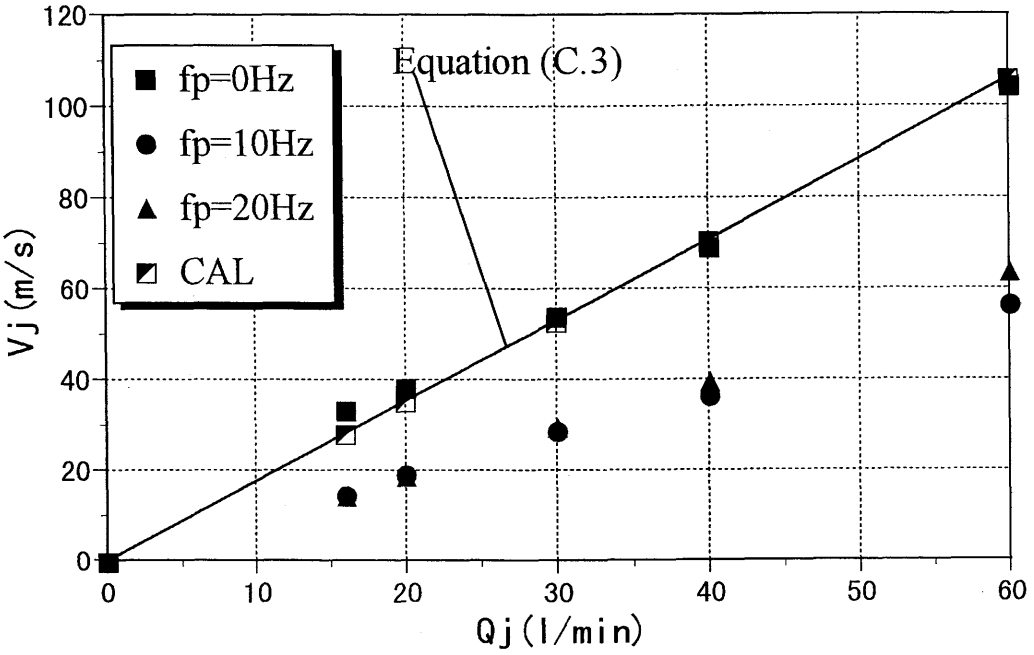

Figure C.3 Jet speed versus jet flow rate (D_j=2 mm); comparison with the values calculated from the continuity equation (CAL).

Table C.1 Values of jet speed along the center axis of jet orifice (ϕ =45 deg)

Pulse Frequency f_p (Hz)	Jet Flow Rate Q_j (l/mim)	Traversing Distance (mm)	Jet Speed (m/s)
0	16	-1.8	3.521
0	16	-1.5	5.292
0	16	-1.2	18.898
0	16	-0.9	29.181
0	16	-0.6	34.394
0	16	-0.3	35.954
0	16	0	35.71
0	16	0.3	35.048
0	16	0.6	33.997
0	16	0.9	30.401
0	16	1.2	24.623
0	16	1.5	19.112
0	16	1.8	11.884
0	20	-1.8	11.488
0	20	-1.5	18.805
0	20	-1.2	25.151
0	20	-0.9	32.351
0	20	-0.6	37.039
0	20	-0.3	39.594
0	20	0	41.516
0	20	0.3	41.418
0	20	0.6	38.977
0	20	0.9	35.389
0	20	1.2	30.655
0	20	1.5	25.378
0	20	1.8	20.892
0	30	-1.8	26.535
0	30	-1.5	35.001
0	30	-1.2	43.558
0	30	-0.9	49.546
0	30	-0.6	55.662
0	30	-0.3	58.478
0	30	0	58.877
0	30	0.3	56.342
0	30	0.6	51.375
0	30	0.9	44.517

Table C.1 Continued

Pulse Frequency f_p (Hz)	Jet Flow Rate Q_j (l/mim)	Traversing Distance (mm)	Jet Speed (m/s)
0	30	1.2	38.574
0	30	1.5	32.527
0	30	1.8	27.016
0	40	-1.8	29.09
0	40	-1.5	38.439
0	40	-1.2	49.57
0	40	-0.9	60.301
0	40	-0.6	68.968
0	40	-0.3	73.282
0	40	0	75.271
0	40	0.3	74.487
0	40	0.6	69.448
0	40	0.9	60.863
0	40	1.2	53.968
0	40	1.5	44.996
0	40	1.8	35.292
0	60	-1.8	52.739
0	60	-1.5	69.463
0	60	-1.2	83.897
0	60	-0.9	96.989
0	60	-0.6	107.457
0	60	-0.3	111.773
0	60	0	112.025
0	60	0.3	109.577
0	60	0.6	100.076
0	60	0.9	86.136
0	60	1.2	72.716
0	60	1.5	59.597
0	60	1.8	47.688
10	16	-1.8	3.616
10	16	-1.5	5.778
10	16	-1.2	8.96
10	16	-0.9	12.745
10	16	-0.6	14.384
10	16	-0.3	15.99
10	16	0	16.175

Table C.1 Continued

Pulse Frequency f_p (Hz)	Jet Flow Rate Q_j (l/mim)	Traversing Distance (mm)	Jet Speed (m/s)
10	16	0.3	15.653
10	16	0.6	14.697
10	16	0.9	12.795
10	16	1.2	9.951
10	16	1.5	7.374
10	16	1.8	5.367
10	20	-1.8	4.284
10	20	-1.5	7.313
10	20	-1.2	11.601
10	20	-0.9	16.428
10	20	-0.6	19.392
10	20	-0.3	19.953
10	20	0	20.499
10	20	0.3	21.923
10	20	0.6	19.648
10	20	0.9	17.98
10	20	1.2	12.892
10	20	1.5	10.659
10	20	1.8	7.33
10	30	-1.8	7.718
10	30	-1.5	13.176
10	30	-1.2	19.745
10	30	-0.9	25.548
10	30	-0.6	27.972
10	30	-0.3	31.694
10	30	0	31.791
10	30	0.3	30.733
10	30	0.6	28.442
10	30	0.9	25.672
10	30	1.2	20.51
10	30	1.5	15.128
10	30	1.8	13.776
10	40	-1.8	13.006
10	40	-1.5	20.179
10	40	-1.2	27.24
10	40	-0.9	33.462

Table C.1 Continued

Pulse Frequency f_p (Hz)	Jet Flow Rate Q_j (l/mim)	Traversing Distance (mm)	Jet Speed (m/s)
10	40	-0.6	37.496
10	40	-0.3	40.973
10	40	0	39.167
10	40	0.3	39.013
10	40	0.6	34.952
10	40	0.9	30.008
10	40	1.2	26.277
10	40	1.5	21.038
10	40	1.8	17.977
20	16	-1.8	5.605
20	16	-1.5	7.749
20	16	-1.2	11.98
20	16	-0.9	12.771
20	16	-0.6	16.122
20	16	-0.3	15.159
20	16	0	15.679
20	16	0.3	14.757
20	16	0.6	14.227
20	16	0.9	11.98
20	16	1.2	10.261
20	16	1.5	8.211
20	16	1.8	6.691
20	20	-1.8	7.349
20	20	-1.5	11.121
20	20	-1.2	14.27
20	20	-0.9	17.1
20	20	-0.6	18.253
20	20	-0.3	20.759
20	20	0	21.986
20	20	0.3	20.342
20	20	0.6	18.465
20	20	0.9	16.135
20	20	1.2	13.384
20	20	1.5	11.483
20	20	1.8	9.431
20	30	-1.8	13.885

Table C.1 Continued

Pulse Frequency f_p (Hz)	Jet Flow Rate Q_j (l/mim)	Traversing Distance (mm)	Jet Speed (m/s)
20	30	-1.5	19.071
20	30	-1.2	24.496
20	30	-0.9	28.804
20	30	-0.6	31.816
20	30	-0.3	33.846
20	30	0	33.642
20	30	0.3	28.858
20	30	0.6	26.516
20	30	0.9	23.076
20	30	1.2	20.647
20	30	1.5	16.548
20	30	1.8	13.569
20	40	-1.8	18.546
20	40	-1.5	24.344
20	40	-1.2	31.808
20	40	-0.9	36.863
20	40	-0.6	38.448
20	40	-0.3	43.924
20	40	0	43.692
20	40	0.3	42.804
20	40	0.6	38.251
20	40	0.9	33.585
20	40	1.2	28.212
20	40	1.5	24.197
20	40	1.8	18.48

APPENDIX D: AUTOMATIC PROBE TRAVERSING UNIT CONTROL / VELOCITY MEASUREMENT PROGRAM

```
/*

 ****************************************************************
 *     <<Automatic Probe Traversing Unit Control Program /      *
 *               Velocity Measurement Program>>                 *
 *                                                              *
 *       INITIALIZATION / PULSE OUTPUT / DATA Acquisition       *
 *                                                              *
 *     THIS PROGRAM is - moving probe traversing unit and       *
 *                   measuring output voltage of hot wire probe.*
 *                                                              *
 *                            1996.9.18                         *
 *                               By                             *
 *                            H.Hasegawa                        *
 *                                                              *
 *                                                              *
 *                  External Program: ad_conv.c                 *
 *                                                              *
 *      set up initial parameter of SMC-3(PC) in program        *
 *                 (set: auto deceleration mode)                *
 *                                                              *
 *          Motor Move & Save Data: Auto Mode Select            *
 *                (WTC1/2:Waiting Time Constant)                *
 ****************************************************************

*/

#include <stdio.h>
#include <conio.h>
#include <dos.h>

#define  WTC1 1e3
#define  WTC2 1e6

unsigned BA = 0x300;              /* Base Address */
int x = 6;
int y = 1;

void cls(void) {
      printf("¥033[2J");                /*** clear screen ***/
}
```

```
void locate(int x, int y) {
      printf("¥033[%d;%dH", y+1, x+1); /**set cursor location**/
}


void cursor(int m) {
      union REGS r;
      switch(m) {
        case 0:                                    /* cursor off */
          r.h.ah = 1;
          r.h.ch = 0x20;
          r.h.cl = 0x20;
        break;
        case 1:                                    /* cursor on */
          r.h.ah = 1;
          r.h.ch = 06;
          r.h.cl = 07;
        break;
      }
      int86(0x10, &r, &r);
}


void title() {
      locate(25, 1);
      printf("*****************************");
      locate(25, 2); printf("*    Pulse Motor     *");
      locate(25, 3); printf("*     MOVE ON !!     *");
      locate(25, 4);
      printf("*****************************");
}


void pls_out(int cr,int mn)
{
      int  st,START;

      cls();
      title();

      outp(BA, mn + 4);
      st = inp(BA + 1);
      START = cr + 1;

      outp(BA, mn);
      outp(BA + 1, START);
}


/*read outputted pulse count loop*/
int pls_cnt(int mn)
{
      int  es = 0;
```

```
int  co,term;
int  st,s;
unsigned int  cplo,cpmi,cpup;
long int  cp;

locate(0, x + 3);
printf("CURRENT OUTPUTTED PULSE COUNT =");

for ( ; ; ) {
       outp(BA, mn);
       co = inp(BA + 1);   /*check termination*/
       if ((co & 1) == 0) {
              locate(y + 50, x + 3);
              printf("OUTPUT IS STOPPED");
              term = 1;
       }
       outp(BA, mn + 1);     /*read current pulse count*/
       cplo = inp(BA + 1);
       outp(BA, mn + 2);
       cpmi = inp(BA + 1);
       outp(BA, mn + 3);
       cpup = inp(BA + 1);
       cp = cpup * 65536 + cpmi * 256 + cplo;
       locate(y + 34, x + 3);
       printf("%ld", cp);

       if (term == 1) break;

/*check pulse output status*/
       locate(y + 50, x + 3);
       outp(BA, mn + 4);
       st = inp(BA + 1);
       s = st & 0x6;
       switch(s) {
         case 0:
           printf("AT MINIMUM SPEED");
           break;
         case 2:
           printf("ACCELERATING    ");
           break;
         case 4:
           printf("DECELERATING    ");
           break;
         case 6:
           printf("AT MAXIMUM SPEED");
           break;
       }
       if (kbhit()) {
         es = 1;
         break;
       }
}
return es;
```

```
}


void insig_ck(int mn)
{
        int  st1,st2;
        char  wait;

        outp(BA, mn + 4);
        st1 = inp(BA + 1);                  /*read status 1 register*/
        locate(0, x + 11);
        if ((st1 & 0x20) != 0x20) printf("PULSES WERE CORRECTLY
OUTPUTTED.¥n");
        else {
          outp(BA, mn + 5);
          st2 = inp(BA + 1);                /*read status 2 register*/
          if ((st2 & 1) == 1) printf("POINT-OF-ORIGIN SIGNAL IS ON.
¥n");
          if ((st2 & 0x80) == 0x80) printf("SLOW-DOWN & STOP SIGNAL
IS ON.¥n");
          if ((st2 & 4) == 4) printf("POSITIVE LIMIT SIGNAL IS ON.¥n");
          if ((st2 & 8) == 8) printf("NEGATIVE LIMIT SIGNAL IS ON.¥n");
          if ((st2 & 2) == 2) printf("EMERGENCY STOP SIGNAL IS ON.¥n");
        }
        printf("¥n");
}

        extern ad_conv(int xdd, int yd, int cn);


main()
{
        long int tp, dp, cp;
        float tp1, tp2;
        int cr, maxs, mins, ar, dr, r, START, term;
        int st, s, co, st1, st2, loop;
        char maxslo, minslo, arlo, drlo;
        unsigned int tplo, tpmi, tpup, tptm;
        unsigned int dplo, dpmi, dpup, dptm;
        unsigned int cpup, cpmi, cplo;
        unsigned int maxsup, minsup, arup, drup;
        char adm, wait, a, eve, evad;
        int  mn, mno, xd, xdd, xe, yd, ye, ydm, i, cn;
        int  iset, cout, cset;
        int  xis, xes, yis, yes;
        float px, py;
        char autm;
        int  aut;
        unsigned long tifc, ti;

        cursor(0);              /*cursor off*/
        cls();                  /*clear screen*/
/*      title();  */            /*display title*/
```

```
    locate(25, 6);  printf("      ARE YOU READY ?      ");
    locate(25, 7);  printf("PRESS '1' TO SET UP PARAMETER : ");
    a = getche();
    while (a != '1')  a = getche();
    locate(25, 6);  printf("                          ");
    locate(25, 7);  printf("                            ");
    locate(25, 5);  printf("ENTER X-INITIAL POSITION > ");
    scanf("%d",&xis);
    locate(25, 6);  printf("ENTER Y-INITIAL POSITION > ");
    scanf("%d",&yis);

for(cout=1;cout<=2;cout++){
    if(cout == 1) {
      mn = 0;
      cr = 0x12;
    }
    if(cout == 2) {
      mn = 0x10;
      cr = 0x10;
      cls();
    }

    /*set of auto-deceleration mode*/

    /*initialize command register*/

    outp(BA, mn);
    outp(BA + 1, cr);

    /*set total pulse register*/

    locate (y, x + 1);
    if(cout == 1){
      printf("ENTER  X-DISTANCE OF 1 MOVE (1~167772 mm)> ");
      scanf("%f", &tp1);
    }
    if(cout == 2){
      printf("ENTER  Y-DISTANCE OF 1 MOVE (1~167772 mm)> ");
      scanf("%f", &tp2);
    }

    locate (y, x + 2);
    if(cout == 1){
     printf("ENTER TOTAL NUMBER OF X-DIRECTION > ");
     scanf("%d",&xe);
    }
    if(cout == 2){
     printf("ENTER TOTAL NUMBER OF Y-DIRECTION > ");
     scanf("%d",&ye);
    }

    if(cout == 1) tp = (long int)(tp1 * 100);
    if(cout == 2) tp = (long int)(tp2 * 100);
```

```
if (tp == 16777216) tp = 0;
tplo = tp % 256;
tptm = (unsigned int)(tp / 256);
tpmi = tptm % 256;
tpup = tptm / 256;
outp(BA, mn + 1);
outp(BA + 1, tplo);
outp(BA, mn + 2);
outp(BA + 1, tpmi);
outp(BA, mn + 3);
outp(BA + 1, tpup);

dp = 0;         /*set deceleration point register*/

dplo = dp % 256;
dptm = (unsigned int)(dp / 256);
dpmi = dptm % 256;
dpup = dptm / 256;
outp(BA, mn + 4);
outp(BA + 1, dplo);
outp(BA, mn + 5);
outp(BA + 1, dpmi);
outp(BA, mn + 6);
outp(BA + 1, dpup);

maxs = 3;     /*set maximum speed register*/
maxslo = maxs % 256;
maxsup = (unsigned int)(maxs / 256);
outp(BA, mn + 7);
outp(BA + 1, maxslo);
outp(BA, mn + 8);
outp(BA + 1, maxsup);

mins = 2;     /*set minimum speed register*/
minslo = mins % 256;
minsup = (unsigned int)(mins / 256);
outp(BA, mn + 9);
outp(BA + 1, minslo);
outp(BA, mn + 0xa);
outp(BA + 1, minsup);

ar = 1;         /*set acceleration rate register*/
arlo = ar % 256;
arup = (unsigned int)(ar / 256);
outp(BA, mn + 0xb);
outp(BA + 1, arlo);
outp(BA, mn + 0xc);
outp(BA + 1, arup);


dr = ar;      /*set deceleration rate register*/
drlo = dr % 256;
drup = (unsigned int)(dr / 256);
outp(BA, mn + 0xd);
```

```
        outp(BA + 1, drlo);
        outp(BA, mn + 0xe);
        outp(BA + 1, drup);


        r = 1;          /*set resolution value register*/
        outp(BA, mn + 0xf);
        outp(BA + 1, r);
}

        locate (y, x + 3);
          printf("ENTER NUMBER OF STORING SAMPLING DATA > ");
          scanf("%d",&cset);

        locate(y, x + 11);  printf("PRESS <ESC> KEY TO QUIT : ");
        locate(y, x + 12);   printf("PRESS ANY OTHER KEY TO START PULSE
OUTPUT : ");

        a = getche();
        if (a == 0x1b) goto end;

        pulseout:                       /*start pulse output*/
        cls();

        xes = xe + xis;
        yes = ye + yis;
        xdd = xis;
        yd = yis;

        locate(30, 6);  printf("Save A/D Data? (y/n)>");
        evad = getche();
        if((evad == 'Y') || (evad == 'y')) {
              for(cn=1;cn<=cset;cn++){
                 ad_conv(xdd,yd,cn);
                 cls();
              }
        }

/*  AUTO MODE SELECT */
        locate (20, 7);
          printf("Motor Move & Save A/D Data AUTO-MODE? (y/n)>");
          autm = getche();
          if((autm == 'Y') || (autm == 'y'))  aut = 1;
          else  aut = 2;

        for(yd=yis;yd<=yes;yd++){
           ydm = yd % 2;
           py = tp2 * yd;
           if(yd != yis){
             cr=0x10;
             mn = 0x10;        /* (Motor-2) */
             if(ydm != 0) xdd = xes;
             if(ydm == 0) xdd = 0;
```

```
        cls();
        if(aut == 2){
              locate(30, 6);  printf("Motor Move? (y/n)>");
              eve = getche();
              if((eve == 'N') || (eve == 'n'))  goto stop;
        }
         else{
           for(ti=0;ti<=WTC1;ti++)  tifc = ti + ti;
         }

         pls_out(cr,mn);
         if(pls_cnt(mn) == 1){
              cls();
              locate(25, 3); printf("****  EMERGANCY STOP!!  ****");
              locate(25, 4); printf("** x >=%5.1f mm(%d) y >= %5.1f
mm(%d)  **",px,xdd,py,yd);
              break;
         }

         cls();
         insig_ck(mn);

         locate(25, 3); printf("X-POSITION >%d Y-POSITION >%d",xdd,
yd);
         locate(25, 4); printf("** X >= %5.1f mm  y >= %5.1f mm **"
,px,py);

  /*  Analog input and storing degital data to files        */
        if(aut == 2){
              locate(30, 6); printf("Save A/D Data? (y/n)>");
              evad = getche();
              if((evad == 'Y') || (evad == 'y')) {

                        for(cn=1;cn<=cset;cn++){
                           ad_conv(xdd,yd,cn);
                           cls();
                        }
              }
         }
          else{
              for(ti=0;ti<=WTC2;ti++)  tifc = ti + ti;
                  for(cn=1;cn<=cset;cn++){
                     ad_conv(xdd,yd,cn);
                     cls();
                  }
          }

      }
      for(xd=xis;xd<xes;xd++){
          if(ydm != 0){
          cr = 0x12; /* output PCW in SM-3(PC)*/ /* (cr = 0x10) */
      /* (cr = 0 : cr = 0x2) */
          xdd = xes - xd -1 + xis;
          px = tp1 * xdd;
```

```
        }
        else{
           cr = 0x10;      /* output DCCW in SM-3(PC)*/
            xdd = xd + 1;
            px = tp1 * xdd;
        }

        mn = 0;   /* (Motor-1) */

        cls();
          if(aut == 2){
             locate(30, 6); printf("Motor Move? (y/n)>");
             eve = getche();
             if((eve == 'N') || (eve == 'n'))  goto stop;
          }
          else{
             for(ti=0;ti<=WTC1;ti++)  tifc = ti + ti;
          }

          pls_out(cr,mn);
          if(pls_cnt(mn) == 1){
             cls();
             locate(25, 3); printf("**** EMERGANCY STOP!! ****");
             locate(25, 4); printf("** x >=%5.1f mm (%d) y >=%5.1f
mm (%d) **",px,xdd,py,yd);
             break;
          }

           cls();
           insig_ck(mn);

           locate(25, 3); printf("X-POSITION >%d  Y-POSITION >%d"
,xdd,yd);
           locate(25, 4); printf("** X >= %5.1f mm  y >= %5.1f mm
**",px,py);

  /*  Analog input and storing degital data to files        */
          if(aut == 2){
             locate(30, 6); printf("Save A/D Data? (y/n)>");
             evad = getche();
             if((evad == 'Y') || (evad == 'y')) {

                 for(cn=1;cn<=cset;cn++){
                    ad_conv(xdd,yd,cn);
                    cls();
                 }
             }
          }
          else{
                for(ti=0;ti<=WTC2;ti++)  tifc = ti + ti;

                for(cn=1;cn<=cset;cn++){
                    ad_conv(xdd,yd,cn);
                    cls();
```

```
                }

            }
          }
        }

        /*check input signal*/
        stop:
/*      insig_ck(mn); */

        end:
        outp(BA, mn);
        outp(BA + 1, 0x12);
        outp(BA, mn+4);
        wait = inp(BA + 1);

        cursor(1);                          //cursor on//
}


/*-------------------------------------------------------------
 * Program of analog input with DMA transfer (ad_conv)
 *
 * THIS PROGRAM is - periodic sampling with internal sampling clock
 *                   and storing converted data to main memory by DMA
 *                   transfer to measure output voltage of probe.
 *
 *       I/O address         = 700h
 *       input gain          = x1
 *       input channel       = multi channel( 0 to 15 ) (use No.0
 *                             channel)
 *       scan clock           = 10usec
 *       sampling clock       = 16000usec
 *       number of samplings = 20
 *       DMA channel          = 5 ( word transfer )
 *
 *    0,1-ch:Voltage of Velocity  2-ch:Voltage of Temperature
 *-------------------------------------------------------------
*/

#include <stdio.h>
#include <dos.h>
#include <math.h>
#include "h306.h"

#define    ADR                    0x0700

int                  aidata[20][16];

void   ad_conv(int xdd, int yd, int cn)
{
   void _far       *ptr = aidata;
   unsigned int    status, dmaseg = FP_SEG(ptr), dmaoff = FP_OFF
ptr);
   unsigned char   errflg = 0;
   unsigned char   gain[] = { 0,0,0,0,0,0,0,0,0,0,0,0,0,0,0,0 };
   unsigned char   channel[] = { 0,1,2,3,4,5,6,7,8,9,10,11,12,13,
```

```
14,15 };
    unsigned char   i, j;
    float   volt;
    int   span = 10;
    int   offset = 0;
    int   n = 12;

    FILE  *fp1;
    char   fnam[20];

    /*--- display title ---*/
    locate(1,6);
    printf( "<< Input analog data and storing converted digital data
>>¥n¥n" );

    /*--- file name ---*/

/*      printf("ENTER FILE NAME =>");
        scanf("%s",&fnam);
*/
        sprintf(fnam,"x%dy%dn%d.dat",xdd,yd,cn);

    while ((fp1 = fopen(fnam, "r")) != NULL) {
       printf(" WARNING >  %s  File Already Exists!¥n",fnam);
       fclose(fp1);
       printf("ENTER FILE NAME =>");
       scanf("%s",&fnam);
    }

    if((fp1 = fopen(fnam, "w")) == NULL) {
       printf("%s not open!!¥n",fnam);
       exit(1);
    }

    /*--- initialize ---*/
    InitBoard( ADR );

    /*--- set AI condition ---*/
    SetAIFunction( ADR, 0x0880 );           /* set function */
    for ( i = 0; i < 16; i++ ) {
        SetAIGain( ADR, i, gain[i] );       /* set input gain */
        SetAIChannel( ADR, i, channel[i] ); /* set input channel */
    }
    SetAIScanClk( ADR, 10000UL );          /* set scan clock */
    SetAISmpClk( ADR, 160000e2 );          /* set sampling clock */
    SetAISmpNum( ADR, 0UL, 20UL, 0UL );    /* set number of samplings
*/

    /*--- set DMA transfer condition ---*/
    SetAIDmaFunc( ADR, 5, 0, 0 );           /* set DMA condition */
    SetPC8237( 5, 0, 0, 0, dmaoff, dmaseg, 319 ); /* set 8237 condition
*/

    /*--- start analog input ---*/
```

```
    StartAI( ADR, 15 );
    do {
       GetStatus( ADR, &status ) ;          /* get sampling status */
    } while ( status & 3 );
    if ( status & 0x80 ) errflg = 1;        /* test sampling error */

    /*--- display data ---*/
    if ( errflg ) {
       printf( "sampling error !!¥n" );
    }
    else {
          for ( i = 0; i < 3; i++ ) {
            printf( "%2dch AIdat:", i );
            for ( j = 0; j < 20; j++ )
               printf( " %04xh", aidata[j][i] );
            printf( "¥n" );
            printf("%2dch Volt :", i );
            printf("          saving  %s ¥n",fnam);
            fprintf(fp1, "%2dch Volt:",i);
            for ( j = 0; j < 20; j++ ){
               volt = aidata[j][i] * span / pow(2,n) - offset;
               fprintf(fp1, "%6.3f ",volt);
             }
            printf( "¥n" );
       }
    }
    fclose(fp1);
}
```

APPENDIX E: IASCSVGJ CONTROL PROGRAM

```
/*
 ************************************************************************
 *       << Program of Active Boundary Layer Control System >>          *
 *                                                                      *
 *                                                                      *
 *    THIS PROGRAM is -  sampling differential pressure and judging     *
 *                    operation of control system to optimize performance *
 *                    under various flow situations.                    *
 *                                                                      *
 *                              1998. 2.17                              *
 *                                  By                                  *
 *                              H.Hasegawa                              *
 *                                                                      *
 *                 External Program : samp_dp.c (Ver.5)                 *
 *                                    Samp_dps.c(Ver.0)                 *
 *                                    cal_avg.c (Ver.4)                 *
 *                                    sig_out.c (Ver.2)                 *
 *                                    int_sig.c (Ver.0)                 *
 *                                                                      *
 *            tg_v: Target Value of Control System                      *
 *            sv: Set Value of Minimum Error                            *
 *            cset:Value of Sampling Set Number                         *
 *            cset:Value of Sampling Set Number                         *
 *                                                                      *
 *         Differential Pressure Transducer: High-Upstream side         *
 *                                           Low- Downstream side       *
 *                                                                      *
 ************************************************************************

*/

#include <stdio.h>
#include <stdlib.h>
#include <math.h>

#define  TW_S  4000
#define TTW_S  4000


void cls(void){
       printf("¥033[2J");
}
```

```
void locate(int x, int y){
       printf("¥033[%d;%dH", y+1, x+1);
}


void title()
{
       char   adm1;

       locate(20, 1); printf("************************************");
       locate(20, 2); printf("*                                  *");
       locate(20, 3); printf("*          Welcome to              *");
       locate(20, 4); printf("*       [ ASCSVGJ ]                *");
       locate(20, 5); printf("* Active Separation Control System*");
       locate(20, 6); printf("*   using Vortex Generator Jets    *");
       locate(20, 7); printf("*                                  *");
       locate(20, 8); printf("************************************");

       locate(20,10); printf("******* SYSTEM START ? > (y/n) *******");
       adm1 = getche();
       if((adm1 == 'N') || (adm1 == 'n')){
          locate(25,15); printf("** SYSTEM SHUT DOWN !! **");
          exit(1);
       }
}


void judge(float *avg,int *q,int *upd,int mno,int *dr_ck,float
          ivol,int *cnrv,int *upd_jr,float *it_avg,float *avg_bf,int
          *kep,int *no_sp,float *jdg_non,float *dp)
{
   float   er_jg;
   float   it_avgmd, avg_md;

   *kep = 0;

    *dp = -3.175 * (*avg - ivol);

    if(mno == 1){
       *cnrv = 0;
       er_jg = 0.0;
       *dr_ck = 1;
       *upd = 1;
       *q = (int)(4/(*dp * 2 + 1) + 0.5);
      printf("**avg[%d]=%6.3f er_jg[%d]=%6.3f **¥n",mno,*avg,mno,er_jg);
    }
    else{
      er_jg = *avg -*avg_bf;
       if((er_jg < 0.002) && (er_jg >= -0.001))  *kep = 1;
       else{
           if(er_jg <= 0.0){
              *dr_ck = 1;
               *cnrv = 0;
           }
```

```
            else{
               *dr_ck = 2;
               *cnrv = *cnrv + 1;
            }
         }

         printf(" +-+-+ cnrv =%d +-+-+-¥n",*cnrv);
         printf("**  AVG[%d]=%6.3f avg[%d]=%6.3f er_jg[%d]=%6.3f dr_ck=%d
**¥n",mno-1,*avg_bf,mno,*avg,mno,er_jg,*dr_ck);

  /* upd=1:flow-increment  upd=2:flow-decrement */
         if((*dr_ck == 1) && (*upd == 1))  *upd_jr = 1;
         if((*dr_ck == 2) && (*upd == 1))  *upd_jr = 2;
         if((*dr_ck == 1) && (*upd == 2))  *upd_jr = 3;
         if((*dr_ck == 2) && (*upd == 2))  *upd_jr = 4;

         printf("!!! upd_jr=%d !!!¥n",*upd_jr);

         if(*upd_jr == 1)  *upd = 1;
         if(*upd_jr == 2)  *upd = 1;
         if(*upd_jr == 3)  *upd = 2;
         if(*upd_jr == 4)  *upd = 2;
         if(*upd_jr >= 5) printf("--- upd : ERROR !! ---¥n");

      }

      it_avgmd = *it_avg - ivol;
      avg_md = *avg - ivol;
      *jdg_non = avg_md / it_avgmd;

      if((it_avgmd <= 0.001) && (it_avgmd >= -0.001))   *no_sp = 3;
      else{
         if((avg_md <= -0.01) && (it_avgmd < -0.001))  *no_sp = *no_sp + 1;
      }


      printf("¥n");
      printf("$$$$ jdg_non=%5.2f,it_avgmd=%6.3f,avg_md=%6.3f &&&&¥n",
*jdg_non,it_avgmd,avg_md);
      printf("¥n");

         *q = (int)(4/(*dp * 2 + 1) + 0.5);

      if(mno > 1){
         if((*upd_jr == 2) && (*cnrv == 3)){
            *upd = 2;
            *q = (int)(4/(*dp * 2 + 1) + 0.5);
            *cnrv = 0;
         }
         if((*upd_jr == 4) && (*cnrv == 3)){
             *upd = 1;
             *q = (int)(4/(*dp * 2 + 1) + 0.5);
             *cnrv = 0;
         }
```

```
    }

        if(*jdg_non <= -0.7)  *q = 0;
}


   extern  samp_dp(int xloc, int mno, int cnt);
   extern  samp_dps(int xloc, int mno, int cnt);
   extern  cal_avg(int mno, int xloc, float *avg, int cset, int cnt, float
*it_avg);
   extern  sig_out(int *q, int upd, int mno, int es, float *volt);
   extern  int_sig(int mno);

void  main(void)
{

        char   ive, adm, lucy;
        char   outfnm[20];
        int    q, upd, mno, i, xloc, es, j_par, dr_ck, sy_ck, fd_ck, end_c;
        int    cnt, cset, cnrv, upd_jr, kep, no_sp, adm_j, kep_par;
        int    ti, tti, twf_s;
        int    mod;
        float  ivol, it_avg, jdg_non;
        float  avg, avg_bf, volt, dp;

        FILE  *fp2;

        cls();
        title();
        cls();

        locate(10, 6); printf("*** ENTER Streamwise Position X(mm) > ");
        scanf("%d",&xloc);
        locate(10, 7); printf("*** ENTER Total Set Number of Sampling > ");
        scanf("%d",&cset);
        locate(10, 8); printf("*** ENTER Initial Voltage (No-Wind) > ");
        scanf("%f",&ivol);
        locate(10, 9); printf("*** ENTER D_P(mmAq) Output File Name > ");
        scanf("%s",&outfnm);

        j_par = 0;
        mno = 0;
        no_sp = 0;
        adm_j = 0;
        sy_ck = 0;
        end_c = 0;
        kep_par = 0;
        fd_ck = 0;
        mod = 0;

        while((fp2 = fopen(outfnm,"r")) != NULL){
         printf("#### WARNING > %s File already exists !!! ###¥n",outfnm);
           fclose(fp2);
           printf("ENTER Output File Name Again > ");
```

```
        scanf("%s",outfnm);
      }
      if((fp2 = fopen(outfnm,"w")) == NULL){
        printf("###  %s not open !!¥n",outfnm);
        exit(1);
      }
      fprintf(fp2,"*** Output D_P(mmAq) ***¥n");

/*-----  Separation Control Loop  ------*/
      mod_1: mod = 0;
      mod_4: mod = 0;
      mod_5:;

      es = 0;
      for( ; ; ){
         mno = mno + 1;
         if(mno == 1){
             int_sig(mno);
             for(ti=1; ti<=TW_S; ti++){
                 for(tti=1; tti<=TTW_S; tti++){
                     twf_s = ti + tti;
                 }
             }
         }

         for(cnt=1; cnt<=cset; cnt++){
             samp_dp(xloc, mno, cnt);
             cls();
         }

         cal_avg(mno, xloc, &avg, cset, cnt, &it_avg);

         judge(&avg, &q, &upd, mno, &dr_ck, ivol, &cnrv, &upd_jr, &it_avg,
&avg_bf, &kep, &no_sp, &jdg_non, &dp);

         if(mod == 5){
             upd = 1;
             mod = 0;
         }

         if(kep  == 1)  kep_par = kep_par + 1;
         else  kep_par = 0;

         fprintf(fp2,"%6.3f¥n",dp);

         avg_bf = avg;
         if(q == 0)  j_par = j_par + 1;
         if((j_par == 1) || (kep_par == 3)){
             break;
         }
         printf("*** q = %d, upd = %d  ***¥n",q,upd);

         if(kbhit()) {
             es = 1;
```

```
            locate(0,10);
            sig_out(&q, upd, mno, es, &volt);
            locate(10,13); printf("***** EMERGENCY STOP!! *****¥n");
            exit(1);
        }

        if(no_sp == 3){
            es = 2;
            locate(0,10);
            sig_out(&q, upd, mno, es, &volt);
            locate(10,13); printf("**** Not Separation !! ****¥n");
            break;
        }

        if((cnrv == 0)&&(q != 0)&&(kep ==0)){
            locate(0,10);
            sig_out(&q, upd, mno, es, &volt);
        }
    }

    locate(10,15); printf("-----  System Standby? (y/n) > ");
    ive = getche();
    if((ive == 'N')||(ive == 'n')) {
        es = 2;
        locate(0,10);
        sig_out(&q, upd, mno, es, &volt);
        locate(10,16); printf("*** System Shut Down!! ***¥n");
        exit(1);
    }

    cls();

/*---------------  Monitor Loop  -------------*/
    j_par = 0;
    kep_par = 0;
/*  mod_2: mod = 0;  */
    mod_3: mod = 0;
    adm_j = 0;

    fprintf(fp2,"----System_Keep-&-Optimizing!!----¥n");
    for( ; ; ){
        mno = mno + 1;

        for(cnt=1; cnt<=cset; cnt++){
            samp_dps(xloc, mno, cnt);
            cls();
        }

        cal_avg(mno, xloc, &avg, cset, cnt, &it_avg);

        judge(&avg, &q, &upd, mno, &dr_ck, ivol, &cnrv, &upd_jr, &it_avg,
&avg_bf, &kep, &no_sp, &jdg_non, &dp);

        avg_bf = avg;
```

```
            fprintf(fp2,"%6.3f¥n",dp);

            if(q == 0)  end_c = end_c + 1;
            if(end_c == 3){
                locate(10,13); printf("------ System Good!!  -----¥n");
                fprintf(fp2,"***Standby(mod_%d)mno=%d ***¥n",mod,mno);
                locate(10,15); printf("----- System Continue?(y/n) > ");
                ive = getche();
                if((ive == 'N')||(ive == 'n')) {
                    break;
                }
                end_c = 0;
                goto mod_3;
            }

            if(no_sp >= 3){
               if((avg - ivol) > 0.0){
                locate(10,13); printf("**** Separation by D_Angle!...
!!.****¥n");
                 mod = 4;
               }
            }
            else{
                if(q >= 5){
                 locate(10,13); printf("**** Separation by F_Stream!...
!!.... *****¥n");
                 mod = 1;
                }

                if((jdg_non > -0.65) && (q < 5)){
                 locate(10,13); printf("******  Jets velocity up!... up!!
.... *****¥n");
                  mod = 5;
                }
            }

/*     ------ Optimizing check --------    */
                if((avg - ivol) <= -0.08){
                   fd_ck = 1;
                    sy_ck = 0;
                }
                locate(1,9); printf("+++++  fd_ck = %d +++++¥n",fd_ck);
/*              if((avg - ivol) <=-0.02) && (no_sp >= 7))   mod = 3; */ /*
For D_A(Not Separation) */

                if((mod == 0) || (mod == 2)){
                    if(fd_ck != 1){
                        if(((it_avg-ivol)<0.075) && ((it_avg-ivol)>0.0) &&
((avg-ivol)<=-0.035))  sy_ck =2;
                    }     /*      Uo:Low speed 20deg-10deg     */

                    if(((no_sp < 3) && ((avg - ivol) <= -0.08)) || (sy_ck ==
2)){
                        if(adm_j == 0){
```

```
                        mod = 2;
                        fprintf(fp2,"*** Standby(mod_%d) mno=%d ***¥n",
mod,mno);
                        locate(10,13); printf("------  System Optimizing?
(y/n) > ");
                         adm = getche();
                     }
                     if((adm == 'Y') || (adm == 'y')){
                        adm_j = 1;
                        end_c = 0;
                        q = 4;
                        upd = 2;
                        locate(0,10);
                        sig_out(&q, upd, mno, es, &volt);
                     }

                     if(volt < 1.99){
                        mod = 3;
                        sy_ck = 0;
                        fprintf(fp2,"*** Standby(mod_%d) mno=%d ***¥n",
mod,mno);
                        es = 2;
                        locate(0,13);
                        sig_out(&q, upd, mno, es, &volt);
                         locate(10,16); printf("-----  Jet Flow Cut :
System Good!!  -----¥n");
                          locate(10,17); printf("----- System Continue?
(y/n) > ");
                        ive = getche();
                        if((ive == 'N')||(ive == 'n')) {
                            break;
                        }
                        no_sp = 3;
                        goto mod_3;
                     }
                  }
               }
/*        ------------------------------------------------------------ */

               if(mod == 1){
                  fprintf(fp2,"*** Standby(mod_%d) mno=%d ***¥n",mod,mno);
                  mno = 0;
                  locate(10,17); printf("---- System Continue? (y/n) > ");
                  ive = getche();
                  if((ive == 'N')||(ive == 'n')) {
                    break;
                  }
                  goto mod_1;
               }

               if(mod == 4){
                  fprintf(fp2,"*** Standby(mod_%d) mno=%d ***¥n",mod,mno);
                  mno = 0;
                  no_sp = 0;
```

```
                locate(10,17); printf("---- System Continue? (y/n) > ");
                ive = getche();
                if((ive == 'N')||(ive == 'n')) {
                    break;
                }
                goto mod_4;
            }

            if(mod == 5){
                fprintf(fp2,"*** Standby(mod_%d) mno=%d ***¥n",mod,mno);
                locate(10,17); printf("---- System Continue? (y/n) > ");
                ive = getche();
                if((ive == 'N')||(ive == 'n')) {
                    break;
                }
                goto mod_5;
            }
/* ------------------------------------------------------------ */

            printf("*** q = %d, upd = %d  ***¥n",q,upd);

            if(kbhit()) {
                es = 1;
                locate(0,10);
                sig_out(&q, upd, mno, es, &volt);
                locate(10,15); printf("**** System - Shut Down !! ****¥n");
                exit(1);
            }
        }
        fclose(fp2);

        locate(10,17); printf("----  Press 's' Key: System Stop!!  ---- >");
        lucy = getche();
        printf("¥n");
        if((lucy == 'S') || (lucy == 's')){
            es = 2;
            sig_out(&q, upd, mno, es, &volt);
        }

}


/*-------------------------------------------------------------------------
 * Program of sampling pressure (samp_dp (Ver.5))
 *
 * THIS PROGRAM is - periodic sampling with internal sampling clock and
 *                   storing converted data to main memory by DMA transfer
 *                   to sample differential pressure.
 *
 *       I/O address          = 700h
 *       input gain           = x1
 *       input channel        = multi channel( 0 to 15 ) (use No.0 channel)
 *       scan clock           = 10usec
 *       sampling clock       = 30000usec
```

```
 *       number of samplings = 10
 *       DMA channel         = 5 ( word transfer )
 *
 *    3-ch:Voltage of Differential Pressure
 *                                                              1998. 2.17
 *-------------------------------------------------------------------------
*/

#include <stdio.h>
#include <dos.h>
#include <math.h>
#include "h306.h"

#define    ADR      0x0700

int                 aidata[40][16];


void samp_dp(int xloc, int mno, int cnt)
{
   void _far      *ptr = aidata;
   unsigned int    status, dmaseg = FP_SEG(ptr), dmaoff = FP_OFF(ptr);
   unsigned char   errflg = 0;
   unsigned char   gain[] = { 0,0,0,0,0,0,0,0,0,0,0,0,0,0,0,0 };
   unsigned char   channel[] = { 0,1,2,3,4,5,6,7,8,9,10,11,12,13,14,15 };
   unsigned char   i, j;
   float  volt;
   int   span = 10;
   int   offset = 0;
   int   n = 12;

   FILE  *fp1;
   char   fnam[25];


   /*--- file name ---*/
   sprintf(fnam,"x%dn%dc%d.dat",xloc,mno,cnt);

/*  while ((fp1 = fopen(fnam, "r")) != NULL) {
      printf(" WARNING >  %s  File Already Exists!¥n",fnam);
      fclose(fp1);
      printf("ENTER FILE NAME =>");
      scanf("%s",&fnam);
   }
*/
   if((fp1 = fopen(fnam, "w")) == NULL) {
      printf("%s not open!! in SAMP_DP.C ¥n",fnam);
      exit(1);
   }

   /*--- initialize ---*/
   InitBoard( ADR );

   /*--- set AI condition ---*/
```

```
    SetAIFunction( ADR, 0x0880 );              /* set function */
    for ( i = 0; i < 16; i++ ) {
       SetAIGain( ADR, i, gain[i] );           /* set input gain */
       SetAIChannel( ADR, i, channel[i] );      /* set input channel */
    }
    SetAIScanClk( ADR, 10000UL );                    /* set scan clock */
    SetAISmpClk( ADR, 30000e3 );                   /* set sampling clock */
    SetAISmpNum( ADR, 0UL, 10UL, 0UL );      /* set number of samplings */

    /*--- set DMA transfer condition ---*/
    SetAIDmaFunc( ADR, 5, 0, 0 );              /* set DMA condition */
    SetPC8237( 5, 0, 0, 0, dmaoff, dmaseg, 159 ); /* set 8237 condition */

    /*--- start analog input ---*/
    StartAI( ADR, 15 );
    do {
       GetStatus( ADR, &status ) ;             /* get sampling status */
    } while ( status & 3 );
    if ( status & 0x80 ) errflg = 1;           /* test sampling error */

    /*--- display data ---*/
    if ( errflg ) {
       printf( "sampling error !!¥n" );
    }
    else {
        for ( i = 3; i < 4; i++ ) {
           printf( "%2dch AIdat:", i );
           for ( j = 0; j < 10; j++ )
               printf( " %04xh", aidata[j][i] );
               printf( "¥n" );
               printf("%2dch Volt :", i );
               printf("          saving  %s ¥n",fnam);
               fprintf(fp1, "%2dch Volt:",i);
               for ( j = 0; j < 10; j++ ){
                  volt = aidata[j][i] * span / pow(2,n) - offset;
                  fprintf(fp1, "%6.3f ",volt);
            }
            printf( "¥n" );
       }
    }
    fclose(fp1);

}


/*-------------------------------------------------------------------------
 * Program of sampling pressure  (samp_dps (Ver.0))
 *
 * THIS PROGRAM is - periodic sampling with internal sampling clock and
 *                storing converted data to main memory by DMA transfer
 *                to sample differential pressure.
 *
 *       I/O address         = 700h
 *       input gain          = x1
```

```
*       input channel       = multi channel( 0 to 15 ) (use No.0 channel)
*       scan clock          = 10usec
*       sampling clock      = 30000usec
*       number of samplings = 60
*       DMA channel         = 5 ( word transfer )
*
*    3-ch:Voltage of Differential Pressure
*                                                              1997.12.27
*-------------------------------------------------------------------------
*/

#include <stdio.h>
#include <dos.h>
#include <math.h>
#include "h306.h"

#define    ADR      0x0700

int                 aidata[40][16];


void samp_dps(int xloc, int mno, int cnt)
{
    void _far      *ptr = aidata;
    unsigned int    status, dmaseg = FP_SEG(ptr), dmaoff = FP_OFF(ptr);
    unsigned char   errflg = 0;
    unsigned char   gain[] = { 0,0,0,0,0,0,0,0,0,0,0,0,0,0,0,0 };
    unsigned char   channel[] = { 0,1,2,3,4,5,6,7,8,9,10,11,12,13,14,15 };
    unsigned char   i, j;
    float   volt;
    int   span = 10;
    int   offset = 0;
    int   n = 12;

    FILE  *fp1;
    char   fnam[25];


    /*--- file name ---*/
    sprintf(fnam,"x%dn%dc%d.dat",xloc,mno,cnt);

/*  while ((fp1 = fopen(fnam, "r")) != NULL) {
      printf(" WARNING >  %s  File Already Exists!¥n",fnam);
      fclose(fp1);
      printf("ENTER FILE NAME =>");
      scanf("%s",&fnam);
    }
*/
    if((fp1 = fopen(fnam, "w")) == NULL) {
      printf("%s not open!! in SAMP_DP.C ¥n",fnam);
      exit(1);
    }

    /*--- initialize ---*/
```

```
    InitBoard( ADR );

    /*--- set AI condition ---*/
    SetAIFunction( ADR, 0x0880 );              /* set function */
    for ( i = 0; i < 16; i++ ) {
       SetAIGain( ADR, i, gain[i] );           /* set input gain */
       SetAIChannel( ADR, i, channel[i] );     /* set input channel */
    }
    SetAIScanClk( ADR, 10000UL );                    /* set scan clock */
    SetAISmpClk( ADR, 30000e3 );                   /* set sampling clock */
    SetAISmpNum( ADR, 0UL, 60UL, 0UL );      /* set number of samplings */

    /*--- set DMA transfer condition ---*/
    SetAIDmaFunc( ADR, 5, 0, 0 );              /* set DMA condition */
    SetPC8237( 5, 0, 0, 0, dmaoff, dmaseg, 959 ); /* set 8237 condition */

    /*--- start analog input ---*/
    StartAI( ADR, 15 );
    do {
       GetStatus( ADR, &status ) ;             /* get sampling status */
    } while ( status & 3 );
    if ( status & 0x80 ) errflg = 1;           /* test sampling error */

    /*--- display data ---*/
    if ( errflg ) {
       printf( "sampling error !!¥n" );
    }
    else {
       for ( i = 3; i < 4; i++ ) {
          printf( "%2dch AIdat:", i );
          for ( j = 0; j < 60; j++ )
          printf( " %04xh", aidata[j][i] );
          printf( "¥n" );
          printf("%2dch Volt :", i );
          printf("          saving  %s ¥n",fnam);
          fprintf(fp1, "%2dch Volt:",i);
          for ( j = 0; j < 60; j++ ){
              volt = aidata[j][i] * span / pow(2,n) - offset;
              fprintf(fp1, "%6.3f ",volt);
          }
          printf( "¥n" );
       }
    }
    fclose(fp1);

}


/*
*-------------------------------------------------------------------------
* Program of calculating average pressure  (cal_avg (Ver.4))
*
*  THIS PROGRAM is - calculating average pressure from output voltage of
*                    differential pressure transducer.
```

```
*
*                                                          1997.11.20
*-------------------------------------------------------------------------
*/

#include <stdio.h>
#include <math.h>

#define SPNUM 40

void  cal_avg(int mno, int xloc, float *avg, int cset, int cnt, float *it_avg)
{
     int    ii, jj;
     char   infnam[25];
     char   dammy;
     float  indat, involt, avg_p;

     FILE  *fp2;


     involt = 0.0;
     for(cnt=1; cnt<=cset; cnt++){
       sprintf(infnam,"x%dn%dc%d.dat",xloc,mno,cnt);

       if((fp2 = fopen(infnam,"r")) == NULL){
         printf("%s File not open!! in CAL_AVG.C ¥n",infnam);
         exit(1);
       }

       indat = 0.0;

       for(ii=1; ii<=10; ii++){
          fscanf(fp2,"%c",&dammy);
       }

       for(jj=0; jj<SPNUM; jj++){
          fscanf(fp2,"%f",&indat);
          fscanf(fp2,"%c",&dammy);

          involt = involt + indat;
       }
       fclose(fp2);
    }

    *avg = involt / (SPNUM * cset);
    avg_p = (*avg - 3.0) / 0.315;
    if(mno == 1)  *it_avg = *avg;
    printf("---- it_avg = %6.3f mno = %d ----¥n",*it_avg,mno);
    printf("*** involt=%6.3f  avg[%d]=%6.3f  Mes_No.=%d¥n",involt,mno,
*avg,mno);
    printf("+++ [Mes.No.]=%d Dif.Press.=%6.3f(mmAq) +++¥n",mno,avg_p);

}
```

```
/*-------------------------------------------------------------------
 * Program of signal output  (sig_out (Ver.2))
 *
 *  THIS PROGRAM is - producing output signal(0-10V) to actuate electric
 *                valve.
 *
 *
 *    I/O address = 700h
 *
 *    n=12   offset=0   span=10   q=ratio_vq * V
 *    ITV:Initial value of metering valve
 *    ITV = 819 = 2(V) = 18(l/min.)
 *
 *                                                          1997.12.20
 *-------------------------------------------------------------------
*/

#include <math.h>
#include <stdio.h>
#include <conio.h>
#include "h306.h"

#define  ADR  0x0700
#define  TW  3000
#define  TTW  2000
#define  ITV  819

void   sig_out (int *q, int upd, int mno, int es, float *volt)
{
   static int     aodata;
   int            offset, span;
   int            ti, tti, twf;
   static float   aodat_jr;
   float          n;
   float          ratio_vq;

   n = 12.0;
   offset = 0;
   span = 10;
   ratio_vq = 0.02;

   if(es == 1){
      aodata = ITV;
      printf("### mno = %d ###¥n",mno);
   }
   if(es == 2)  aodata = 0;

   if((es != 1) && (es != 2)){
      if(mno == 1){
         aodata = ITV;
         aodat_jr = (float)aodata;
      }
      else{
```

```
    /*-------set flow rate- up or down-------*/
        if (upd == 1)
          aodat_jr = aodat_jr + ((ratio_vq*pow(2.0,n))/span)*(*q);
        if (upd == 2)
          aodat_jr = aodat_jr - ((ratio_vq*pow(2.0,n))/span)*(*q);
          aodata = (int)(aodat_jr + 0.5);
        }
/* printf("*** mno=%d aodat_jr=%7.3f aodata=%d ***¥n",mno,aodat_jr,aodata);
*/
   }

   /*-----------initialize-------------*/
   InitBoard( ADR );

   /*-----------set AO data----------*/
   SetAOData( ADR, aodata );

   /*------make time delay------*/
   for (ti=1; ti<=TW; ti++){
     for (tti=1; tti<=TTW; tti++){
        twf = ti + tti;
     }
   }

   *volt =(float)((aodata *span) / pow(2.0,n) - offset);

   /*----------display data---------*/
/* printf("output data: %04xh¥n",aodata);  */
   if(es != 1){
      printf("output data: %d¥n",aodata);
      printf("output voltage : %6.4f¥n",*volt);
   }
}


/*-------------------------------------------------------------------------
* Program of signal output for non-jet situation  (int_sig)
*
*  This PROGRAM is - producing output signal to cut off jet flow
*
*
*                                                          1997.11.18
-------------------------------------------------------------------------
*/

#include <stdio.h>
#include "h306.h"


#define ADR 0x0700

void int_sig (int mno)

{
```

```
  int aodata;

  aodata = 0;

  InitBoard( ADR );

  SetAOData( ADR, aodata);

/*  printf("Now, initial aodata is 0 !"); */
}
```